Fisheries New Zealand
Tini a Tangaroa

Characterisation and stock assessment of scampi (*Metanephrops challengeri*) in SCI 3 (Mernoo Bank) and SCI 4A for the 2024–25 fishing year

New Zealand Fisheries Assessment Report 2026/27

A. Dunn, S.D, Hoyle, D.N. Webber

ISSN 1179-5352 (online)
ISBN 978-1-997337-47-8 (online)

July 2026

New Zealand Government

Disclaimer

Enquiries should be directed to:

Fisheries Science Editor
Fisheries New Zealand
Ministry for Primary Industries
PO Box 2526
Wellington 6140
NEW ZEALAND

Email: Fisheries-Science.Editor@mpi.govt.nz
Telephone: 0800 00 83 33

This publication is also available on the Ministry for Primary Industries websites at:
http://www.mpi.govt.nz/news-and-resources/publications
http://fs.fish.govt.nz go to Document library/Research reports

Please cite this report as:
Dunn, A.; Hoyle, S.D.; Webber, D.N. (2026). Characterisation and stock assessment of scampi (*Metanephrops challengeri*) in SCI 3 (Mernoo Bank) and SCI 4A for the 2024–25 fishing year. *New Zealand Fisheries Assessment Report 2026/27*. 87 p.

Table of Contents

PLAIN LANGUAGE SUMMARY

The 2026 stock assessment of scampi (*Metanephrops challengeri*, a small deep-water lobster) on the Mernoo Bank (fishery area SCI 3) off New Zealand found the population to be in a healthy state. Current abundance was estimated at about two-thirds of the stock's original, unfished level; comfortably above the 40% management target used for this stock and well clear of the lower limits that would trigger concern.

The smaller neighbouring fishery, SCI 4A, also appears to be above target, but with much greater uncertainty because far less information is available; the combined trawl/photographic survey in 2024 provided the first reliable abundance data for this area.

Drawing on commercial catch and catch-rate records, trawl and photographic surveys, and two independent population models, the report concludes that current catch limits are likely to be sustainable over the next five years — provided the recent strong numbers of young scampi entering the fishery continue to occur rather than dropping back to the long-term average.

EXECUTIVE SUMMARY

Dunn, A.[1]; Hoyle, S.D.[2]; Webber, D.N.[3] (2026). Characterisation and stock assessment of scampi (*Metanephrops challengeri*) in SCI 3 (Mernoo Bank) and SCI 4A for the 2024–25 fishing year.

***New Zealand Fisheries Assessment Report 2026/27*. 87 p.**

This report characterises the SCI 3 and SCI 4A scampi (*Metanephrops challengeri*) fisheries, updates the catch-per-unit-effort (CPUE) analysis for these areas, and provides stock assessments for both Fishstocks, fulfilling the objectives of Fisheries New Zealand project SCI2024-02. SCI 3 is treated as three separate stocks, each assumed to represent a separate biological stock: Mernoo north (MN), Mernoo original (MO), and Mernoo west (MW); and SCI 4A as two stocks, SCI 4A east (4AE) and SCI 4A west (4AW). The SCI 3 fishery began in the late 1980s and has a Total Allowable Commercial Catch (TACC) of 408 t; the smaller and more recently developed SCI 4A fishery has a TACC of 120 t.

The assessment used a descriptive summary of catch and effort since the onset of the fisheries, updated standardised CPUE indices, trawl and photographic (burrow and visible-scampi) resource survey indices including the 2024 survey, which extended the surveys to SCI 4A for the first time, commercial and survey length compositions, and a length-weight relationship estimated specifically for Chatham Rise scampi for the first time. Standardised CPUE indices were estimated using generalised additive models (GAMs) with a Tweedie distribution, by stock and time step, for the 1990–2024 model years.

An integrated, two-sex, length-based stock assessment was carried out for the three SCI 3 stocks (MN, MO, and MW), implemented in Casal2. The conversion of the model from the CASAL implementation used in the previous assessment was validated by reproducing the previous base case; the CASAL and Casal2 implementations gave very similar results at both the MPD and MCMC levels. The model assumed natural mortality M=0.25 y^{-1} and Beverton-Holt stock recruitment with steepness h=0.75; recruitment variability was estimated to be higher ($\sigma_R \approx 1.1$) than assumed in previous assessments. A separate Bayesian state-space surplus production model was also fitted to all five stocks (SCI 3 MN, MO, and MW, and SCI 4A east and west) in a model that jointly estimated some of the parameters, providing the only quantitative assessment available for the data-limited SCI 4A stocks.

For the integrated assessment, the SCI 3 stock as a whole was estimated to have an initial spawning-stock biomass (B_0) of 5687 t (95% credible interval (CI) 4713–7209 t) and a current biomass of about 68% B_0 (95% CI 46–100%). The stock was assessed as Very Likely (> 90%) to be at or above the 40% B_0 management target and Exceptionally Unlikely (< 1%) to be below the soft (20% B_0) or hard (10% B_0) limits. At the sub-stock level, MO was well above the target (about 112% B_0) while MN and MW were each at about 58% B_0. Overfishing (exploitation above the rate at the target biomass) was estimated to be Likely (> 60%) to be occurring in the MW stock, but Very Unlikely (< 10%) for the total SCI stock. These conclusions were robust across a wide range of model sensitivity runs, although the estimated scale of the stock was sensitive to the choice of abundance index.

The surplus production model gave results broadly consistent with the integrated assessment for SCI 3, with stock-specific carrying capacity (K) estimates of the same order of magnitude as the integrated B_0 estimates and all three SCI 3 stocks estimated to be above target. All five stocks, including both SCI 4A stocks, were estimated to be above the 40% K target reference point in 2026;

[1] Ocean Environmental Ltd., Wellington, New Zealand.
[2] Hoyle Consulting Ltd. Nelson, New Zealand.
[3] Quantifish Ltd., Tauranga, New Zealand.

however, the SCI 4A results were considerably more uncertain, and for SCI 4A west the posterior for carrying capacity closely tracked its prior, indicating that the available data were largely uninformative about the scale of this stock.

Projections under TACC catches indicated that the total SCI 3 stock is Very Likely to remain above the 40% B_0 target over the next five years if recent recruitment levels are maintained. If future recruitment instead reverts to the long-term average, stock status was projected to decline, and the probability of MN and, in particular, MW remaining above the target was appreciably lower. The probability of the stock declining below the soft or hard limits under TACC catches was low throughout the projection period.

Overall, the SCI 3 scampi stock is assessed to be in a healthy state and likely to remain so under current catches provided recent recruitment continues; the data-limited SCI 4A stocks appear to be above the target but are assessed with considerably lower confidence. Areas for future work include continuation of the trawl and photographic survey series (including for SCI 4A), further development of the photographic survey reader calibration, improved information on scampi growth, natural mortality, and stock structure, and continued monitoring of recruitment variability and its possible links to environmental variability, including climate change.

1. INTRODUCTION

Scampi (*Metanephrops challengeri*) are important fisheries within New Zealand, with major scampi fisheries based in SCI 1, SCI 2, SCI 3, and SCI 6A. A smaller fishery, based in SCI 4A, has become more notable over recent years.

The current management for scampi divides it into nine main Fishstocks (Figure 1): (i) SCI1 - Auckland (east) Fisheries Management Area (FMA); (ii) SCI 2 - Central (east) FMA: (iii) SCI 3 and SCI 4A - Chatham Rise; (iv) SCI 5 - Southland FMA; (v) SCI 6A- the Auckland Islands shelf; (vi) SCI 6B - the remainder of FMA 6 not covered by SCI 6A; (vii) SCI 7 – Challenger/Central Plateau FMA; (viii) SCI 8 Central (Egmont) FMA; and (ix) SCI 9 – Auckland (west) FMA. An administrative Fishstock (with no recorded landings) is also defined for the Kermadec FMA (SCI 10) (Fisheries New Zealand 2025).

Scampi are widely distributed around the New Zealand coast, principally in depths between 200 and 600 m on the continental slope (Tuck 2019, McGregor et al. 2022). Catches are generally in 300–550 m depths using trawl fishing gear. The stock structure of scampi in New Zealand waters is not well known, but larval development for scampi is probably very short and may be less than three days in the wild (Fisheries New Zealand 2025) suggesting that different areas are separate biological stocks. There is some evidence to suggest that scampi in SCI 6A are genetically distinct from those in other areas and there was heterogeneity in samples between SCI 1, SCI 2, and SCI 4A (Fisheries New Zealand 2025). In 2000, a review of stock boundaries between SCI 3 and SCI 4A and between SCI 6A and SCI 6B was conducted prior to introduction of scampi into the Quota Management System (Cryer 2000). Following this review, the management boundaries were changed on 1 October 2004, to reflect the distribution of scampi stocks and fisheries (Fisheries New Zealand 2025).

This report characterises the SCI 3 and SCI 4A scampi fisheries, updates the CPUE (catch-per-unit-effort) analysis for these areas, and provides stock assessments for both SCI 3 and SCI 4A scampi Fishstocks and fisheries up to 2025–26. The main area of SCI 3 is split into three regions, each assumed to represent a separate stock: Mernoo north (MN), Mernoo original (MO), and Mernoo west (MW). SCI 4A is split into two areas SCI 4A east (SCI 4AE) and SCI 4A west (SCI 4AW) (see Figure 2). In this report, we update the integrated length-based assessment using abundance and length composition data for the MN, MO, and MW areas in SCI 3; as well as developing state-space surplus production models for SCI 3 (MN, MO, and MW) and SCI 4AE and SCI 4AW within a single multi-stock model.

SCI 3 has the largest Total Allowable Commercial Catch (TACC) of all the scampi stocks, which is currently 408 t per year, a level it has been at since the 2018–19 fishing year (Fisheries New Zealand 2025). The TACC for SCI 4A is 120 t, a level that it has remained at since it was set in 2004–05. The SCI 3 fishery began in the late 1980s and scampi was introduced into the QMS (Quota Management System) on 1 October 2004 (Fisheries New Zealand 2025).

The SCI 3 targeted scampi fishing has been concentrated on the area on the western end of the Chatham Rise and straddles the boundary between the Fisheries Management Areas (FMA) 3 and 4, on and around the Mernoo Bank. SCI 4A was sporadically fished up until 2011, when a more consistent fishery developed, The SCI 4A fishery has been concentrated into two areas (See Figure 2), labelled SCI 4A east and SCI 4A west. Minimal scampi catch (< 1%) has been taken outside of these areas on the Chatham Rise.

Scampi have been modelled with an integrated length-based stock assessments using two-sex and area based models with the most recent assessment of SCI 3 by McGregor et al. (2022) for the 2019–20 fishing year, updating the analysis of Tuck (2019) for 2017–18. No previous assessments have been undertaken for SCI 4A, although a CPUE analysis was carried out by Tuck (2020) and a single resource survey in the second half of 2023 (Wieczorek et al. 2024) provides the only fishery independent abundance information from that area for the 2024 model year.

This report provides a descriptive summary of catch and catch-effort data since the onset of the fisheries, a summary of available data from resource surveys, commercial length compositions, an update of the length-weight parameters, and revision of the analysis of the CPUE data for scampi for both the SCI 3 and SCI 4A stocks for the fishing years 1990–91 (1991) to 2023–24 (2024). In addition, we provide an integrated assessment for SCI 3 (areas MN, MO, and MW), and a state-space surplus production model for these areas in combination with scampi in SCI 4A.

This report fulfils the objectives of the Fisheries New Zealand Project SCI2024-02. The overall Objective was "To carry out a stock assessment of scampi (*Metanephrops challengeri*) in SCI 3 and SCI 4A including estimating biomass and sustainable yields" with the specific objectives: (1) To update the descriptive analysis of the commercial catch and effort and observer data for scampi SCI 3 and SCI 4A; and (2) To carry out a stock assessment for SCI 3 including estimating biomass and sustainable yields, the status of the stock in relation to management reference points, and future projections of stock status as required to support management. An assessment for SCI 4A should also be carried out using the best available information.

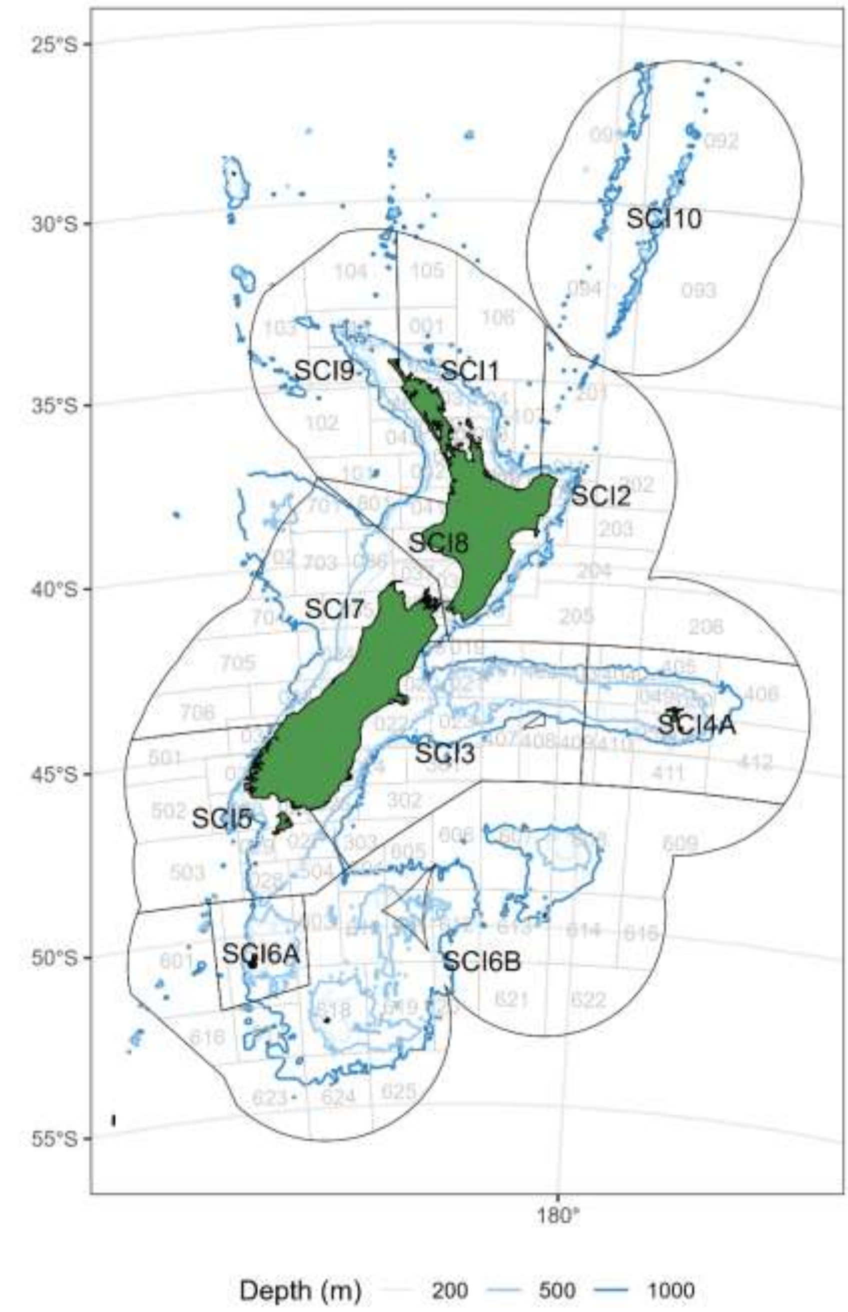

Figure 1: The scampi Quota Management Areas (QMAs) in New Zealand (black lines), statistical areas (grey), with depth contours at 200, 500, and 1000 m shown as blue lines.

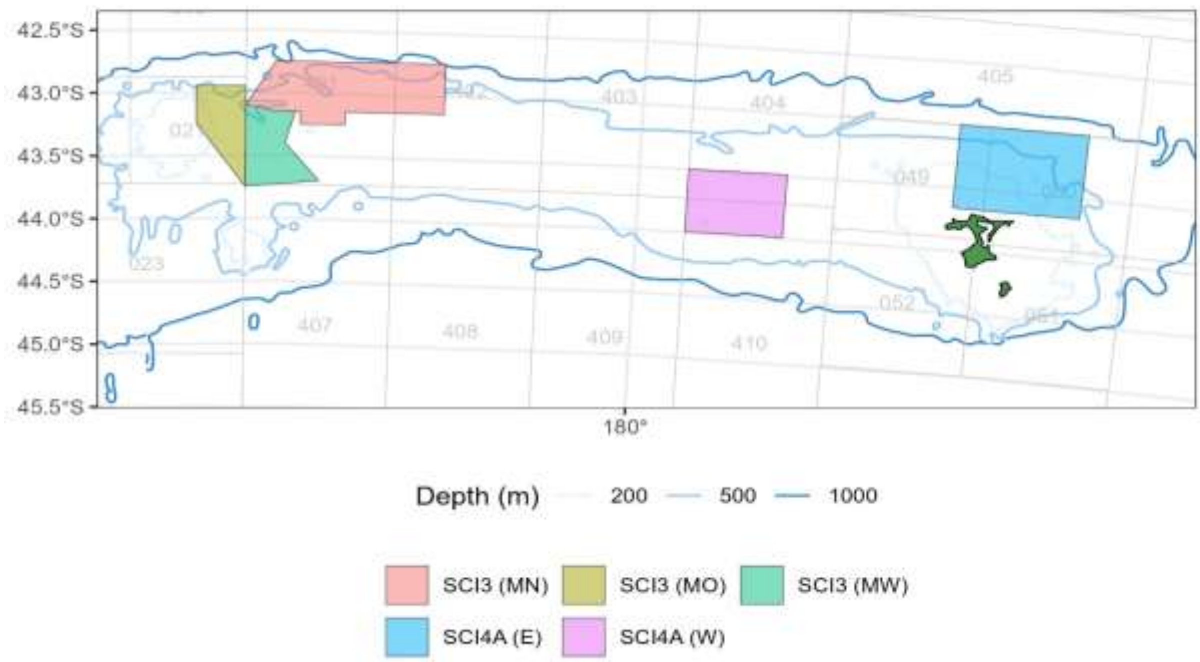

Figure 2: Quota Management Areas (QMAs) SCI 3 and SCI 4A on the Chatham Rise showing the statistical areas and 180° line (light grey), SCI 3 scampi stocks (MN (red), MO (olive), MW (green)), and SCI 4A scampi stocks (west (W) and east (E)). Depth contours at 200, 500, and 1000 m area shown as blue lines.

2. FISHERY SUMMARY AND MODEL INPUTS

2.1 Available data

Catch and effort data were extracted by Fisheries New Zealand for the period from October 1989 to September 2024 (REPLOG 16220) which included all available data at the date of the extract (15th November 2024). The data extract included all data from trips where scampi (*Metanephrops challengeri*) were reported as either targeted, caught, processed, or landed, and all fishing recorded on trawl catch, effort and processing returns (TCEPRs); trawl catch and effort returns (TCERs); catch, effort and landing returns (CELRs); lining catch and effort returns (LCERs); lining trip catch and effort returns (LTCERs); netting catch, effort and landing returns (NCELRs); electronic reporting system returns for all methods (ERS); and any high seas reports.

Observer data for scampi from the Fisheries New Zealand observer sampling programme were also extracted, and data included all observer trips that reported hoki, hake, or ling as of 15th November 2024 (REPLOG 16220). Biological and length frequency data from these trips were also extracted. In addition, all data from the research survey database that recorded scampi or were from scampi surveys were also extracted.

2.2 Catch history

The reported catch history of scampi in each of the stocks within SCI 3 and SCI 4A is given in Table 1 for the years assumed in the assessment models (i.e., July–June). Across SCI 3 and SCI 4A, total reported landings have generally increased slightly since the beginning of the fisheries and peaked at over 590 t in 2022. Area MO has been fished consistently since 1990, but in 2004, with the introduction of scampi to the QMS, catches in this area were substantially reduced and now only contribute about a tonne of catch each year.

Due to the current hypotheses about growth and moult cycles of male and female scampi (see Tuck 2019), the fishery is split into an annual cycle that starts in July and ends in June in the following year, and we define the model year as the period from July- June and labelled with the second year of the period (Figure 3). The annual cycle consists of two time-steps (time-step one and time-step two) that cover the first and second six monthly periods of the model year respectively.

The catch history for scampi for each stock within SCI 3 and SCI 4A for each time-step and model year is given as Table 1 and in Figure 4. While scampi fishing has been focused on depths between 300–400 m, there have been some systematic changes over time as the fishery first moved slightly deeper and now operates over a wider depth range than in the early years of the fishery. The change in depth distribution over time in each of the areas is given in Figure 5 and the distribution of the fishery is given in Figure 6.

Table 1: Total catches (t) by stock for scampi in SCI 3 MN, MO, and MW, and in SCI 4A east and west from 1990 to 2025 for the model year (where 1990 is 1 July 1989–30 June 1990) by time-step (1=Jul–Dec, 2=Jan–Jun). '0' indicates a positive catch rounded to zero and '–' represents nil catch.

Model year	SCI 3 MN		SCI 3 MO		SCI 3 MW		SCI 4 AE		SCI 4 AW		Total
	1	2	1	2	1	2	1	2	1	2	
1990	–	–	–	–	–	–	–	–	–	–	0
1991	–	0	–	0	–	–	–	2	–	–	2
1992	0	116	–	–	1	2	45	37	–	–	230
1993	104	105	55	25	1	1	–	11	–	–	311
1994	74	189	60	1	1	1	–	–	–	–	335
1995	135	56	66	0	1	1	–	0	–	–	274
1996	217	23	75	0	1	1	–	0	–	–	327
1997	100	113	68	–	0	16	0	–	–	–	302
1998	214	6	62	0	22	–	–	0	–	0	308
1999	204	10	60	0	4	4	27	0	0	0	318
2000	158	59	76	0	7	7	21	0	0	0	334
2001	202	20	74	0	44	0	0	0	0	0	348
2002	207	0	72	0	22	0	30	–	0	0	334
2003	152	0	69	0	38	0	79	0	0	–	343
2004	204	0	65	0	5	0	41	–	0	0	318
2005	89	69	0	2	23	91	33	16	0	25	351
2006	53	72	1	3	63	131	19	0	29	21	398
2007	46	30	1	0	73	115	19	2	26	21	335
2008	23	72	1	0	91	60	2	7	2	1	261
2009	27	44	0	0	65	9	0	0	0	0	146
2010	14	64	0	0	91	52	0	–	0	0	223
2011	191	18	0	0	160	33	0	43	0	0	448
2012	133	55	0	0	24	12	0	41	0	0	267
2013	127	85	0	0	59	13	22	33	0	–	341
2014	142	79	0	0	25	3	48	40	0	–	343
2015	236	130	1	0	42	12	68	33	0	0	523
2016	174	95	1	0	47	1	95	34	0	0	450
2017	184	128	0	0	15	17	80	47	0	0	473
2018	220	122	0	0	23	23	118	27	0	0	541
2019	175	170	0	0	42	52	66	55	0	0	561
2020	55	114	0	0	32	131	75	48	–	0	463
2021	85	93	0	3	89	134	79	22	–	0	509
2022	163	120	0	0	87	89	87	41	0	0	590
2023	85	59	1	9	136	121	88	15	0	0	514
2024	143	56	1	0	118	97	54	45	0	0	514
Total	4 335	2 372	810	44	1 452	1 229	1 219	600	62	68	12 366

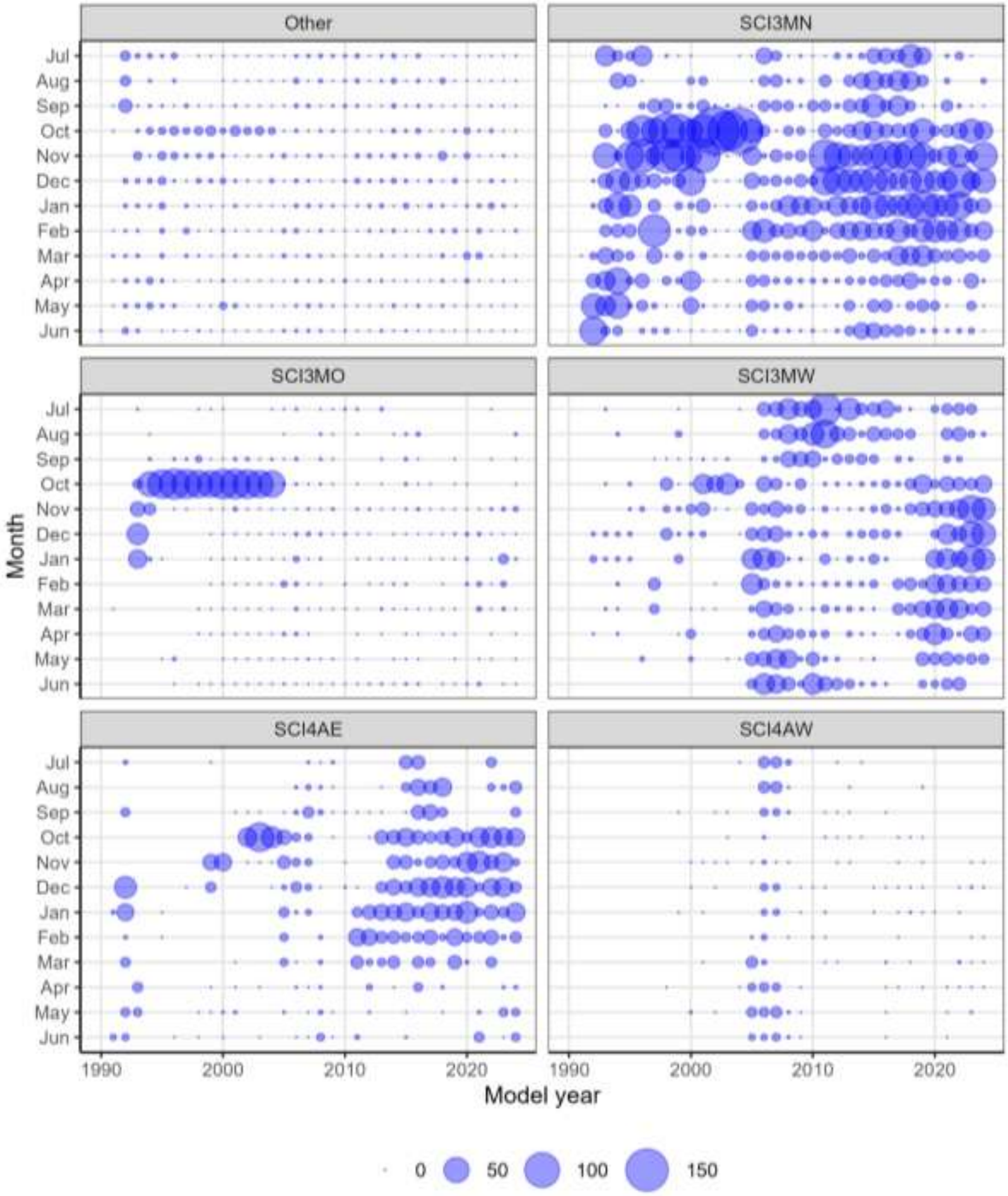

Figure 3: Total catch of scampi in SCI 3 and SCI 4A by month and model year, 1990–2024 (scale in tonnes).

Figure 4: Total catches (t) by stock for scampi in SCI 3 MN, MO, and MW, SCI 4A east and west, and areas outside the defined stock areas ('other') for SCI 3 and SCI 4A from model years 1990 to 2024 (where model year 1990 is 1 July 1989–30 June 1990).

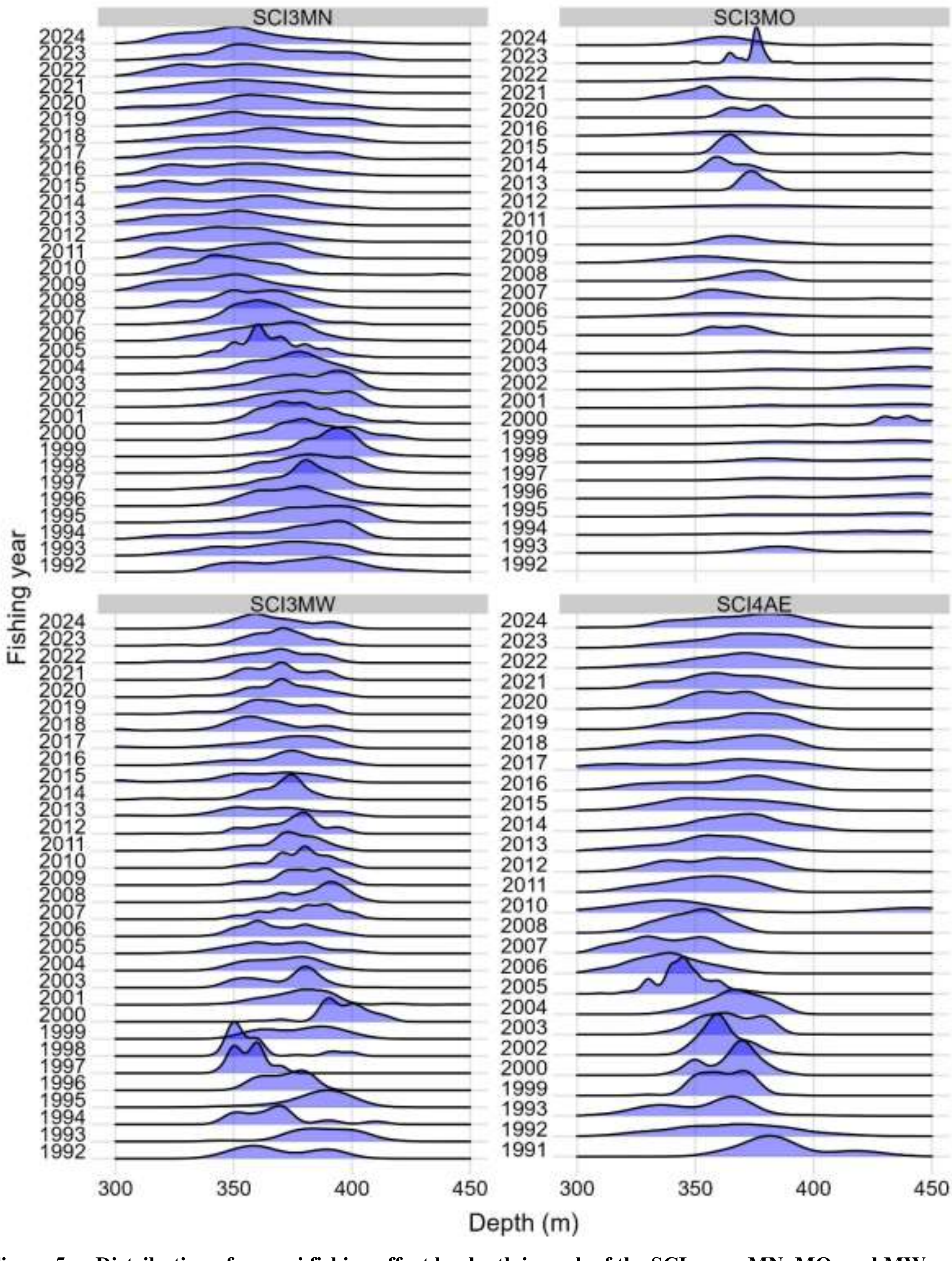

Figure 5: Distribution of scampi fishing effort by depth in each of the SCI areas MN, MO, and MW, and in SCI 4A east, for the years 1991–2024.

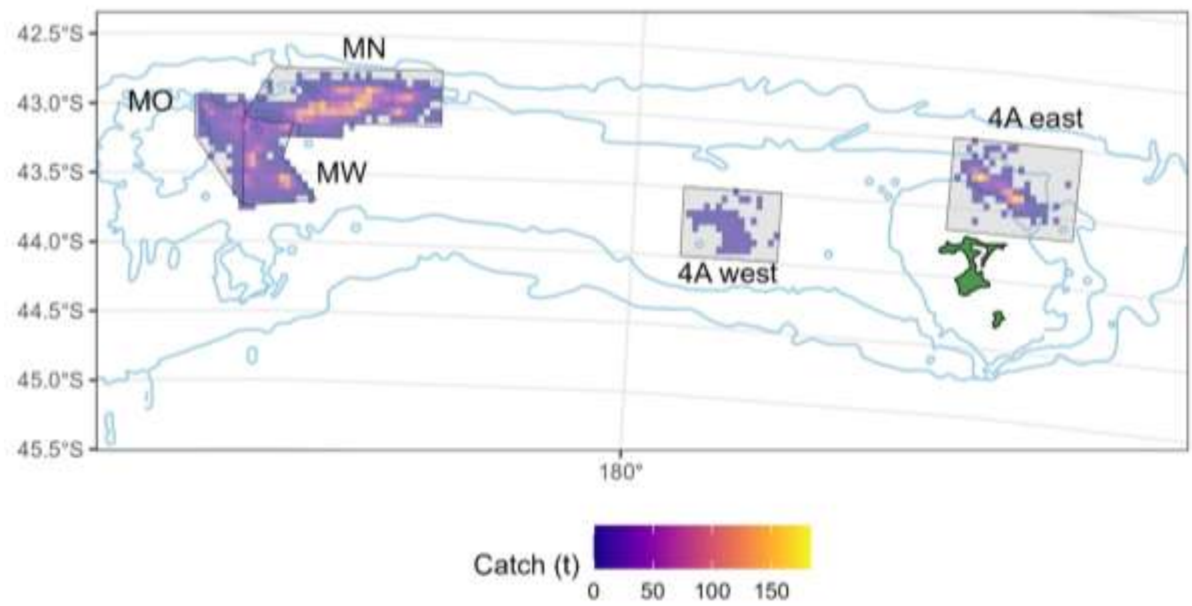

Figure 6: Distribution of total scampi catch over the years 1990–2024 in SCI 3 (areas MN, MO, and MW) and SCI 4A (areas east and west).

2.3 Biological parameters

Previously, the length-weight parameters for scampi on the Chatham Rise were assumed from the relationship derived by Cryer & Stotter (1997) for scampi in SCI 1 & 2. However, samples from Chatham Rise resource surveys (predominantly dedicated scampi surveys) have collected length (Orbital Carapace Length, OCL) and weight samples for male (n=522) and female (n=275) scampi that are adequate to estimate a length weight relationship for scampi on the Chatham Rise. The numbers of length-weight observations by year for males and females in the MN, MO, and MW areas of SCI 3 and in SCI 4A east and west is shown in Figure 7.

A log-linear regression was applied to the available length (OCL) and weight parameters, where weight=$a \cdot (\text{length})^b$, to estimate the a and b parameters for each sex separately (see Table 2 and Figure 8). Plots of residuals indicated reasonable fits to the data with the length-weight relationship, with no apparent pattern or trend over time (Figure 9). The resulting parameter estimates suggested that scampi on the Chatham Rise grow to be longer/thinner than those found in SCI 1 & 2.

Table 2: Estimated scampi length-weight parameters from Cryer & Stotter (1997) for SCI 1 & 2 and the updated estimates for SCI 3 and SCI 4A from this analysis (weight in g, OCL in mm).

Sex	N	Parameter	Cryer & Stotter (1997)	This analysis
Male	522	a	3.73×10^{-4}	7.855×10^{-4}
		b	3.145	2.908
Female	275	a	4.61×10^{-4}	3.886×10^{-4}
		b	3.083	2.493
Both	797	a	–	1.11×10^{-4}
		b	–	2.818

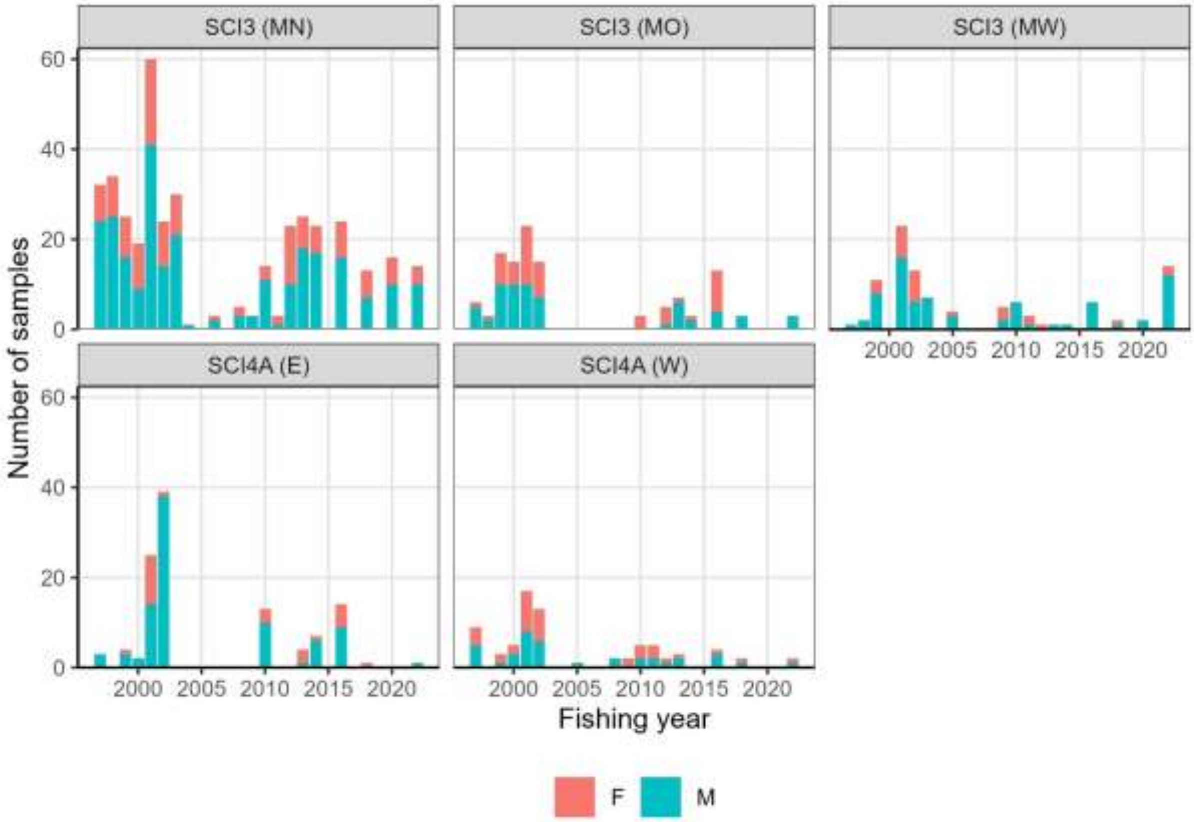

Figure 7: Numbers of male and female scampi samples with both length (OCL) and weight measurements in each of the stocks within SCI 3 and SCI 4A.

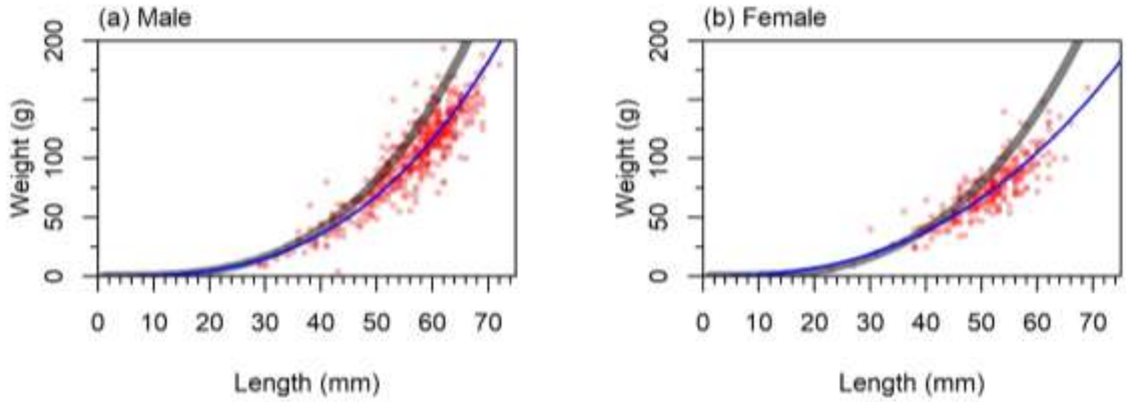

Figure 8: Estimated relationship between length (OCL) and weight (blue line) for SCI 3 and SCI 4A compared with the estimates previously assumed for SCI 3 that were derived by Cryer & Stotter (1997) for SCI 1 & 2 (grey line). The length-weight observations are shown as red points.

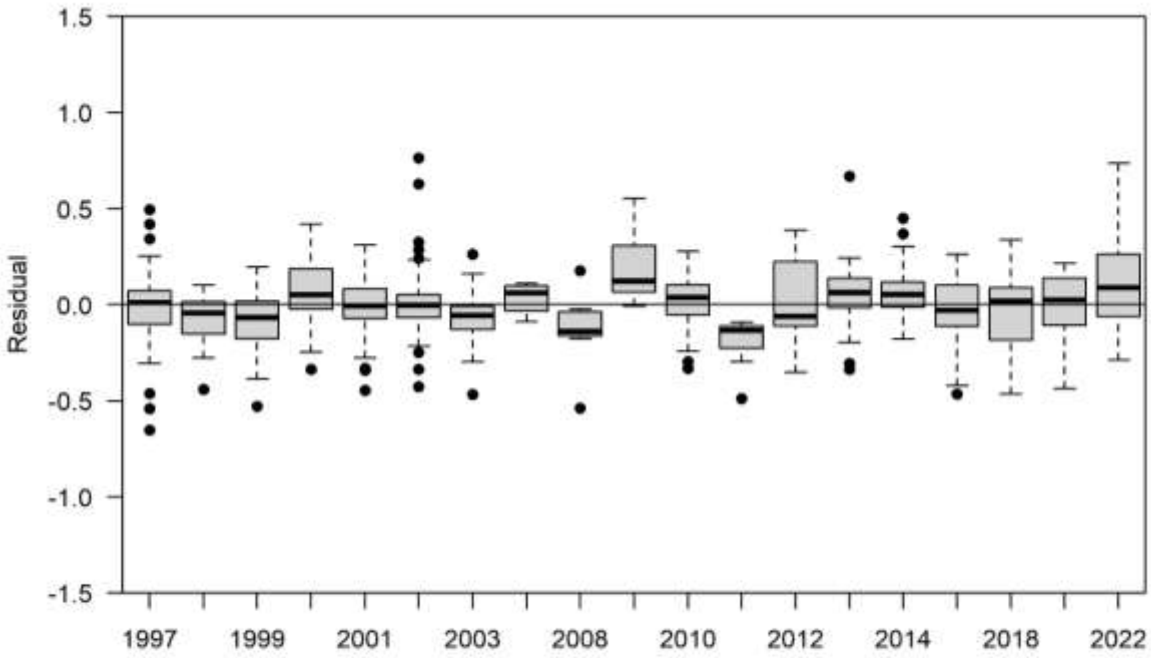

Figure 9: Boxplots of the length weight relationship residuals (dark line=median; grey box=interquartile range; and values more than 1.5 times the interquartile range plotted as black circles) by year (1997 to 2022), of the fitted length-weight relationship for scampi in SCI 3 and SCI 4A , with the residuals for both sexes combined.

The maximum age for scampi in New Zealand is not known although "aquarium trials suggest that this species may be quite long lived" (Fisheries New Zealand 2025) and with longevity estimated (with high uncertainty) indirectly at around 18–23 years from tag-derived growth parameters (Cryer & Stotter 1999). Tuck (2019) reviewed the biological parameters for scampi, and noted that while the instantaneous rate of natural mortality (*M*) has not been estimated directly for any scampi species, estimates have been made (0.2–0.25 y^{-1}) based on the estimate of the *k* parameter from a von Bertalanffy growth curve (Cryer & Stotter 1999) using a correlative method (Pauly 1980, Charnov 1993). Tuck (2019) also reported that Morizur (1982) used length distributions from 'quasi-unexploited' Nephrops stocks to obtain estimates for *M* of 0.2–0.3 y^{-1}. For New Zealand scampi, *M* has previously been fixed at 0.2 y^{-1} (Tuck & Dunn 2012) or both 0.2 and 0.3 y-^{1} (Tuck 2014), and recent assessments for SCI 3 have assumed *M*=0.25 y^{-1} (Tuck 2019, McGregor et al. 2022) with sensitivity runs with *M*=0.2 y^{-1} and 0.3 y^{-1}.

Relatively little is known of the growth rate of any of the Metanephrops species in the wild (Tuck 2019), but males grow to a larger size than females. Tagging of *M. challengeri* to determine growth rates was undertaken in the Bay of Plenty in 1995, and the bulk of recaptures were made late in 1996 (see Tuck 2019 for a summary) and have been used within some scampi stock assessment models in other areas to estimate growth rates.

Estimates of the stock recruitment relationship and the associated Beverton-Holt steepness (*h*) and variability parameters are not known. Previous analyses of scampi within New Zealand have assumed a Beverton-Holt relationship (Beverton & Holt 1957) with steepness *h*=0.75 and variability σ_R=0.4. In this report, preliminary model fits suggested that the value of σ_R=0.4 was not consistent with the changes in stock levels seen over the life of the fisheries in SCI 3, with values closer to σ_R=1.1 being more plausible (see later).

The assumed biological parameters used for scampi in SCI 3 are given in Table 3.

Table 3: Assumed biological parameters for SCI 3 and SCI 4A scampi.

Relationship	Reference	Parameter (units)	Value Both	Male	Female
Natural mortality[1]	(Tuck 2019)	M (y^{-1})		0.25	0.25
Length-weight	(This analysis)	a ($g.mm^{-1}$)		7.855×10^{-4}	3.886×10^{-4}
		b		2.908	2.493
Stock recruitment relationship	(Tuck 2019)				
Stock recruitment steepness		h	0.75		
Recruitment variability[2]	(This analysis)	σ_R	1.1		
Proportion male at birth	(Tuck 2019)		0.5		
Proportion of mature that spawn	(Tuck 2019)		1.0		
Maximum exploitation rate[3]		U_{max}	0.99		

1. Assumed value but also sensitivity runs considered higher and lower values.
2. Assumed prior updated within this analysis
3. Assumed maximum exploitation rate to constrain implausible model estimates.

2.4 Catch-effort indices

Standardised catch-per-unit effort (CPUE) indices were updated using generalised additive models (GAMs) rather than Generalised Linear Models (GLMs), as these are mathematically equivalent when excluding smooth terms (Wood 2003, 2011, 2017) while allowing greater flexibility to include spatial and cyclic smoothers than GLMs. CPUE indices were calculated for the tow-by-tow data (SCI target TCEPR and ERS-trawl tows) using *mgcv* (Wood 2003, 2004, 2011, 2017, Wood et al. 2016) for the model years 1990–2024. Effort data from catch-effort data other than TCEPR and ERS trawl data were ignored as these comprised a very small proportion of the total recorded catch of scampi in both of SCI 3 and SCI 4A.

Unstandardised CPUE indices were calculated as the mean of catch (kg) per hour (Figure 10). Standardised indices were calculated using the mean catch per tow for the non-zero catch tows only, as the proportion of zero tows was extremely small (<1%).

Initial models were run using similar explanatory variables as those used by Tuck (2019) and McGregor et al. (2022) in previous analyses. The GAM considered all terms in the model, but used automatic smoothing parameter selection and variable selection, allowing the model to shrink smooth terms towards zero and effectively remove non-informative predictors from the final model by penalising the smoothing parameters towards infinity (Marra & Wood 2011). The data were filtered to include only core vessels with bottom trawl (BT) gear using TCEPR and ERS data from vessels that were ≥28 m in length (to maintain consistency in the vessels present in the TCEPR and ERS data) and fished in the areas MN, MO, or MW in SCI 3, or in SCI 4A east or west. Target scampi tows using bottom fishing gear (BT) were selected when fishing was between the depths of 250 and 500 m with a duration of between 0.5 and 20 hours. The core vessel set was defined to ensure that the catch data represented vessels with a consistent presence in the fishery using a consistent method. The core vessel data set was then created from all those vessels with a presence of at least five years in the fishery (comprising 95% of the total reported catch). This resulted in a data set comprising fourteen unique vessels (Figure 11) and the relative contribution of effort in each year of each vessel is shown in Figure 12. For these vessels, additional data on the number of nets used and the use of ling bycatch reduction gear modifications were manually identified using analyses updated from Tuck (2017).

For the core vessel data, CPUE indices were modelled where CPUE was defined as catch per tow. A separate analysis was carried out for each of the areas MN, MO, and MW in SCI 3 and in SCI 4A east and west; and for each time-step (one/two). Stock/time-step/year combinations with fewer than ten effort observations were excluded from the analysis to ensure adequate sample sizes for model fitting. The predictor variables were processed as follows: model year, month, and vessel were treated as factors; number of nets (NNets) was treated as an ordered factor; bycatch reduction gear presence was coded as a binary factor; and fishing location coordinates (start longitude and latitude) were included as continuous spatial covariates.

The CPUE standardisation used Generalized Additive Models (GAMs) fitted separately for each stock area. In addition, lognormal (using log(CPUE)) and Gamma, and Tweedie models with a log link were fitted to evaluate the most appropriate model that accounted for the residual errors in the model fits. The final model, based on the residuals, used the Tweedie distribution with a log link function that better accommodated the continuous, positive, and right-skewed nature of the catch data (see Figure 13–Figure 22 for the Tweedie model diagnostics). The GAM model formula for each model was:

```
cpue ~ year + month + s(vessel, by=NNets, bs="re") +
s(BottomDepth, bs="ts", k=6) + s(log(FishingDuration), bs="ts", k=6) +
s(time.mid.hr, bs="cc", k=6) + Bycatch + NNets +
s(moon.phase, bs="cc") + te(long, lat, k=c(6,6))
```

Where:

- Year (model year) was the focal predictor of interest, included as a fixed factor effect
- Month was included as ordered factor effects to account for seasonal patterns
- Vessel × number of nets (NNets) interaction was modelled as a random effect smoother to account for vessel-specific fishing power that varied with gear configuration
- Bottom depth and log(Fishing duration) were included as thin plate regression splines (bs="ts") with basis dimension k=6 to model non-linear relationships with depth and fishing duration
- Time of day at midpoint of tow (time.mid.hr) was included as a cyclic cubic spline (bs="cc", k=6) to capture diel patterns
- Bycatch reduction gear presence was included as a linear fixed effect
- Number of nets was included as a linear fixed effect
- Moon phase was included as a cyclic cubic spline to account for potential lunar effects on catchability
- Spatial location (longitude and latitude) was modelled using a tensor product smooth (te()) with k=6 for each marginal to capture potential spatial variation in abundance

Models were fitted using the *mgcv* package in *R* with a gamma value of 1.4 for increased smoothing penalty and select=TRUE to enable automatic term selection via additional penalties. This approach allows the model to effectively remove non-significant smooth terms during estimation. The model terms, log-likelihood, AIC, and degrees of freedom for each term in each model is given in Table 4.

Standardised CPUE indices were derived using the influence function approach (Bentley et al. 2012) implemented in *gamInflu* (Dunn 2025). This method calculates the marginal effect of the year term while accounting for the influence of all other covariates in the model. Indices were extracted using a prediction-based approach rather than coefficient-based calculations, which provides more robust estimates when dealing with complex smooth terms and interactions.

Model performance was evaluated through multiple diagnostic procedures. Model fits were investigated using standard residual diagnostics and plots. For each model, a plot of residuals against fitted values and quantile-quantile plots were evaluated to check for departures from model assumptions including standard GAM diagnostic plots using gratia::appraise() (Simpson 2024) to assess residual patterns, Q-Q plots, and basis dimension adequacy. Influence plots (Bentley et al. 2012, Dunn 2025) were made for each variable in the CPUE standardisation, which show the effect of each variable on the standardisations and the annual influence of each variable. Post model residual analysis was carried out (see residual pattern analysis in Dunn 2025) to identify if any additional parameters should be considered in the model.

The CPUE indices (Table 5) had r^2 values between 43% and 76% (see Table 4). The standardised Tweedie indices were generally an initial high index, dropping to a low around 2005–2010, then increasing to a second mode at 2017–2020, and then fluctuating thereafter (Figure 23). For Tweedie models, the diagnostic plots of the indices were similar for each of the models and did not suggest strong evidence of departure from model assumptions, although the residuals did suggest a small amount of overdispersion in the tails (Figure 13–Figure 22). The patterns in the indices for the lognormal and Gamma models were very similar (not shown) although the diagnostics for both did suggest departure from the distributional assumptions of both the Gamma and the lognormal models — much more so than for the Tweedie model. Where the CPUE indices and survey indices overlapped (i.e., after 2010), there was reasonable similarity in the trends between the CPUE and survey indices.

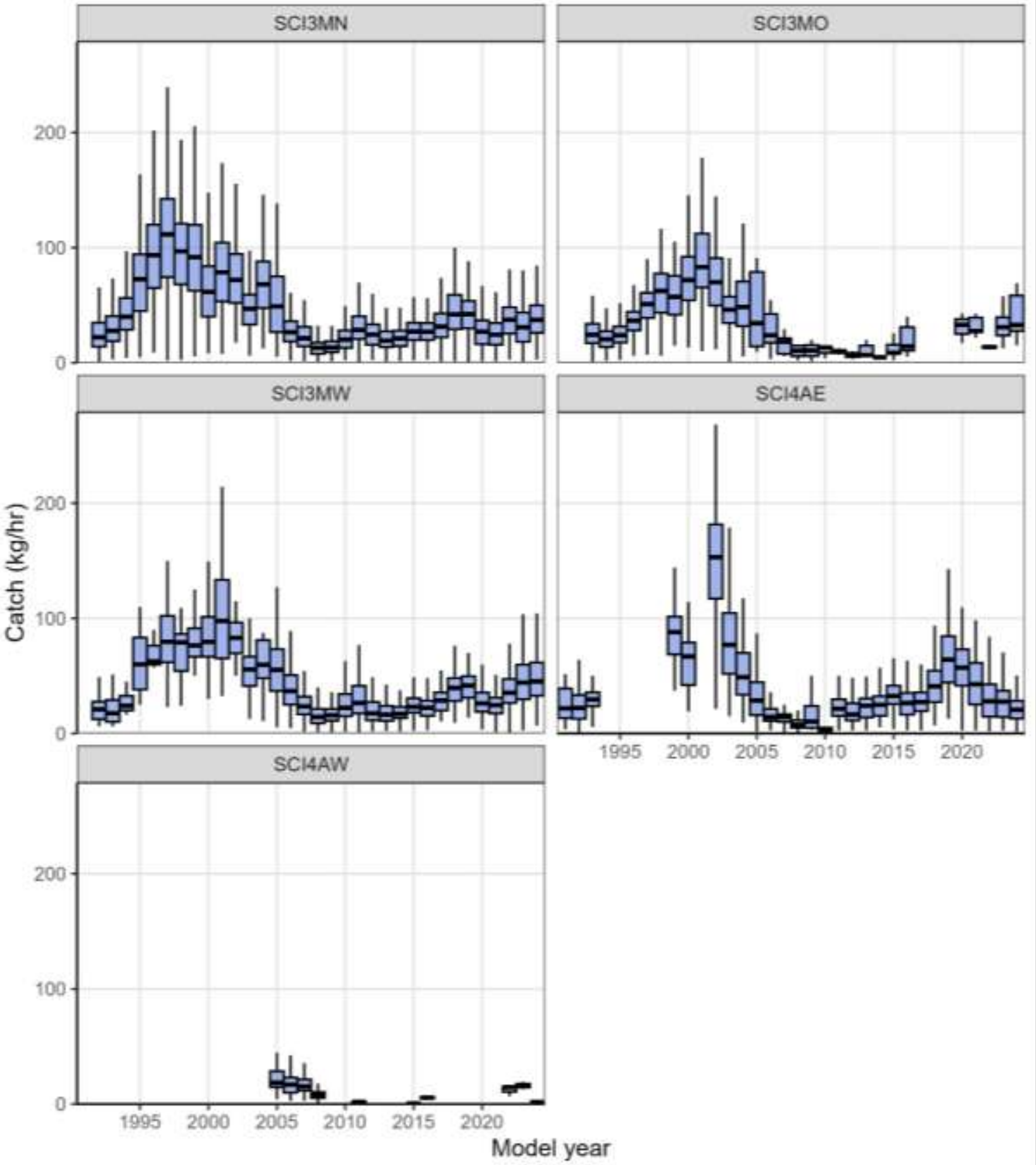

Figure 10: Boxplots of the raw catch per hour (kg/hr) for scampi by model year, from 1990–91 to 2023–24 for each stock in SCI 3 and SCI 4A (dark line=median; blue box=interquartile range; and values up to 1.5 times the interquartile range plotted as vertical black lines) by model year (1990 to 2024).

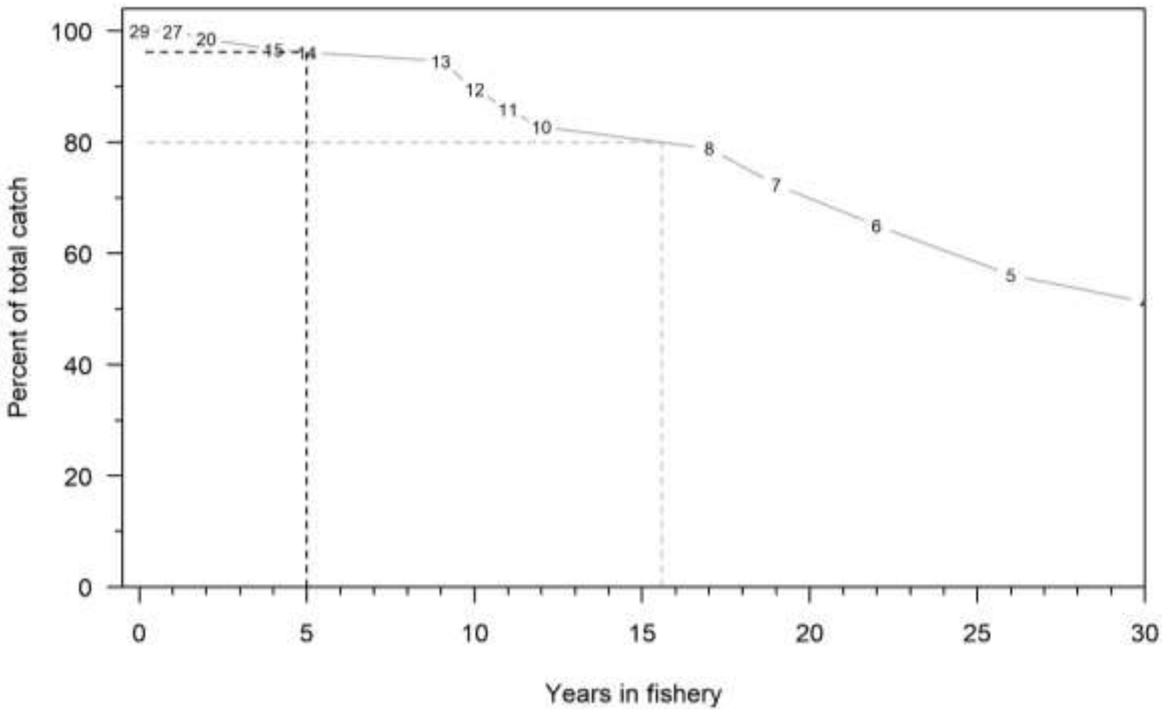

Figure 11: Percentage of catch for different numbers of years in the fishery used to determine core vessels in the tow-by-tow CPUE standardisation. Dashed lines indicate the effect of selecting the years in the fishery for core vessels that give 90% of total catch (14 vessels) or 80% of total catch (8 vessels).

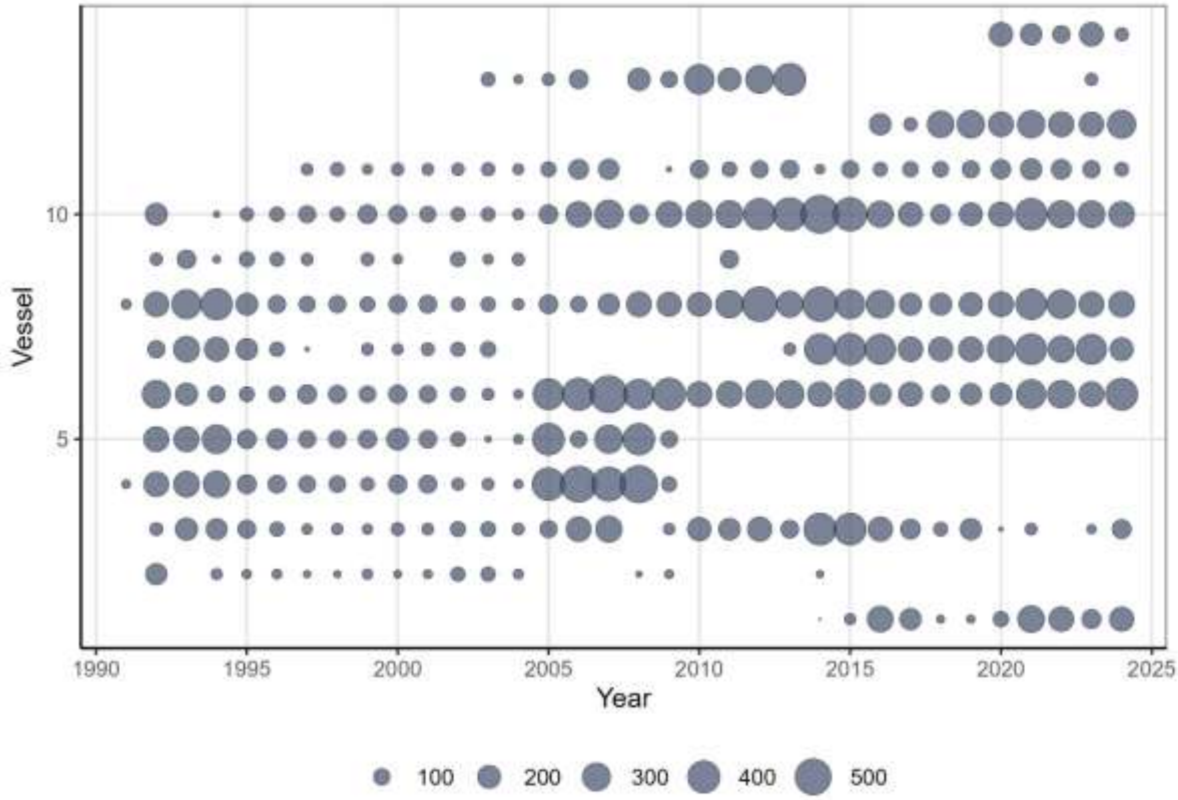

Figure 12: Relative effort (numbers of hauls) by scampi vessels and model year for the core data used in the tow-by-tow CPUE standardisation for 1989–90 to 2023–24.

Table 4: CPUE model terms for the Tweedie model for each stock (SCI 3 MN, MO, and MW, and SCI 4A east and west) and time-step (one and two), showing the log-likelihood (Log.Lik), AIC, r^2, and degrees of freedom (d.f.) for each term in each model.

Stock	Term	LogLik.	AIC	r^2	d.f.
SCI 3 MN	Intercept	6 857.4	-13 708.9	0.00	0.00
Time-step 1	Year	10 639.1	-21 210.2	0.43	31.00
	Month	10 905.9	-21 733.8	0.45	5.00
	s(vessel, by=NNets, bs="re")	11 322.5	-22 533.6	0.49	16.14
	s(BottomDepth, bs="ts", k=6)	11 413.3	-22 706.3	0.49	4.13
	s(log(FishingDuration), bs="ts", k=6)	11 774.3	-23 418.1	0.52	4.58
	s(time.mid.hr, bs="cc", k=6)	13 154.0	-26 169.1	0.59	4.37
	Bycatch	13 158.4	-26 176.5	0.59	0.71
	NNets	13 161.4	-26 180.1	0.59	0.82
	s(moon.phase, bs="cc")	13 161.4	-26 180.0	0.59	0.01
	te(long, lat, k=c(6, 6))	13 280.9	-26 384.8	0.60	13.56
SCI 3 MN	Intercept	9 248.4	-18 490.7	0.00	0.00
Time-step 2	Year	11 457.3	-22 850.7	0.32	29.00
	Month	12 006.0	-23 938.0	0.38	5.00
	s(vessel, by=NNets, bs="re")	12 298.6	-24 488.3	0.43	16.53
	s(BottomDepth, bs="ts", k=6)	12 311.8	-24 508.7	0.43	2.41
	s(log(FishingDuration), bs="ts", k=6)	12 428.9	-24 736.9	0.44	3.12
	s(time.mid.hr, bs="cc", k=6)	14 093.2	-28 050.8	0.58	7.01
	Bycatch	14 101.4	-28 065.3	0.58	1.04
	NNets	14 105.2	-28 072.4	0.58	0.33
	s(moon.phase, bs="cc")	14 122.1	-28 099.4	0.58	2.61
	te(long, lat, k=c(6, 6))	14 252.0	-28 329.9	0.59	11.90
SCI 3 MO	Intercept	2 242.4	-4 478.9	0.00	0.00
Time-step 1	Year	3 716.8	-7 405.6	0.57	11.00
	month	3 754.5	-7 473.0	0.58	4.00
	s(vessel, by=NNets, bs="re")	3 798.2	-7 556.5	0.59	1.95
	s(BottomDepth, bs="ts", k=6)	3 798.2	-7 556.5	0.59	0.01
	s(log(FishingDuration), bs="ts", k=6)	3 955.8	-7 860.2	0.61	4.98
	s(time.mid.hr, bs="cc", k=6)	4 000.8	-7 943.2	0.62	2.92
	NNets	4 000.8	-7 943.2	0.62	0.02
	s(moon.phase, bs="cc")	4 007.9	-7 952.0	0.62	1.98
	te(long, lat, k=c(6, 6))	4 073.6	-8 058.4	0.64	9.97
SCI 3 MO	Intercept	229.9	-453.8	0.00	0.00
Time-step 2	Year	278.8	-545.7	0.44	3.00
	Month	281.0	-542.1	0.46	4.00
	s(vessel, by=NNets, bs="re")	288.7	-555.5	0.48	0.91
	s(BottomDepth, bs="ts", k=6)	289.8	-556.1	0.46	0.55
	s(log(FishingDuration), bs="ts", k=6)	292.2	-558.8	0.47	0.81
	s(time.mid.hr, bs="cc", k=6)	308.8	-585.4	0.57	2.76
	Bycatch	308.5	-584.9	0.57	-0.01
	NNets	308.5	-584.9	0.57	0.08
	s(moon.phase, bs="cc")	342.8	-645.7	0.66	3.32
	te(long, lat, k=c(6, 6))	342.8	-645.2	0.66	0.00
SCI 3 MW	Intercept	4 201.0	-8 396.1	0.00	0.00
Time-step 1	Year	5 720.1	-11 384.2	0.42	25.00
	Month	5 749.9	-11 433.8	0.42	5.00
	s(vessel, by=NNets, bs="re")	5 815.4	-11 552.8	0.44	5.76
	s(BottomDepth, bs="ts", k=6)	5 830.0	-11 574.2	0.44	3.05
	s(log(FishingDuration), bs="ts", k=6)	5 942.3	-11 790.0	0.46	3.83
	s(time.mid.hr, bs="cc", k=6)	6 981.1	-13 858.3	0.61	4.71
	Bycatch	6 981.2	-13 856.5	0.61	0.92
	NNets	6 980.8	-13 856.2	0.61	-0.46
	s(moon.phase, bs="cc")	6 997.7	-13 882.8	0.61	2.69
	te(long, lat, k=c(6, 6))	7 098.4	-14 045.2	0.63	16.75

Stock	Term	LogLik.	AIC	r^2	d.f.
SCI 3 MW	Intercept	4 819.1	-9 632.3	0.00	0.00
Time-step 2	Year	6 169.0	-12 286.1	0.35	23.00
	Month	6 306.7	-12 551.5	0.39	5.00
	s(vessel, by=NNets, bs="re")	6 351.9	-12 630.2	0.40	5.45
	s(BottomDepth, bs="ts", k=6)	6 364.6	-12 653.3	0.40	0.94
	s(log(FishingDuration), bs="ts", k=6)	6 483.9	-12 884.4	0.42	3.14
	s(time.mid.hr, bs="cc", k=6)	7 212.9	-14 339.2	0.56	1.95
	Bycatch	7 213.0	-14 337.5	0.56	0.73
	NNets	7 213.2	-14 338.0	0.56	-0.15
	s(moon.phase, bs="cc")	7 251.8	-14 400.7	0.56	5.80
	te(long, lat, k=c(6, 6))	7 291.7	-14 457.5	0.57	8.65
SCI 4A east	Intercept	2 602.6	-5 199.2	0.00	0.00
Time-step 1	Year	3 802.3	-7 554.5	0.44	22.00
	Month	3 879.8	-7 699.6	0.46	5.00
	s(vessel, by=NNets, bs="re")	3 932.4	-7 782.1	0.48	10.17
	s(BottomDepth, bs="ts", k=6)	3 950.7	-7 810.8	0.48	2.62
	s(log(FishingDuration), bs="ts", k=6)	3 996.2	-7 891.8	0.49	4.62
	s(time.mid.hr, bs="cc", k=6)	5 315.0	-10 517.7	0.71	6.56
	Bycatch	5 320.8	-10 530.1	0.71	-0.72
	NNets	5 322.8	-10 532.5	0.71	0.89
	s(moon.phase, bs="cc")	5 325.3	-10 533.6	0.71	1.29
	te(long, lat, k=c(6, 6))	5 359.4	-10 577.9	0.71	9.26
SCI 4A east	Intercept	3 028.9	-6 051.8	0.00	0.00
Time-step 2	Year	3 700.5	-7 357.1	0.38	19.00
	Month	4 103.7	-8 153.4	0.50	5.00
	s(vessel, by=NNets, bs="re")	4 274.4	-8 465.9	0.54	13.82
	s(BottomDepth, bs="ts", k=6)	4 274.7	-8 464.7	0.54	0.21
	s(log(FishingDuration), bs="ts", k=6)	4 356.8	-8 622.2	0.56	2.88
	s(time.mid.hr, bs="cc", k=6)	5 253.1	-10 404.8	0.75	5.04
	Bycatch	5 253.7	-10 404.7	0.75	0.59
	NNets	5 267.5	-10 426.0	0.75	2.74
	s(moon.phase, bs="cc")	5 271.5	-10 429.5	0.75	1.55
	te(long, lat, k=c(6, 6))	5 280.4	-10 441.5	0.76	2.03
SCI 4A west	Intercept	716.5	-1 426.9	0.00	0.00
Time-step 1	Year	747.3	-1 482.6	0.13	3.00
	Month	779.0	-1 536.0	0.22	5.00
	s(vessel, by=NNets, bs="re")	779.0	-1 536.0	0.22	0.00
	s(BottomDepth, bs="ts", k=6)	779.3	-1 535.9	0.22	0.21
	s(log(FishingDuration), bs="ts", k=6)	799.9	-1 575.6	0.25	0.82
	s(time.mid.hr, bs="cc", k=6)	838.3	-1 644.0	0.38	3.29
	Bycatch	842.9	-1 650.3	0.39	1.35
	NNets	843.0	-1 650.9	0.39	0.18
	s(moon.phase, bs="cc")	851.5	-1 662.1	0.42	2.10
	te(long, lat, k=c(6, 6))	854.5	-1 663.3	0.43	1.53
SCI 4A west	Intercept	669.1	-1 332.2	0.00	0.00
Time-step 2	Year	683.1	-1 356.3	0.05	2.00
	Month	687.1	-1 354.2	0.07	5.00
	s(vessel, by=NNets, bs="re")	698.5	-1 375.1	0.10	0.94
	s(BottomDepth, bs="ts", k=6)	699.0	-1 375.1	0.10	0.30
	s(log(FishingDuration), bs="ts", k=6)	720.1	-1 410.8	0.15	2.57
	s(time.mid.hr, bs="cc", k=6)	819.8	-1 603.1	0.48	3.19
	Bycatch	819.6	-1 601.6	0.48	0.33
	NNets	820.1	-1 601.5	0.48	0.68
	s(moon.phase, bs="cc")	820.1	-1 601.5	0.48	0.00
	te(long, lat, k=c(6, 6))	823.4	-1 604.2	0.48	1.27

Table 5: CPUE unstandardised (Unstd.) and standardised index (Index), with the CV and upper and lower 95% confidence intervals for the Tweedie model for each stock (SCI 3 MN, MO, and MW, and SCI 4A east and west) and time-step (one and two).

Stock	Time-step	Year	Unstd.	Index	CV	Lower CI	Upper CI	Time-step	Unstd.	Index	CV	Lower CI	Upper CI
SCI 3 MN													
	One	1992	-	-	-	-	-	Two	0.58	0.90	0.04	0.81	0.99
		1993	0.66	0.83	0.03	0.77	0.89		0.76	1.05	0.04	0.95	1.14
		1994	0.92	1.16	0.04	1.06	1.25		1.22	1.50	0.04	1.37	1.63
		1995	1.59	1.86	0.03	1.73	2.00		1.75	1.75	0.05	1.56	1.93
		1996	1.86	2.18	0.03	2.03	2.34		2.09	3.48	0.06	3.02	3.93
		1997	2.19	2.76	0.04	2.53	2.99		2.26	2.80	0.04	2.53	3.08
		1998	1.84	2.21	0.03	2.05	2.37		0.81	1.64	0.08	1.36	1.93
		1999	1.83	2.18	0.03	2.02	2.35		0.64	1.43	0.06	1.23	1.64
		2000	1.45	1.79	0.03	1.65	1.92		1.24	2.05	0.05	1.84	2.26
		2001	1.54	1.89	0.03	1.76	2.03		1.60	2.22	0.06	1.92	2.53
		2002	1.48	1.71	0.03	1.59	1.84		-	-	-	-	-
		2003	0.97	1.21	0.04	1.11	1.30		-	-	-	-	-
		2004	1.51	1.66	0.03	1.53	1.79		-	-	-	-	-
		2005	1.42	1.50	0.03	1.39	1.61		1.23	1.31	0.03	1.22	1.40
		2006	0.84	0.97	0.03	0.90	1.03		0.92	0.90	0.03	0.84	0.96
		2007	0.74	0.76	0.03	0.71	0.81		0.71	0.67	0.03	0.62	0.72
		2008	0.37	0.34	0.03	0.32	0.37		0.50	0.43	0.03	0.40	0.45
		2009	0.40	0.37	0.03	0.34	0.39		0.55	0.44	0.03	0.41	0.47
		2010	0.52	0.52	0.04	0.47	0.57		0.79	0.62	0.03	0.58	0.67
		2011	0.86	0.73	0.02	0.70	0.76		0.81	0.67	0.04	0.60	0.73
		2012	0.78	0.58	0.02	0.55	0.61		0.73	0.55	0.03	0.51	0.58
		2013	0.60	0.51	0.02	0.48	0.53		0.65	0.49	0.03	0.45	0.52
		2014	0.69	0.57	0.02	0.54	0.60		0.72	0.59	0.03	0.55	0.62
		2015	0.81	0.74	0.02	0.70	0.77		0.93	0.75	0.03	0.70	0.79
		2016	0.79	0.69	0.02	0.65	0.72		0.99	0.74	0.03	0.69	0.79
		2017	0.84	0.79	0.02	0.75	0.83		1.41	1.12	0.03	1.04	1.20
		2018	1.41	1.30	0.02	1.24	1.37		1.46	1.22	0.03	1.14	1.30
		2019	1.25	1.07	0.02	1.01	1.12		1.55	1.18	0.03	1.10	1.26
		2020	0.91	0.75	0.03	0.70	0.81		0.95	0.78	0.03	0.73	0.83
		2021	0.78	0.66	0.03	0.62	0.69		0.89	0.68	0.03	0.63	0.72
		2022	1.03	0.87	0.02	0.83	0.92		1.47	0.97	0.03	0.91	1.04
		2023	1.07	0.87	0.03	0.82	0.92		0.93	0.90	0.03	0.84	0.97
		2024	1.10	0.89	0.02	0.85	0.94		1.36	0.97	0.04	0.90	1.05
SCI 3 MO													
	One	1993	0.42	0.43	0.05	0.38	0.47		0.46	0.63	0.09	0.51	0.75
		1994	0.39	0.45	0.03	0.42	0.49		-	-	-	-	-
		1995	0.54	0.57	0.03	0.53	0.61		-	-	-	-	-
		1996	0.86	0.79	0.03	0.74	0.85		-	-	-	-	-
		1997	1.24	1.16	0.03	1.07	1.24		-	-	-	-	-
		1998	1.37	1.43	0.04	1.32	1.55		-	-	-	-	-
		1999	1.38	1.31	0.03	1.22	1.41		-	-	-	-	-
		2000	1.79	1.63	0.03	1.51	1.75		-	-	-	-	-
		2001	1.79	1.84	0.03	1.71	1.97		-	-	-	-	-
		2002	1.59	1.59	0.04	1.46	1.71		-	-	-	-	-
		2003	0.99	1.01	0.04	0.93	1.09		-	-	-	-	-
		2004	1.08	1.08	0.04	0.98	1.18		-	-	-	-	-
		2006	-	-	-	-	-		0.94	0.89	0.17	0.57	1.21
		2021	-	-	-	-	-		1.57	1.37	0.24	0.70	2.03
		2023	-	-	-	-	-		1.47	1.30	0.16	0.87	1.73

Stock	Time-step	Year	Unstd.	Index	CV	Lower CI	Upper CI	Time-step	Unstd.	Index	CV	Lower CI	Upper CI
SCI 3 MW													
	One	1992	-	-	-	-	-	Two	0.54	0.61	0.09	0.49	0.73
		1993	-	-	-	-	-		0.30	0.43	0.13	0.30	0.55
		1994	0.58	0.72	0.12	0.53	0.91		-	-	-	-	-
		1997	-	-	-	-	-		1.99	2.60	0.06	2.26	2.95
		1998	1.74	1.95	0.06	1.68	2.22		-	-	-	-	-
		1999	-	-	-	-	-		1.73	2.18	0.09	1.72	2.63
		2000	2.03	2.58	0.08	2.12	3.05		2.65	3.37	0.08	2.73	4.02
		2001	1.86	2.45	0.05	2.20	2.71		-	-	-	-	-
		2002	1.70	2.03	0.06	1.78	2.28		-	-	-	-	-
		2003	1.13	1.42	0.05	1.27	1.57		-	-	-	-	-
		2005	1.62	1.71	0.05	1.52	1.90		1.45	1.61	0.03	1.49	1.72
		2006	1.03	1.04	0.03	0.97	1.12		1.34	1.29	0.02	1.22	1.36
		2007	0.93	0.88	0.03	0.82	0.94		0.85	0.82	0.02	0.77	0.86
		2008	0.54	0.55	0.03	0.51	0.58		0.48	0.48	0.03	0.45	0.51
		2009	0.49	0.48	0.03	0.45	0.51		0.66	0.69	0.05	0.61	0.76
		2010	0.73	0.72	0.03	0.67	0.76		0.98	0.91	0.03	0.84	0.97
		2011	0.97	0.87	0.03	0.82	0.92		0.80	0.69	0.03	0.64	0.74
		2012	0.64	0.62	0.04	0.57	0.68		0.55	0.53	0.04	0.48	0.59
		2013	0.54	0.52	0.03	0.49	0.55		0.54	0.51	0.05	0.45	0.57
		2014	0.59	0.62	0.04	0.56	0.68		0.50	0.51	0.08	0.41	0.60
		2015	0.80	0.71	0.03	0.66	0.76		0.96	0.88	0.05	0.79	0.98
		2016	0.75	0.69	0.03	0.64	0.74		-	-	-	-	-
		2017	0.63	0.62	0.11	0.47	0.77		1.31	1.15	0.05	1.01	1.28
		2018	1.33	1.28	0.04	1.16	1.40		1.49	1.52	0.04	1.39	1.66
		2019	1.53	1.38	0.04	1.27	1.50		1.56	1.52	0.03	1.41	1.63
		2020	1.23	1.02	0.04	0.94	1.11		1.02	0.98	0.03	0.92	1.03
		2021	0.91	0.80	0.03	0.74	0.85		0.91	0.78	0.02	0.74	0.82
		2022	1.01	0.90	0.03	0.84	0.96		1.62	1.33	0.03	1.24	1.41
		2023	1.51	1.30	0.03	1.21	1.38		1.56	1.32	0.03	1.24	1.39
		2024	1.76	1.48	0.03	1.37	1.59		1.65	1.32	0.03	1.24	1.41
SCI 4A east													
	One	1991	-	-	-	-	-	Two	0.52	1.16	0.12	0.87	1.45
		1992	0.59	0.61	0.05	0.54	0.67		0.59	0.89	0.08	0.73	1.04
		1993	-	-	-	-	-		1.01	1.66	0.10	1.31	2.00
		1999	1.91	1.62	0.06	1.42	1.83		-	-	-	-	-
		2000	1.38	1.29	0.05	1.14	1.45		-	-	-	-	-
		2002	2.82	2.47	0.05	2.18	2.77		-	-	-	-	-
		2003	2.04	1.83	0.04	1.65	2.00		-	-	-	-	-
		2004	1.32	1.15	0.05	1.03	1.27		-	-	-	-	-
		2005	1.08	1.05	0.05	0.94	1.16		1.01	1.63	0.06	1.41	1.85
		2006	0.49	0.49	0.04	0.44	0.54		0.42	0.28	0.12	0.21	0.35
		2007	0.43	0.44	0.04	0.41	0.48		0.38	0.51	0.09	0.41	0.60
		2008	0.35	0.37	0.09	0.30	0.44		1.11	0.97	0.03	0.90	1.04
		2013	0.81	0.80	0.05	0.71	0.89		0.85	0.68	0.03	0.63	0.73
		2014	0.90	0.92	0.04	0.83	1.01		0.99	0.74	0.03	0.69	0.79
		2015	1.03	1.10	0.04	1.00	1.21		1.02	0.88	0.03	0.82	0.93
		2016	0.94	1.01	0.04	0.92	1.11		1.66	1.28	0.03	1.21	1.36
		2017	0.96	1.06	0.04	0.96	1.16		0.91	1.07	0.03	1.00	1.14
		2018	1.26	1.31	0.04	1.18	1.43		1.22	0.94	0.03	0.88	0.99
		2019	1.81	1.71	0.05	1.54	1.88		1.81	1.42	0.03	1.31	1.53
		2020	1.81	1.71	0.05	1.54	1.88		2.57	2.37	0.03	2.22	2.51
		2021	1.38	1.41	0.04	1.27	1.54		2.20	1.55	0.03	1.45	1.64
		2022	1.01	1.08	0.04	0.98	1.18		1.42	1.45	0.04	1.32	1.58
		2023	0.88	0.90	0.04	0.81	0.98		1.06	1.00	0.03	0.94	1.06
		2024	0.64	0.70	0.04	0.64	0.77		0.78	0.79	0.04	0.72	0.85
		2025	0.48	0.56	0.05	0.50	0.62		0.96	0.78	0.03	0.74	0.83

Stock	Time-step	Year	Unstd.	Index	CV	Lower CI	Upper CI	Time-step	Unstd.	Index	CV	Lower CI	Upper CI
SCI 4A west													
	One	2005	-	-	-	-	-	Two	1.02	0.96	0.05	0.87	1.06
		2006	0.87	0.98	0.06	0.86	1.11		1.12	1.27	0.07	1.11	1.44
		2007	1.15	1.10	0.05	0.98	1.23		0.88	0.82	0.05	0.74	0.89
		2008	0.61	0.49	0.10	0.38	0.60		-	-	-	-	-
		2025	1.64	1.86	0.17	1.17	2.55		-	-	-	-	-

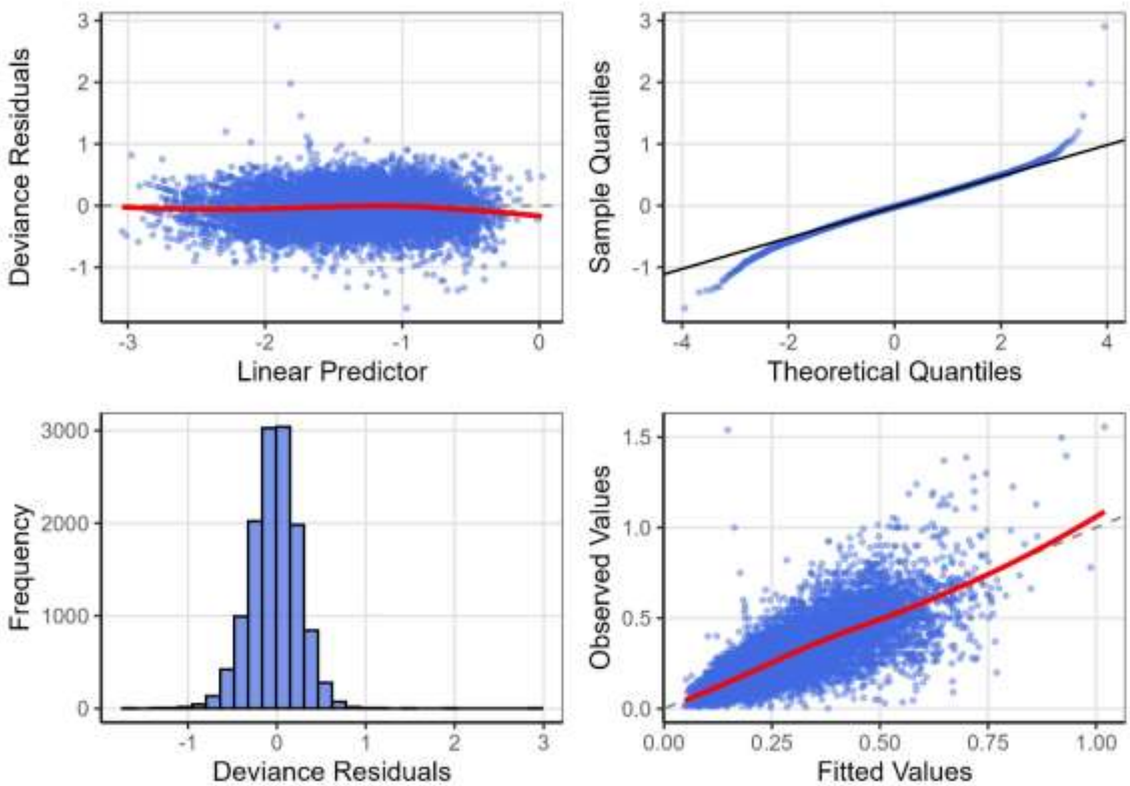

Figure 13: Residual plots for the CPUE (abundance) of scampi for SCI 3 (MN) in time-step one, showing deviance residuals (top left), quantile-quantile plot (top right), residual histogram (bottom left), and the observed versus expected (bottom right). Red lines show loess fits to the deviance residuals and the observed versus expected.

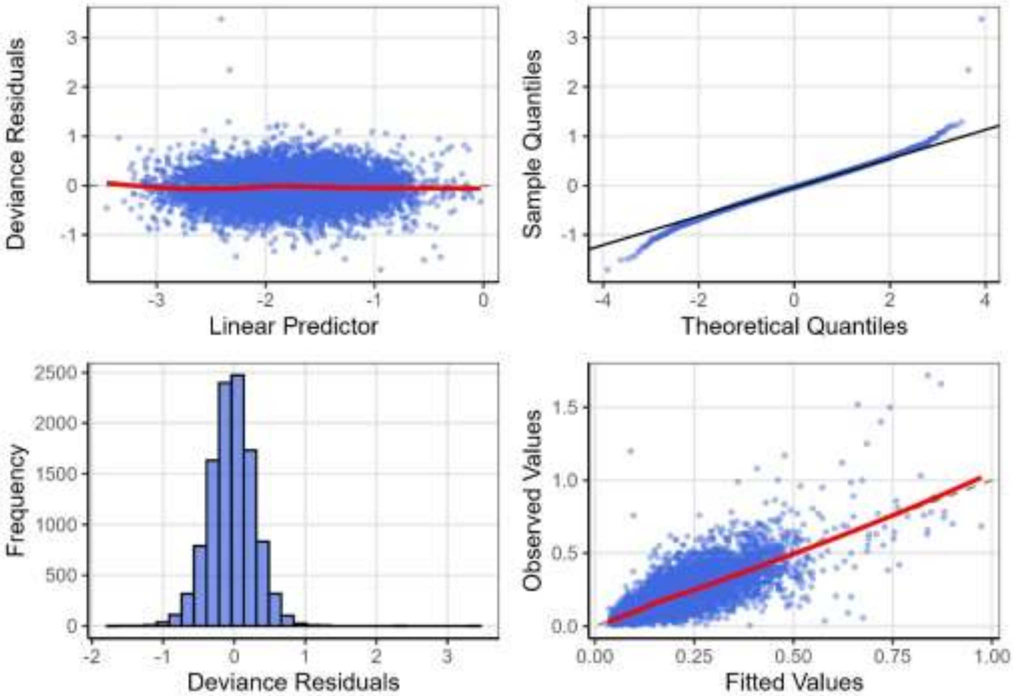

Figure 14: Residual plots for the CPUE (abundance) of scampi for SCI 3 (MN) in time-step two, showing deviance residuals (top left), quantile-quantile plot (top right), residual histogram (bottom left), and the observed versus expected (bottom right). Red lines show loess fits to the deviance residuals and the observed versus expected.

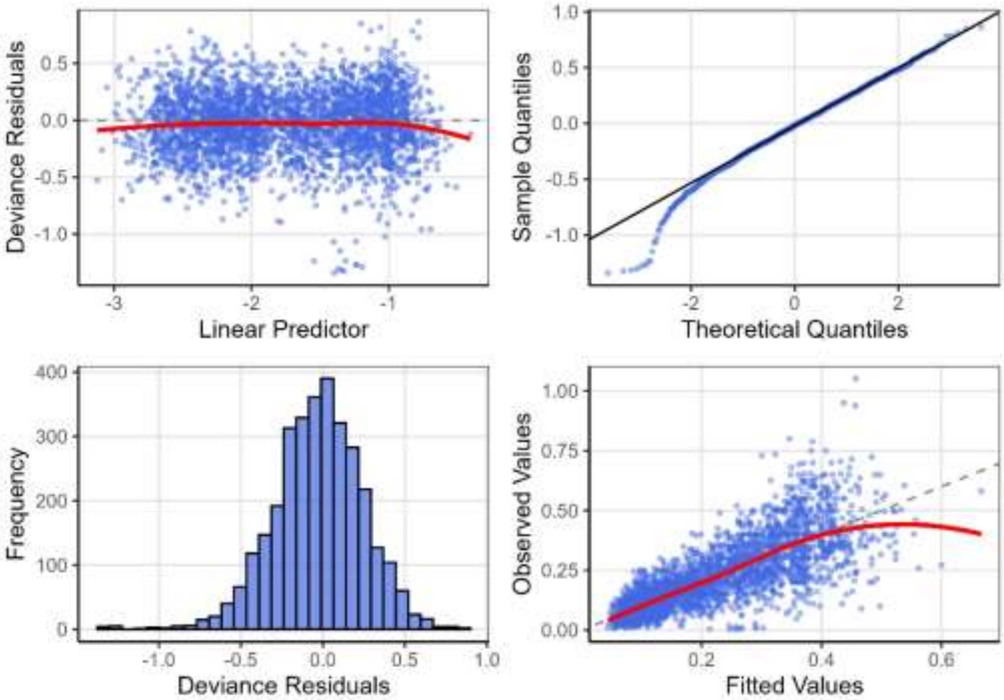

Figure 15: Residual plots for the CPUE (abundance) of scampi for SCI 3 (MO) in time-step one, showing deviance residuals (top left), quantile-quantile plot (top right), residual histogram (bottom left), and the observed versus expected (bottom right). Red lines show loess fits to the deviance residuals and the observed versus expected.

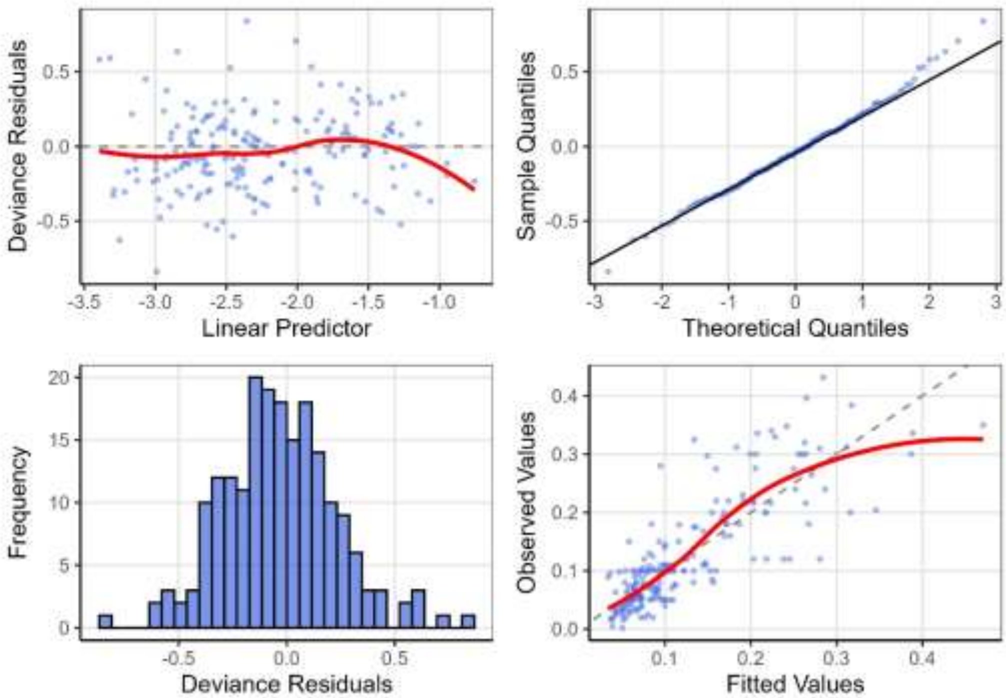

Figure 16: Residual plots for the CPUE (abundance) of scampi for SCI 3 (MO) in time-step two, showing deviance residuals (top left), quantile-quantile plot (top right), residual histogram (bottom left), and the observed versus expected (bottom right). Red lines show loess fits.

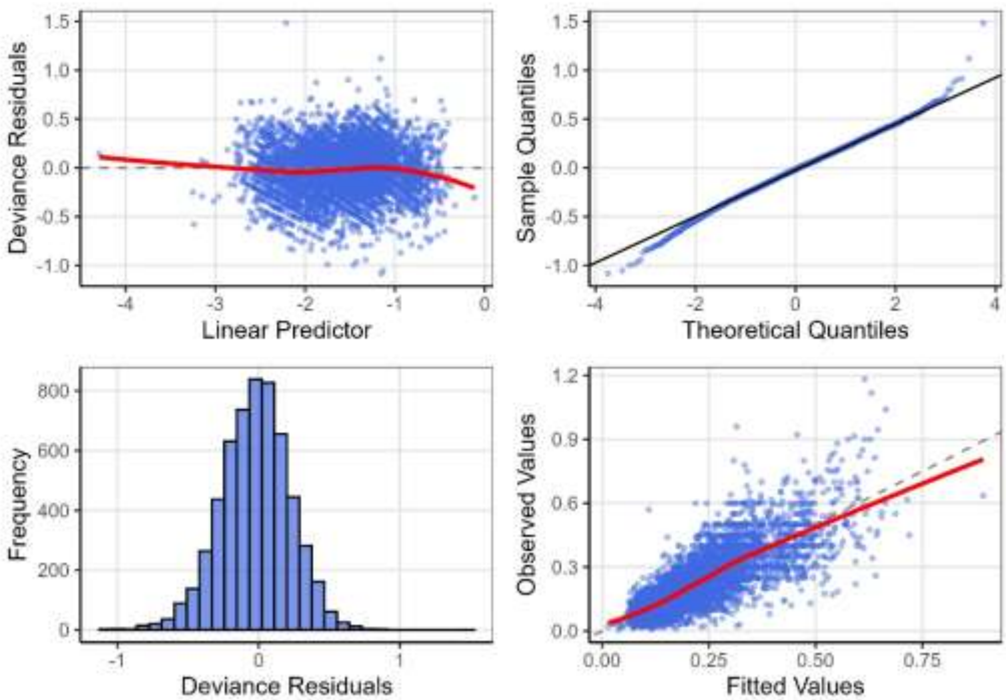

Figure 17: Residual plots for the CPUE (abundance) of scampi for SCI 3 (MW) in time-step one, showing deviance residuals (top left), quantile-quantile plot (top right), residual histogram (bottom left), and the observed versus expected (bottom right). Red lines show loess fits to the deviance residuals and the observed versus expected.

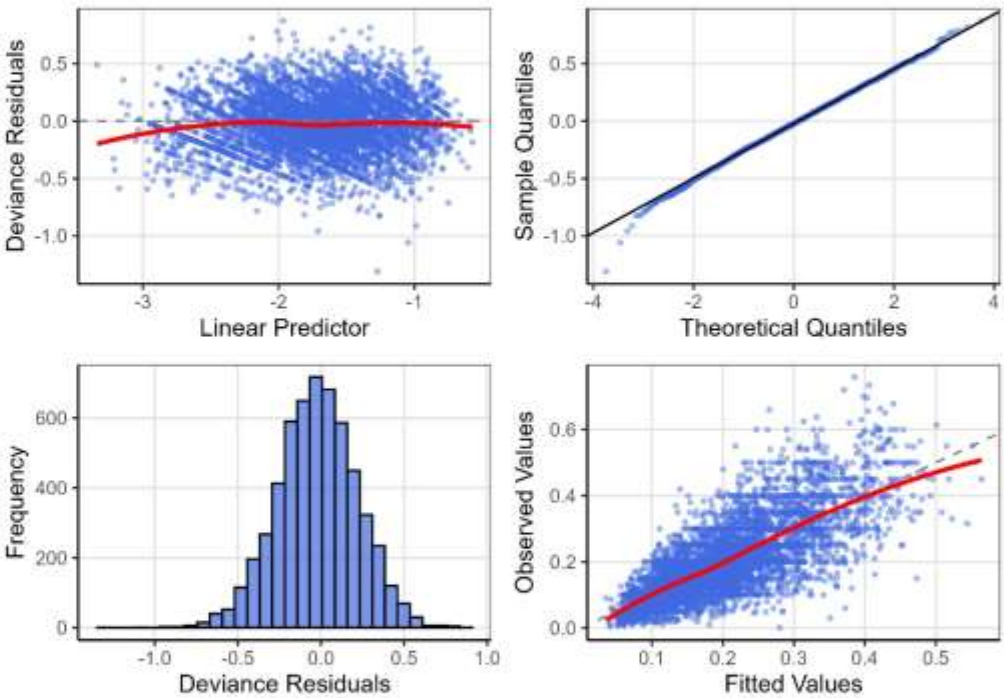

Figure 18: Residual plots for the CPUE (abundance) of scampi for SCI 3 (MW) in time-step two, showing deviance residuals (top left), quantile-quantile plot (top right), residual histogram (bottom left), and the observed versus expected (bottom right). Red lines show loess fits to the deviance residuals and the observed versus expected.

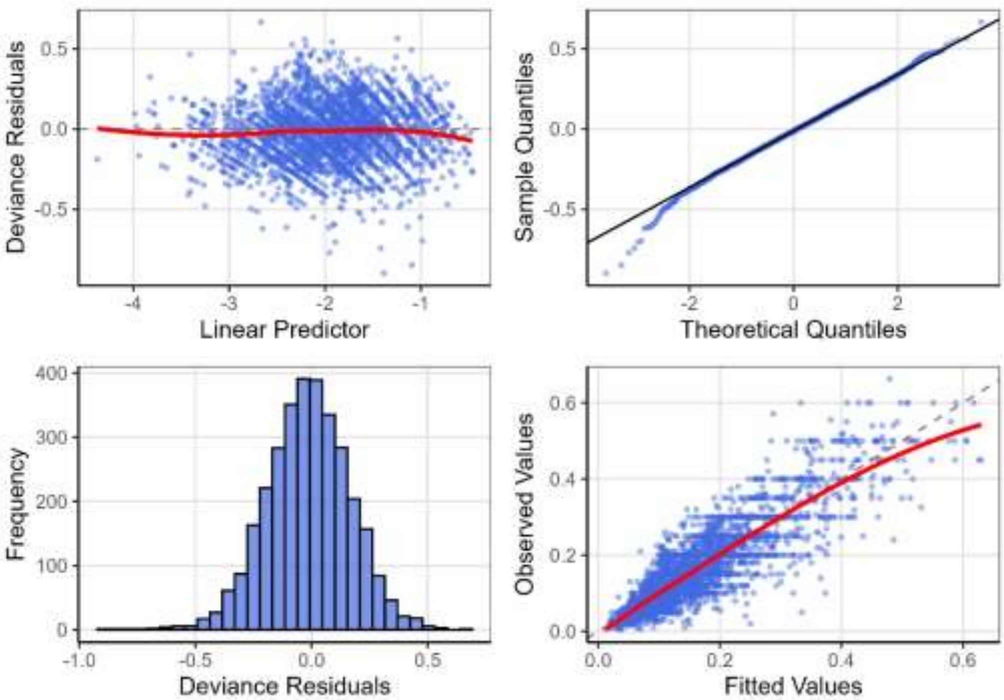

Figure 19: Residual plots for the CPUE (abundance) of scampi for SCI 4A (east) in time-step one, showing deviance residuals (top left), quantile-quantile plot (top right), residual histogram (bottom left), and the observed versus expected (bottom right). Red lines show loess fits.

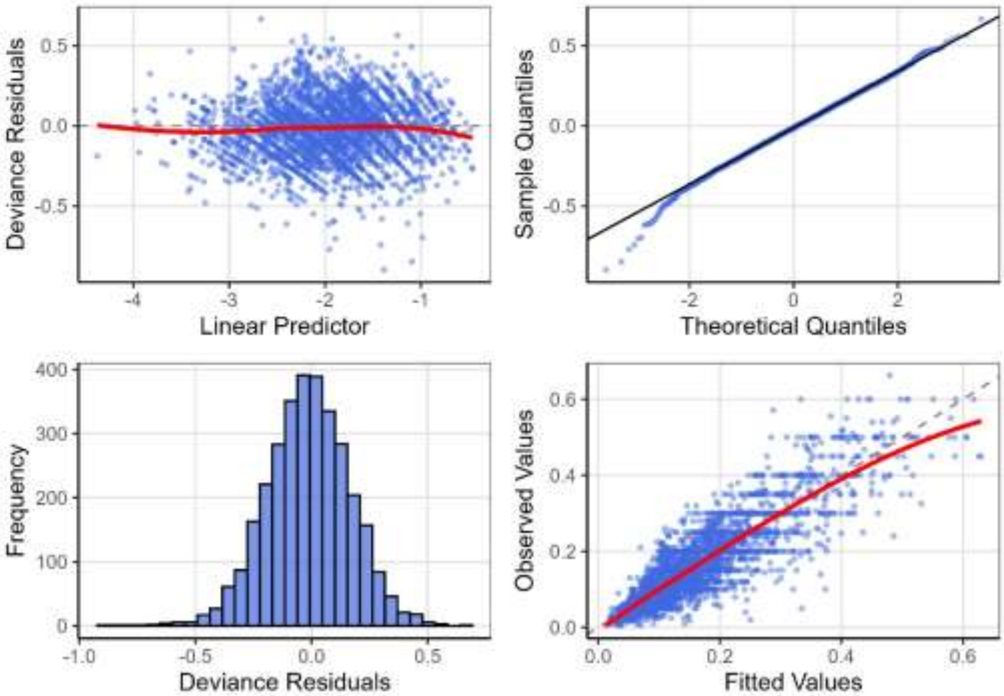

Figure 20: Residual plots for the CPUE (abundance) of scampi for SCI 4A (east) in time-step two, showing deviance residuals (top left), quantile-quantile plot (top right), residual histogram (bottom left), and the observed versus expected (bottom right). Red lines show loess fits to the deviance residuals and the observed versus expected.

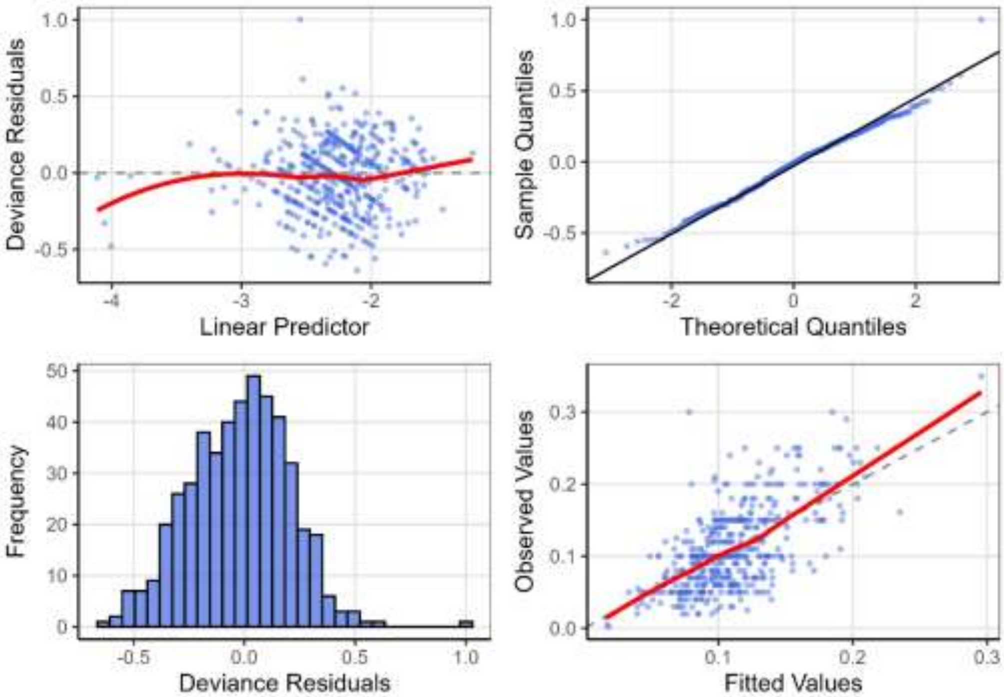

Figure 21: Residual plots for the CPUE (abundance) of scampi for SCI 4A (west) in time-step one, showing deviance residuals (top left), quantile-quantile plot (top right), residual histogram (bottom left), and the observed versus expected (bottom right). Red lines show loess fits to the deviance residuals and the observed versus expected.

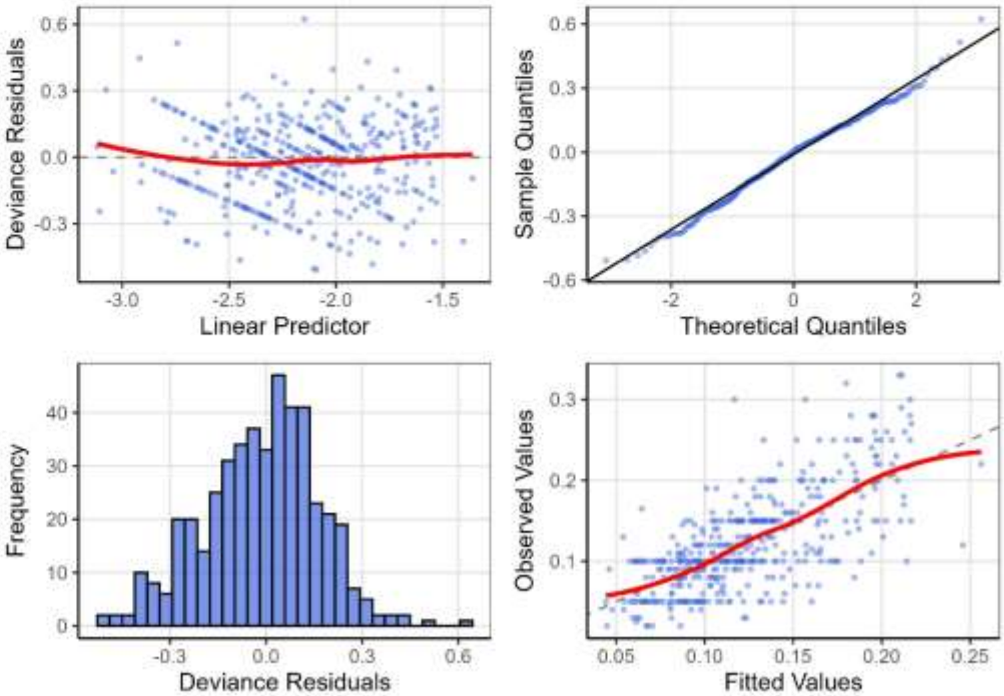

Figure 22: Residual plots for the CPUE (abundance) of scampi for SCI 4A (west) in time-step two, showing deviance residuals (top left), quantile-quantile plot (top right), residual histogram (bottom left), and the observed versus expected (bottom right). Red lines show loess fits to the deviance residuals and the observed versus expected.

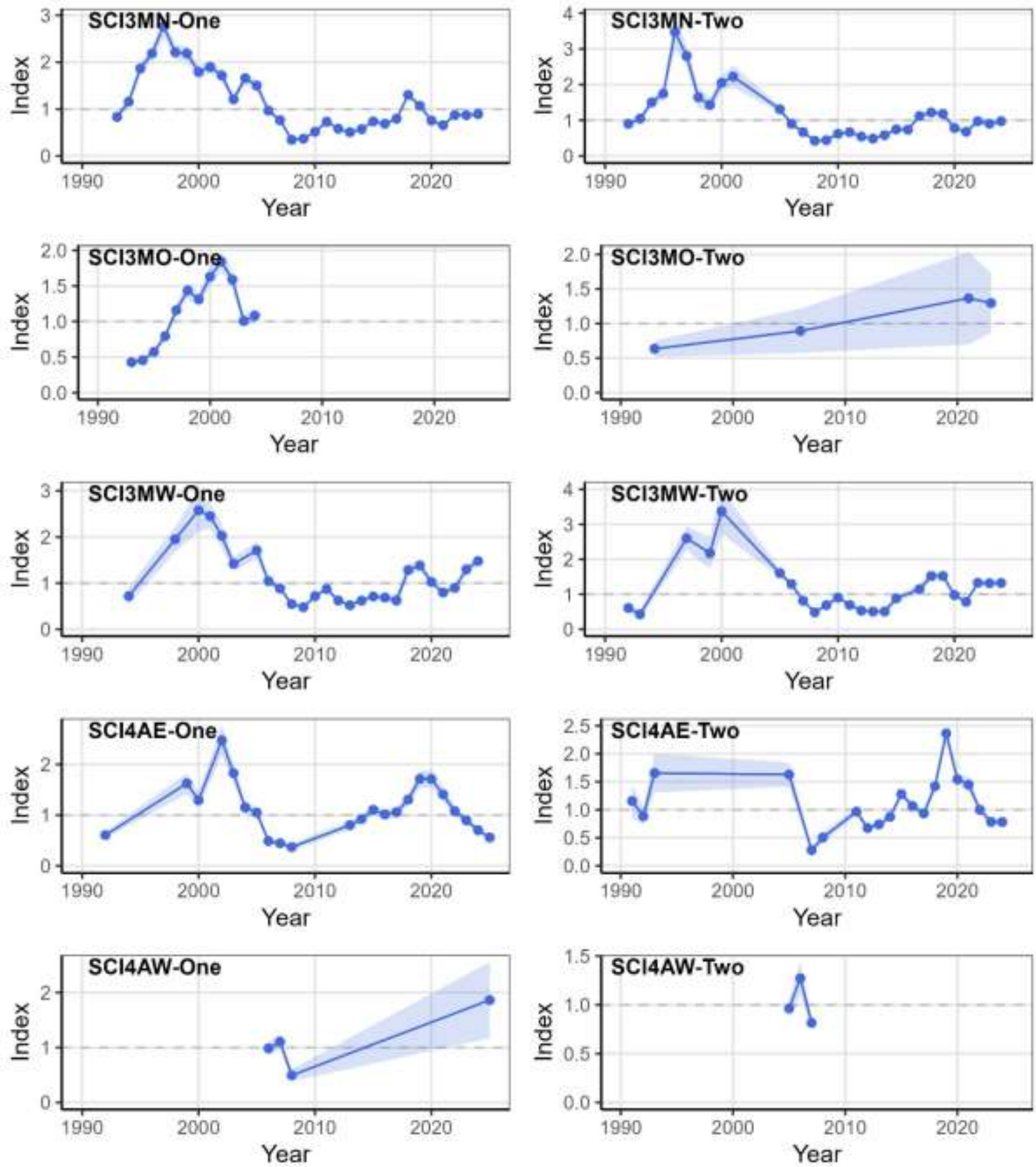

Figure 23: Tweedie CPUE indices for SCI 3 MN, MO, and MW and SCI 4A east and west for time-steps one and two, for the scampi target tow-by-tow analysis by model year, from 1990 to 2024.

2.5 Resource surveys

The Chatham Rise resource surveys have conducted both trawl (Table 6) and photographic surveys (Table 7) (Wieczorek et al. 2024). The photographic surveys provide two main abundance indices, the abundance of major burrow openings and the abundance of visible scampi. It is recognised that the interpretation of the photographic indices by readers of the images may change over time, potentially due to differences in visibility, reader experience, or other factors. The indices were calibrated for reader effects using a Poisson GLM (M. Underwood, Earth Sciences NZ, pers. comm.), with the method described by McGregor et al. (2024).

The patterns of the biomass from the CPUE and trawl indices, and the abundance from the uncalibrated photo surveys were broadly similar across all of the SCI 3 stocks (Figure 24), although the trend in the CPUE index was flatter in the most recent few years than either of the trawl survey and the uncalibrated photo indices. However, estimates from the calibrated analysis of readers were more similar, and suggested a slightly flatter trend since 2019 (Figure 25).

The abundance of major burrow openings has been used as the main resource survey abundance index in recent stock assessments for SCI 3 (Tuck 2019, McGregor et al. 2022) with the visible scampi index used in sensitivity runs by Tuck (2019). In 2024, the survey was extended to SCI 4A for areas SCI4AE and SCI4AW for the first time (Wieczorek et al. 2024).

Length composition observations for the survey series were available for each of the surveys (Figure 26) and were included as sexed length compositions. Commercial length compositions were available for most years (Figure 26) and were also included as sexed length composition proportions. Length compositions were fitted using multinomial likelihoods.

Lognormal errors, with known CVs, were assumed for the resource survey biomass observations. The CVs for those observations allow for sampling error only. Additional variance (termed process error), assumed to arise from differences between model simplifications and real-world variation, was added to the sampling variance. Here, a constant process error was estimated at MPD and was fixed at MCMC.

The effective sample sizes (*N*) for the length composition observations were generated using a two-step process. First, the sample sizes were derived by assuming the relationship between the observed proportions, E_i, and estimated CVs, c_i, followed that for a multinomial with unknown sample size N_j. The estimated sample sizes were then derived using robust non-linear least squares fits of $\log(c_i) \sim \log(P_i)$ (labelled the initial sample size). Second, estimates of the effective sample size, $N_j{}'$, were made for the multinomial, from iterative model fitting using method TA1.8 in appendix A of Francis (2011). A summary of the observations with initial and effective sample sizes and their likelihoods for the base case model is given as Figure 27.

Table 6: SCI 3 trawl survey biomass indices (tonnes) and CVs for SCI 3 areas MO, MN, and MW; and SCI 4A areas 4AE and 4AW.

Year	SCI 3 MO		SCI 3 MN		SCI 3 MW		SCI 4AE		SCI 4AW	
	Index (t)	CV	Index (t)	CV	Index (t)	CV	Index (t)	CV	Index (t)	CV
2002	254.3	0.24	–	–	–	–	–	–	–	–
2010	40.2	0.37	82.3	0.25	295.0	0.36	–	–	–	–
2011	49.0	0.11	199.1	0.07	347.0	0.06	–	–	–	–
2014	126.5	0.27	246.6	0.06	177.0	0.30	–	–	–	–
2017	139.6	0.14	454.7	0.20	318.8	0.19	–	–	–	–
2020	158.3	0.19	505.7	0.06	572.7	0.12	–	–	–	–
2024	196.3	0.15	508.2	0.08	597.5	0.09	92.70	0.59	121.7	0.19

Table 7: SCI 3 scampi burrow photo survey abundance index (numbers) and CVs for SCI 3 areas MO, MN, and MW.

Year	SCI 3 MO		SCI 3 MN		SCI 3 MW	
	Index (n)	CV	Index (n)	CV	Index (n)	CV
2002	242 783 173	0.12	–	–	–	–
2010	68 617 984	0.15	138 890 270	0.07	153 078 504	0.13
2011	77 344 717	0.11	200 893 579	0.05	139 080 948	0.12
2014	170 790 096	0.10	375 344 283	0.09	173 975 776	0.10
2017	181 168 433	0.11	445 359 711	0.07	259 439 693	0.16
2020	178 497 927	0.15	436 930 735	0.13	252 385 202	0.12
2024	190 396 607	0.12	356 759 549	0.10	305 760 260	0.10

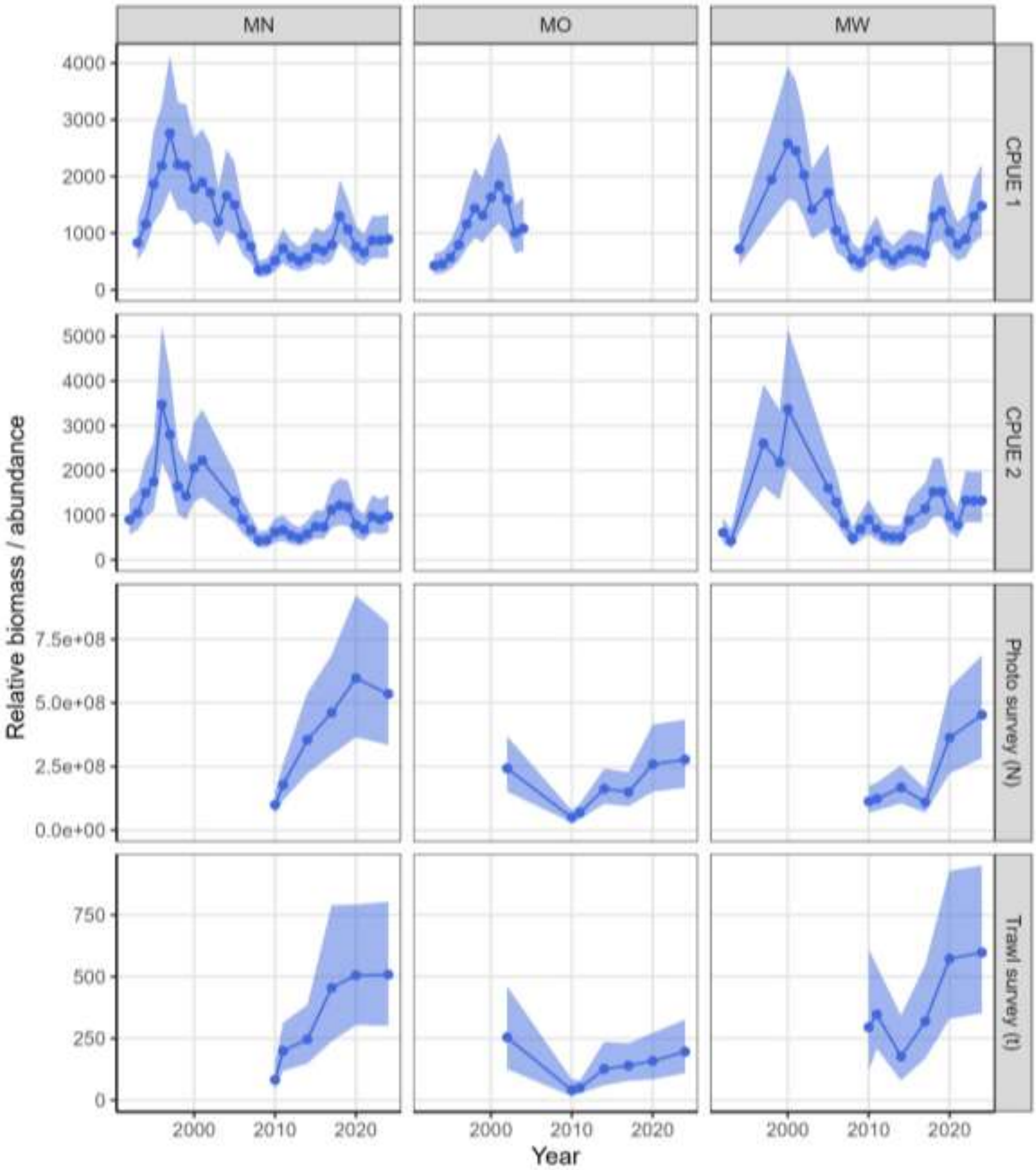

Figure 24: Biomass and uncalibrated abundance indices for the SCI 3 scampi resource surveys for areas SCI 3 MN, MO, and MW for standardised CPUE (relative scale with mean = 1000), the trawl survey (t) and uncalibrated photographic surveys (emerged, visible, and major burrows, in numbers) 1990–2024.

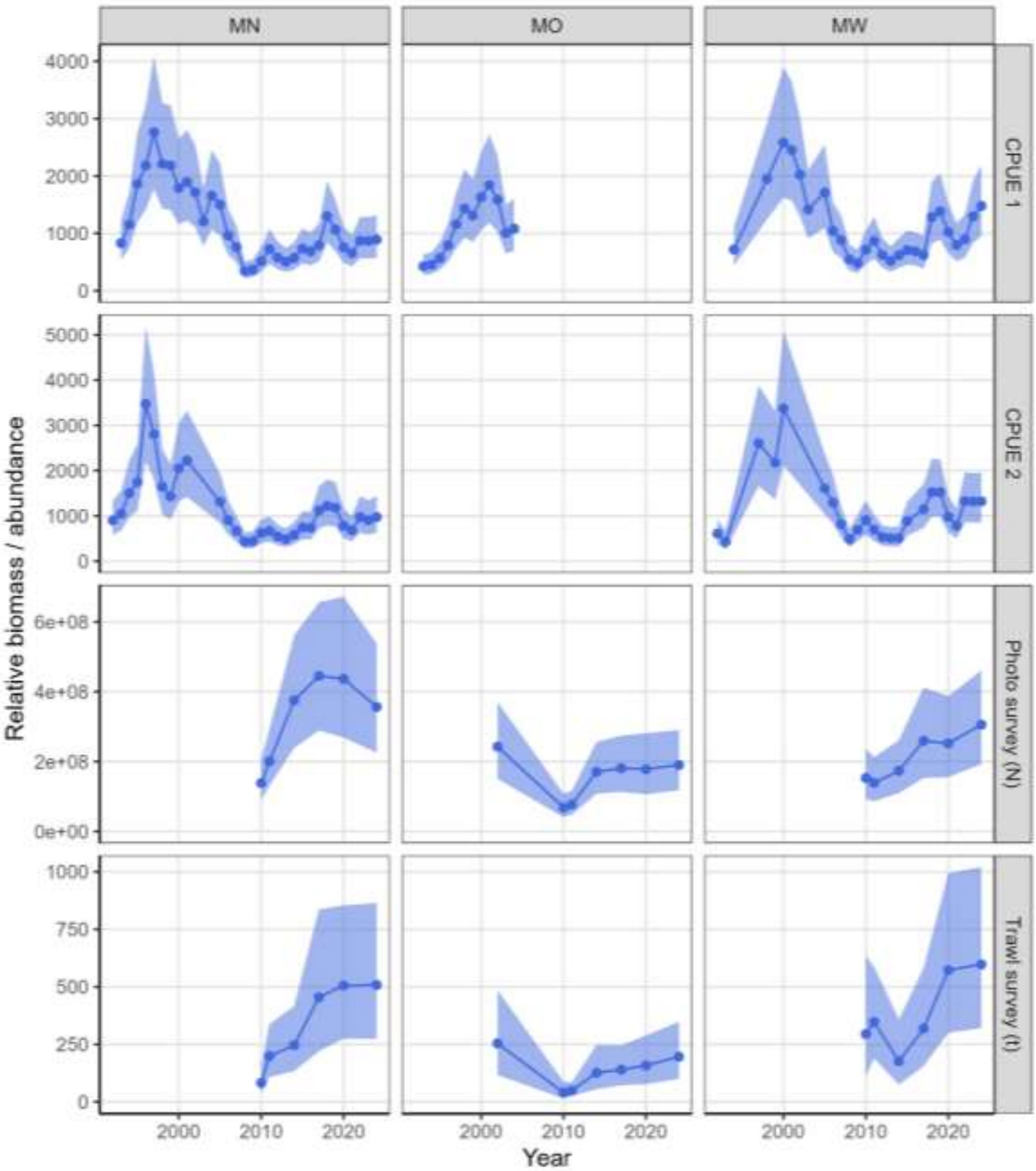

Figure 25: Biomass and calibrated abundance indices for the SCI 3 scampi resource surveys for areas SCI 3 MN, MO, and MW for standardised CPUE (relative scale with mean = 1000), the trawl survey (t) and photographic surveys (emerged, visible, and major burrows, in numbers) 1990–2024.

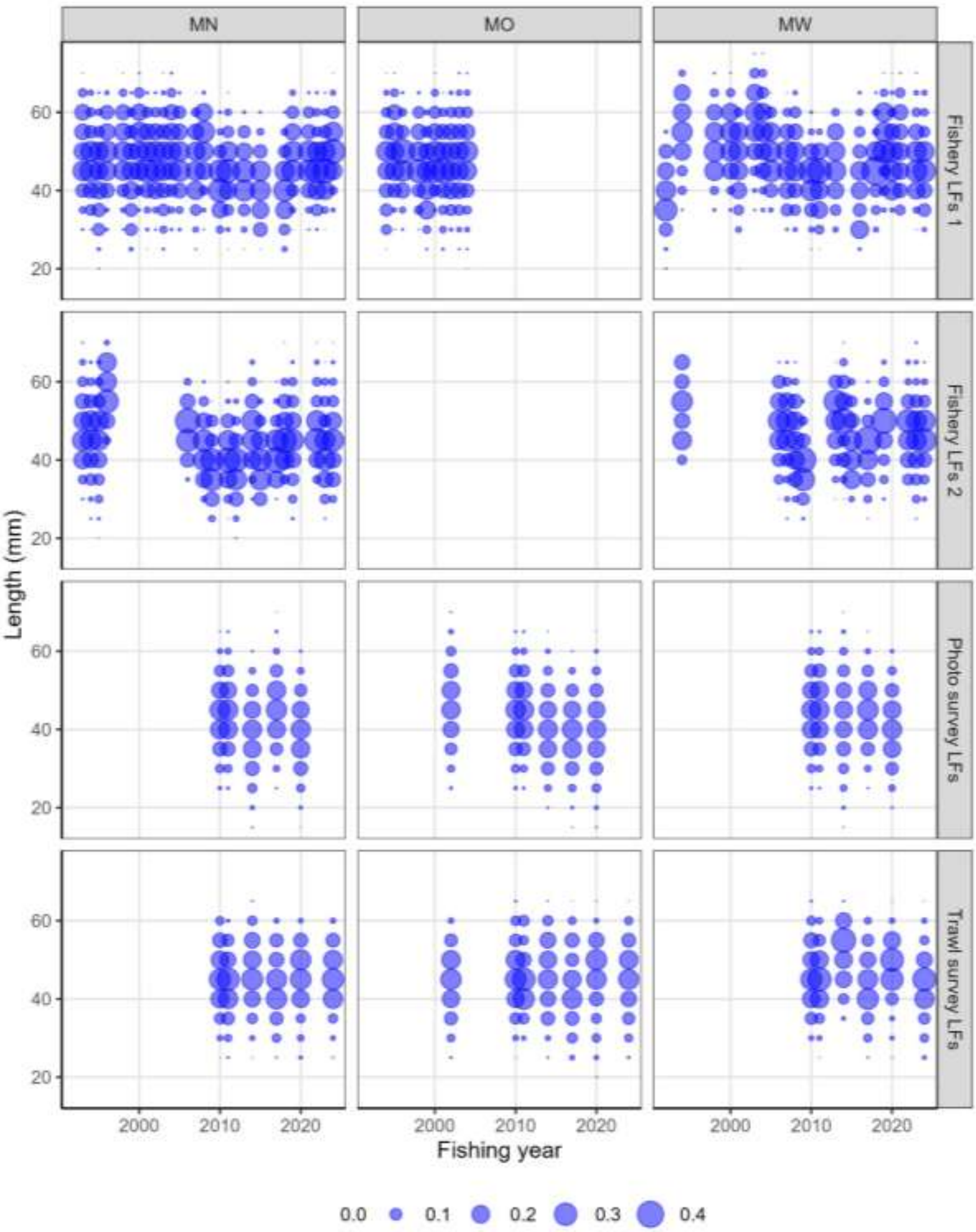

Figure 26: Relative observed length compositions (LFs) for the SCI 3 MN, MO, and MW stocks for the commercial fishery in time-steps one and two, and the photo and trawl surveys, 1990–2024.

2.6 Integrated length-based model structure

Stock assessments for scampi in SCI 3 have been carried out using an integrated length-based stock assessment implemented in CASAL (Bull et al. 2012). This report updates the assessment using Casal2 (Casal2 Steering Group 2026), with post-processing in R (R Core Team 2022) using the Rlibraries *Casal2* (Casal2 Steering Group 2026) and *r4Casal2* (Marsh & Dunn 2024). Validations of the conversion from CASAL to Casal2 are given below.

The model was structured as a sex (male and female) and length-structured model for three spatially distinct sub-stocks (MN, MW and MO), with length classes from 1 to 75 mm tracked separately for each stock, whereby the number of male and female scampi in each 1 mm length class was tracked through time, and the last length class was a plus group (i.e., an aggregate of all scampi 76 mm and longer).

The population in each stock was initialised assuming an unfished equilibrium length structure, obtained iteratively over 200 years until convergence, at an initial (unfished) biomass (B_0) specific to that stock. The initial biomass for each stock was estimated independently by the model.

The model was run from the 1985 to 2026 fishing years, with projections to 2031, and the annual cycle was broken into two discrete time steps: time step one (July–December) and time step two (January–June). Unlike an age-structured model, there was no discrete ageing or age-incrementation step; growth instead occurred as a continuous, length-based growth-increment process applied within time step one. The annual cycle assumed in the model is described in Table 8.

In time step one, growth was applied to all length classes for both sexes, moving individuals between length classes according to the estimated growth-increment relationship, before mortality was applied. Biomass calculations at any point in the model were made by multiplying the numbers of scampi in each length class by the length-weight relationship for each sex separately.

Recruitment was assumed to occur at the beginning of time step two (January–June), to be 50:50 male to female, and to follow a Beverton–Holt stock-recruitment relationship specific to each stock, with steepness (h) fixed at 0.75. New recruits were assumed to enter the population at a mean length of 10 mm with a coefficient of variation of 0.40. Annual year class strengths (recruitment multipliers) were estimated independently for each stock for the 1984–2022 period using a simplex transformation and were assumed constant (equal to 1) outside this period. Future (projected) recruitment was assumed to be resampled from the distribution of the estimated 2013–2022 year class strengths for each stock.

The catch history for the fishery was applied separately by stock and time step (six methods in total: MN, MW and MO, each split into a July–December and a January–June component), reflecting the seasonal pattern of reported landings in each area. Total mortality for each method was applied by removing half of the natural mortality for the time step, then mortality from the fishery, and then the remaining half of the natural mortality for the time step. Natural mortality (M=0.25 y^{-1}) was assumed constant across length, sex and stock, and was not estimated.

The fishing selectivity parameters were assumed logistic by sex and were estimated in the model through the fitting of the fishery length-composition data, with separate ogives estimated for time step one and time step two. The a_{50} and a_{to95} parameters were shared across the three stocks within each time step (i.e., one fishery selectivity ogive per sex per time step, common to MN, MW and MO), while the α (steepness) parameter was estimated for males and shared across stocks, with the female α fixed at 1. Maturity was specified as a time-invariant logistic relationship between length and the proportion of scampi mature, shared between males and females, estimated in the model by fitting to maturity-at-length data, and used to calculate spawning-stock biomass at the middle of time step two (January–June).

The primary sources of abundance information were a research trawl survey and a research photographic (camera) survey, each conducted within time step one (July–December) for each of the three stocks, providing relative biomass (trawl survey) and relative abundance (photographic survey) indices respectively, together with associated trawl-survey length-frequency data. Commercial catch-per-unit-effort (CPUE) series, standardised by stock and time step, provided an additional relative abundance index for most stock/time-step combinations. Survey selectivities were assumed logistic by sex and were estimated by the model by fitting the trawl-survey length-composition data; the photographic-survey selectivity alpha parameter was fixed at 1.

Model parameters were estimated by minimising the total objective function, which was the sum of the negative log-likelihoods from the data (fishery and survey length compositions, CPUE indices, survey biomass/abundance indices, and maturity-at-length data), the negative log-priors, Jacobians from any transformations where the prior was applied in natural space, and the penalty functions used to apply model constraints. A penalty (*CatchMustBeTaken*) would have been applied to catch data if the biomass from the model was too small to allow the catch to be taken, but this did not enter the model in any of the scenarios modelled.

Initial fits were evaluated at the mode of the posterior distribution (MPD). MPD model fits were evaluated by investigating jitter start values to confirm the MPD had been achieved, evaluating MPD fits and residual patterns, and by qualitative assessment of the MPD profile distributions (i.e., by evaluating the minimum objective function while fixing one parameter, such as a stock's initial biomass, and allowing all other parameters to vary). Residual patterns in the length compositions were investigated using standardised multinomial residual diagnostics appropriate to length-frequency data.

The initial biomass (B_0) for each of the three stocks was estimated in the model (via a log transformation), as were the annual year class strengths, the growth parameters, and the selectivity ogives. Trawl- and photographic-survey selectivity ogives, and fishery selectivity ogives, were each fitted as logistic curves. Selectivities were assumed to be constant for all years within each stock, time step, fishery and survey. The parameters estimated, prior distributions, prior parameters, and bounds are summarised in Table 9.

Most priors were intended to be relatively non-informative and were specified with wide bounds. A Student's-t distribution with 3 degrees of freedom, with a wide standard deviation, was used for most non-informative parameters (selectivities and maturity). Uniform priors with wide bounds were used for the initial biomass (in log space), the growth-increment parameters, and the commercial CPUE catchabilities. The exceptions were the informative lognormal priors specified for the trawl- and photographic-survey catchabilities (q), which differed between the two survey types to reflect their different observation processes (biomass versus abundance).

Bayesian inference was used to obtain samples from the posterior distribution of model parameters using a random-walk Metropolis–Hastings algorithm (Gelman et al. 1995, Gilks et al. 1998). The MCMC chain was initialised at the MPD and run for a total of 3×10^6 iterations, with a burn-in length of 1×10^6 iterations, and every 2000th sample taken from the subsequent 2×10^6 iterations (i.e., a final sample of length 1000 was taken after the burn-in to sample from the posterior distribution). The step size of the random-walk proposal (a multivariate Student's-t distribution with 4 degrees of freedom) was adapted during the burn-in period (500 000 iterations), subject to a maximum allowed correlation of 0.8 between parameters.

Chains were investigated for evidence of non-convergence with qualitative investigation of MCMC traces and multiple-chain comparisons (i.e., three chains of 1000 samples each), and $\hat{r}$ statistics and the effective sample size estimates (Gelman et al. 2015, Vehtari et al. 2017). Based on the recommendations of Monnahan (2024), $\hat{r}$ values less than 1.05 are considered evidence of acceptable convergence and effective sample sizes above 400 are considered adequate.

Table 8: Annual cycle of the scampi (SCI) stock assessment model, giving the time steps and the order of biological processes (growth, recruitment, natural and fishing mortality, spawning), and the observations (resource surveys, CPUE indices, and associated length frequencies) made within each time step.

Time step	Period	Biological processes (in order)	Catch taken (methods)	Resource surveys / CPUE	Length frequencies
1	Jul–Dec	Growth (both sexes); natural mortality (0.5×M); fishing mortality; natural mortality (0.5×M)	TrawlMN1, TrawlMW1, TrawlMO1	Trawl survey (biomass) and photographic survey (abundance), MN/MW/MO (2002–2024); CPUE-MN1, MW1, MO1	Fishery LFs (TrawlMN1/MW1/MO1); trawl-survey LFs, MN/MW/MO
2	Jan–Jun	Recruitment (start of step, 50:50 M:F); natural mortality (0.5×M); fishing mortality; natural mortality (0.5×M); SSB calculated mid-step	TrawlMN2, TrawlMW2, TrawlMO2	CPUE-MN2, MW2	Fishery LFs (TrawlMN2/MW2)

Table 9: The assumed priors for key parameters (when estimated) for the scampi (SCI) stock assessment. The parameters (and the transformation used) are mean (mu), and either σ (scale parameter for the Student's-t) or CV (for the lognormal). Parameters without an informative mu/sigma/CV were given uniform priors over the bounds.

Parameter (transformation)	Distribution	Mu	Sigma/ CV	Lower bound	Upper bound
B_0 (log), MN/MW/MO	Uniform (log)	–	–	6	11
Year class strengths (simplex), per sub-stock	Lognormal (μ, CV)	1.0	1.1	–	–
Trawl survey q, MN/MW/MO	Lognormal (μ, CV)	0.0665	0.706	1×10^{-8}	10
Photographic survey q, MN/MW/MO	Lognormal (μ, CV)	4.38	0.30	1×10^{-8}	10
CPUE q (each area × time step)	Uniform	–	–	1×10^{-8}	10
Fishery selectivity a50 (M & F, time steps 1 & 2)	Student's-t (μ, σ)	35	20	15	40
Fishery selectivity ato95 (M & F, time steps 1 & 2)	Student's-t (μ, σ)	10	10	3	20
Fishery selectivity alpha (M only, time steps 1 & 2)	Student's-t (μ, σ)	1	10	0.3	20
Trawl survey selectivity a50	Student's-t (μ, σ)	35	100	15	45
Trawl survey selectivity ato95	Student's-t (μ, σ)	10	100	3	20
Trawl survey selectivity alpha	Student's-t (μ, σ)	1	10	0.3	2
Photographic survey selectivity a50	Student's-t (μ, σ)	35	100	10	45
Photographic survey selectivity ato95	Student's-t (μ, σ)	10	10	5	50
Photographic survey selectivity alpha	Uniform (fixed)	–	–	1	1
Maturity a50 (M & F, shared)	Student's-t (μ, σ)	43	100	10	60
Maturity ato95 (M & F, shared)	Student's-t (μ, σ)	10	100	1	50
Growth g_alpha (M)	Uniform	–	–	1	60
Growth g_beta (M)	Uniform	–	–	−8	50
Growth g_alpha (F)	Uniform	–	–	1	60
Growth g_beta (F)	Uniform	–	–	−10	50
Trawl survey process error	Student's-t (μ, σ)	0	0.2	0.0001	1.0
CPUE process error	Student's-t (μ, σ)	0.2	0.5	0.0001	1.0

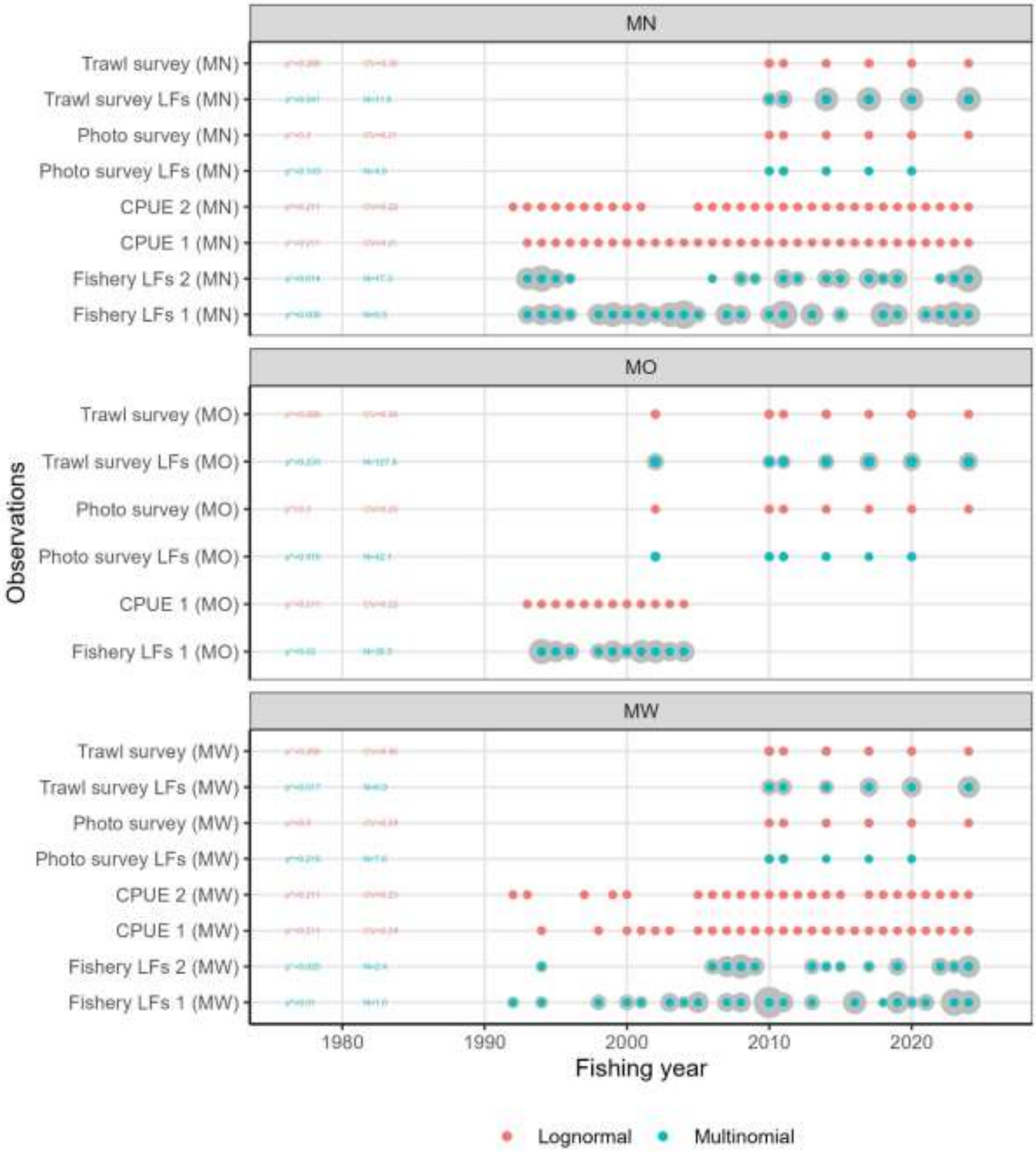

Figure 27: Model observations for the base case assessment model (02d). The coloured points represent the relative effective sample sizes (mean-adjusted for comparability between observation types) for each year and observation type (rows: trawl survey biomass (t) or photo survey abundance (n) and length-compositions (LFs)) and likelihood (colour), with the grey outline indicating the initial sample size before reweighting. *p was the multiplier used to adjust the multinomial *N*s in each observation from the Francis reweighting (multinomial likelihoods) or the process error CV (lognormal likelihoods).**

2.7 Surplus production models

For all the stocks in SCI 3 (MN, MO, and MW) and in SCI 4A (SCI 4AW and SCI 4AE), a Bayesian surplus production assessment based on the Pella-Tomlinson biomass-dynamic model (Pella & Tomlinson 1969) was fitted. A Bayesian surplus production model was used for SCI 4AE and SCI 4AW because these stocks are currently data-limited: the SCI 4A fishery is relatively recent, survey information is sparse (effectively a single recent survey year), and the biological and length-composition data needed for an integrated length-based assessment were not yet available. SCI 3 MN, MO, and MW were modelled in the same framework so the data-rich SCI 3 stocks could both benchmark the simpler approach against the integrated assessment (where results were broadly consistent) and support a joint shared-parameter fit, providing a coherent basis to estimate productivity and status across all five stocks, including those in SCI 4A.

The surplus production model was fitted separately to the five scampi stocks, but in a joint model, with annual biomass (B_t) in each stock evolving according to:

$$B_{t+1} = \left(B_t + \frac{r}{z} B_t \left(1 - \left(\frac{B_t}{K}\right)^z\right) - C^t\right) e^{\varepsilon_t^p}$$

where r is the intrinsic rate of increase, K is carrying capacity, z is the Pella-Tomlinson shape parameter, and C_t is annual catch (tonnes). The shape parameter defines a Schaefer (1954) model if $z = 1$, and as z tends towards zero it becomes the modified Fox (1970) model.

Initial biomass was assumed to be close to the carrying capacity:

$$B_{t=1} = K e^{\varepsilon_{t=1}^p}$$

Annual process deviations were assumed lognormal (Polacheck et al. 1993, Punt 2003):

$$\varepsilon_t^p \sim N(0, \sigma_p^2)$$

Where σ_p is the process error standard deviation.

Relative abundance indices (commercial CPUE, trawl survey, and photo survey) were assumed proportional to biomass (Hilborn & Walters 1992, Harley et al. 2001), i.e.,

$$I_t = q B_t \varepsilon_t^o$$

with lognormal observation error and observation standard deviation defined as the quadrature sum of the index-specific GLM uncertainty and an estimated additional observation-error term

$$\varepsilon_t^o \sim N(0, \sigma_t^2)$$
$$\sigma_t = \sqrt{\left(\sigma_t^{\mathrm{GLM}}\right)^2 + \tau^2}$$

where τ is the additional observation error (or data set / likelihood weight) over all abundance series.

All estimable parameters were fitted on the log scale. The intrinsic growth rate (r), shape parameter (z), process error (σ_p), and additional observation error (τ) were assumed common across stocks, whereas carrying capacity (K) was estimated separately for each stock. Catchability coefficients were assumed time-invariant, with stock-specific CPUE catchabilities and shared catchabilities for the trawl and photo survey series as specified in the model setup (Figure 28). The reference model used normal priors on the log scale and parameter estimation was constrained using bounds (Table 10). No prior was assigned to (q). The model was coded in RTMB (Kristensen 2026) and Markov chain Monte Carlo was done using Stan (Stan Development Team 2020).

Table 10: Model parameters, priors, and bounds.

Parameter	Structure across stocks	Prior	Bounds	
			Lower	Upper
r	Common to all stocks	$\log(r) \sim N(\log(0.35), 0.5^2)$	exp(-5)	1
z	Common to all stocks	$\log(z) \sim N(\log(1), 0.5^2)$	0	2.5
K	Stock-specific	$\log(K) \sim N(\log(500), 1^2)$	10	10000
q	Stock / series specific		exp(-25)	1
τ	Common to all stocks / series	$\log(\tau) \sim N(\log(0.5), 0.5^2)$	0	2
σ_p	Common to all stocks	$\log(\sigma_p) \sim N(\log(0.5), 0.5^2)$	0	2
B_t	Stock-specific annual latent state		$-\infty$	∞

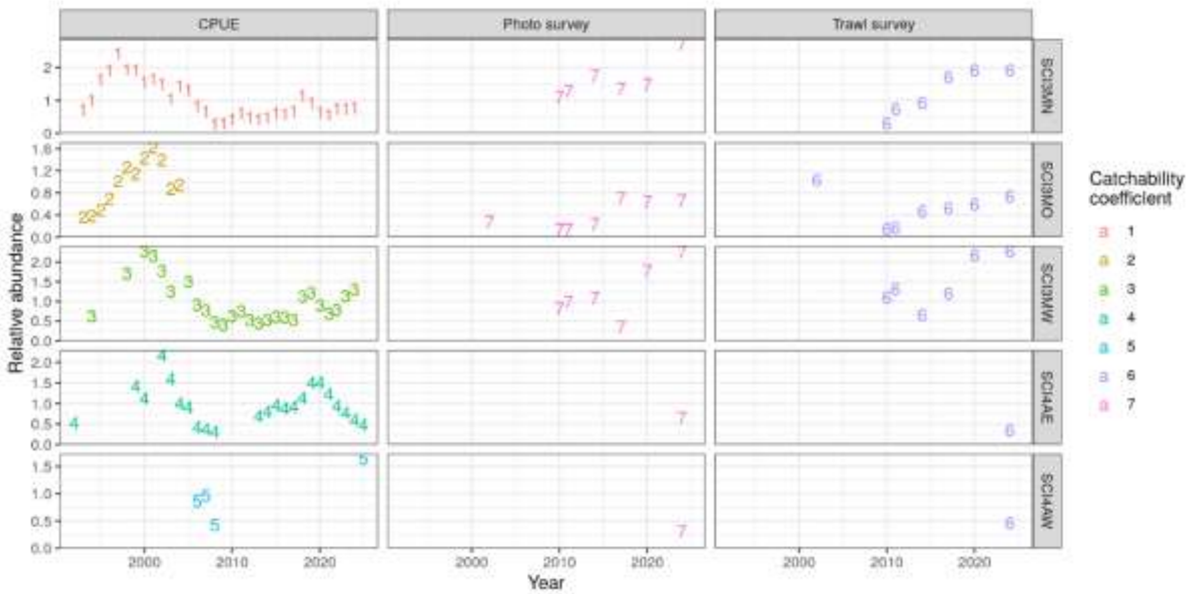

Figure 28: Relative abundance indices by year for each stock indicating the catchability coefficients assumed for each stock.

3. INTEGRATED LENGTH-BASED STOCK ASSESSMENT RESULTS

3.1 CASAL and Casal2 comparison

The 2020 assessment base case for SCI 3 in areas MN, MO , and MW (McGregor et al. 2022) were implemented using CASAL (Bull et al. 2012). The updated models presented here were implemented in Casal2 (Casal2 Development Team 2024). A comparison between the 2020 assessment model in CASAL and in Casal2 was made using the same model structure, parameters, and observations as for the 2020 base case to validate the length-based implementation in Casal2. No parameter transformations were applied, and penalties were used to constrain YCS to have mean one in Casal2 in the same manner as in CASAL.

Model estimates of B_0 and current biomass (B_{2020}) from the 2020 CASAL and Casal2 implementations were similar with very similar SSB trajectories (Figure 29) values for the components of the objective function, and YCS estimates (Figure 30). At MCMC the models also had very similar SSB trajectories (Figure 31) and estimates of YCS (Figure 32).

These results confirm that the Casal2 length-based implementation reproduced the 2020 CASAL base case closely at both the MPD and MCMC level, providing confidence that the implementation of the length-based model in Casal2 did not introduce material differences in model behaviour or stock status estimates.

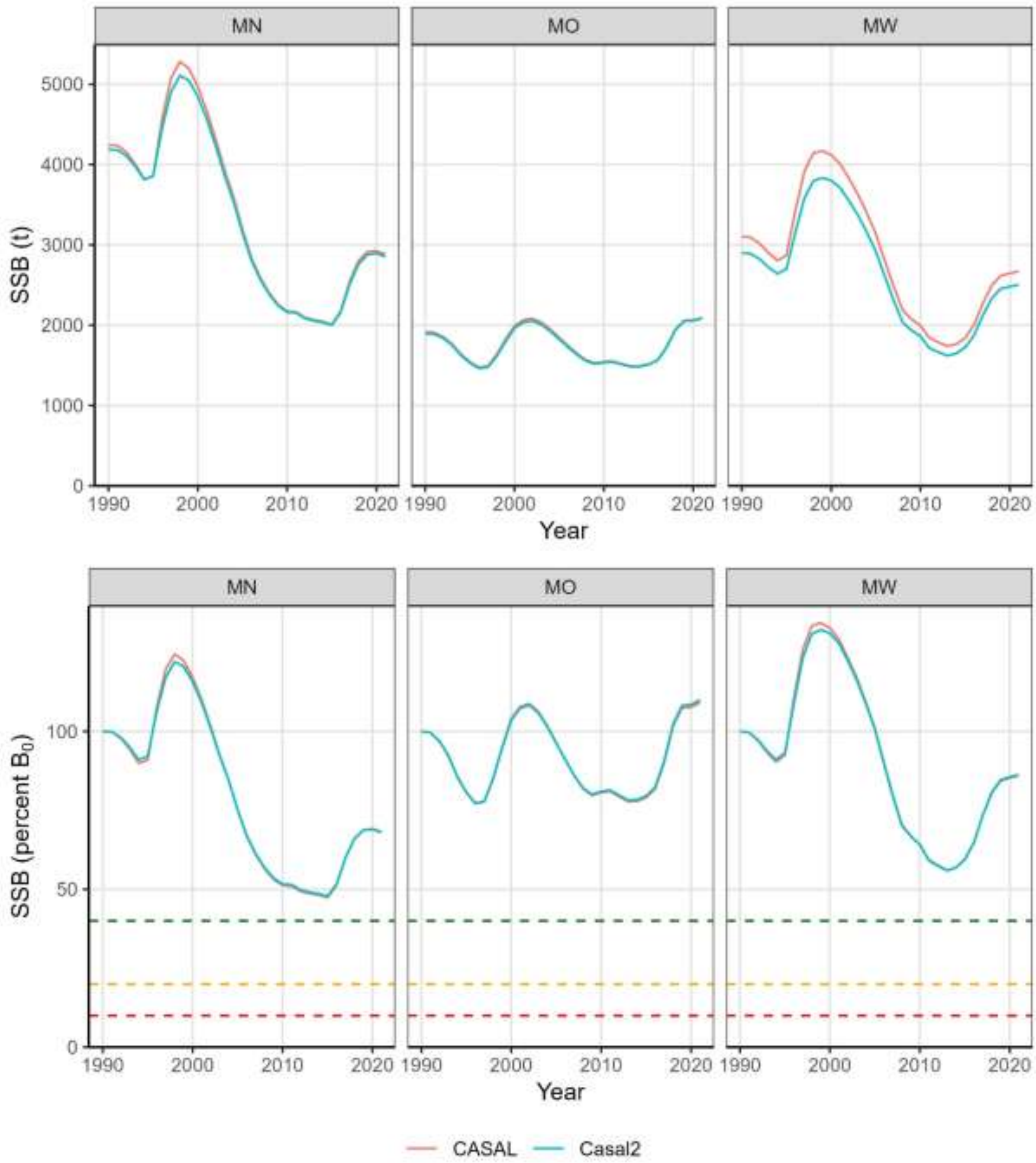

Figure 29: 2020 MPD base case CASAL model and the equivalent Casal2 model for (top) SSB by year and (bottom) SSB as a percentage of B_0 for 1990–2021.

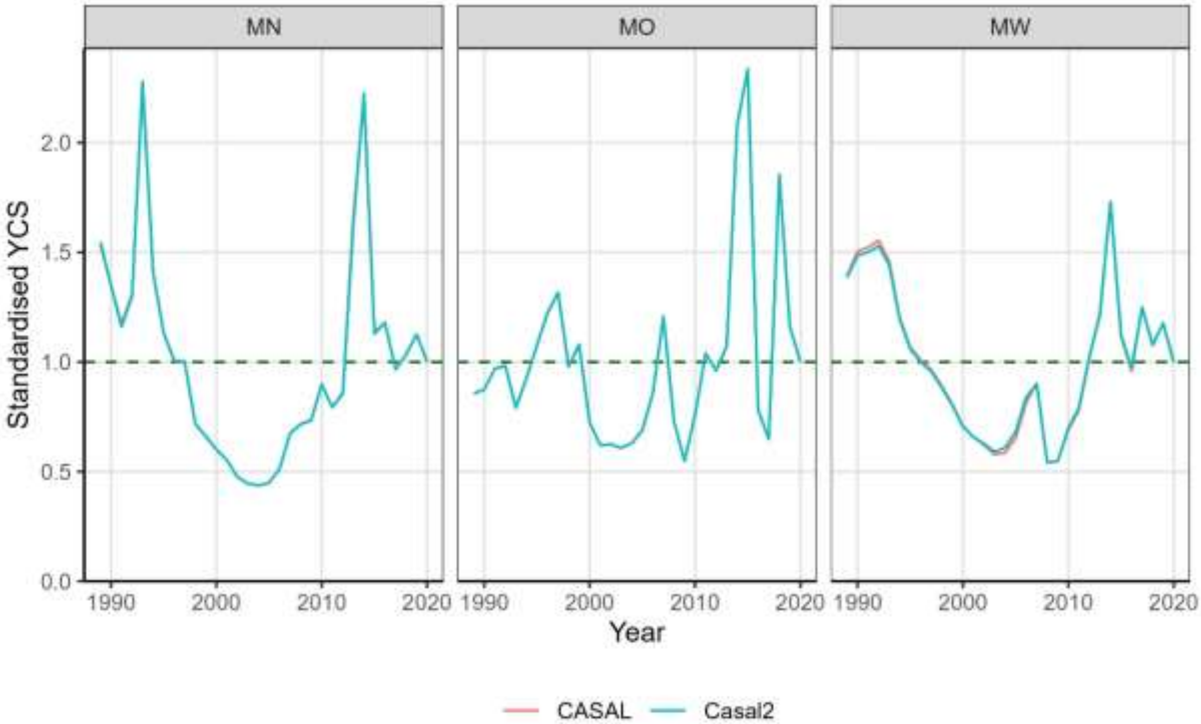

Figure 30: 2020 MPD base case CASAL model and the equivalent Casal2 model for estimates of year class strengths (1989–2019) for the years 1989–2020.

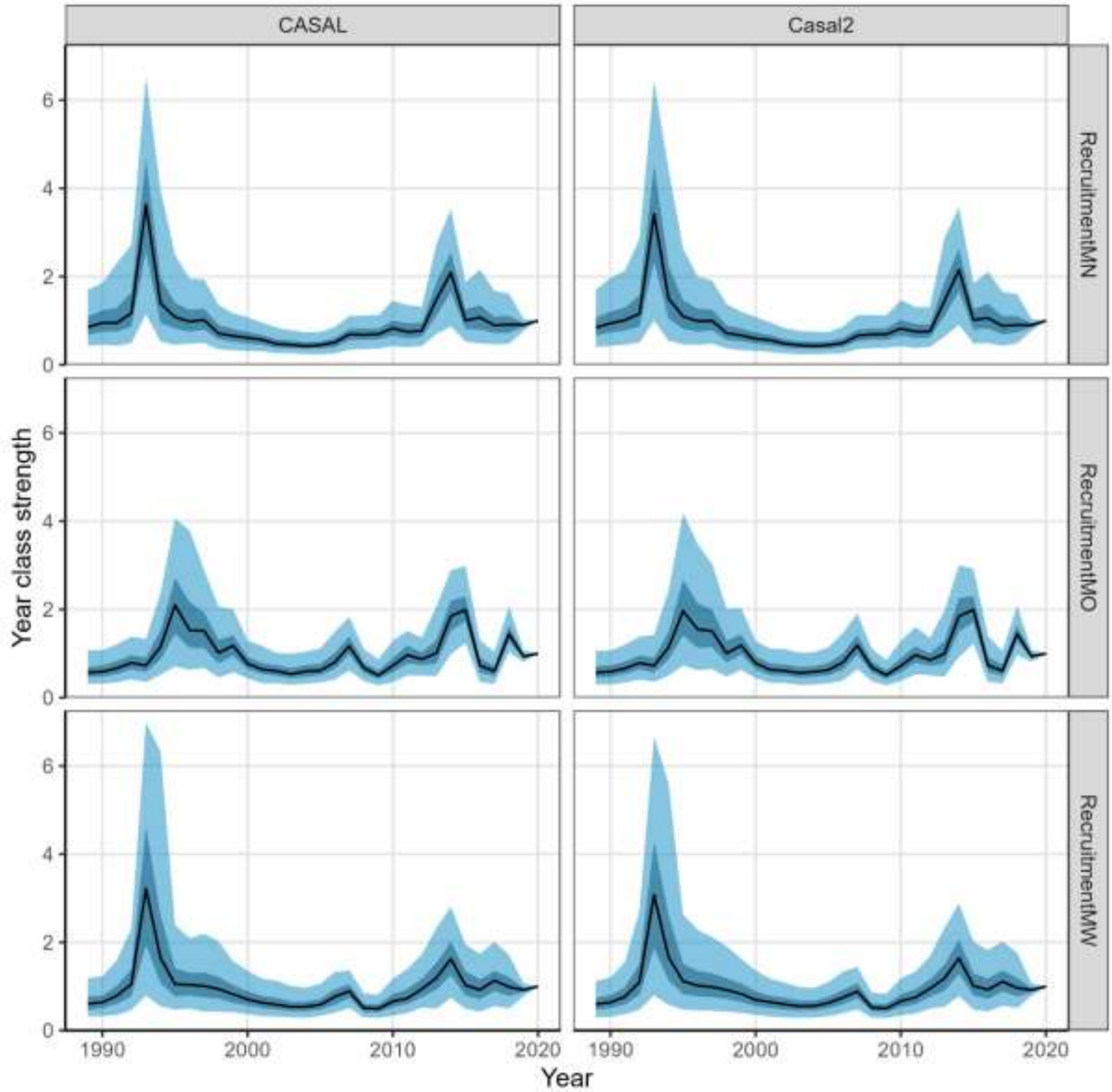

Figure 31: 2020 MCMC base case CASAL (left) and the equivalent Casal2 (right) model for estimates of year class strengths relative to one (1989–2019) for the years 1989–2020.

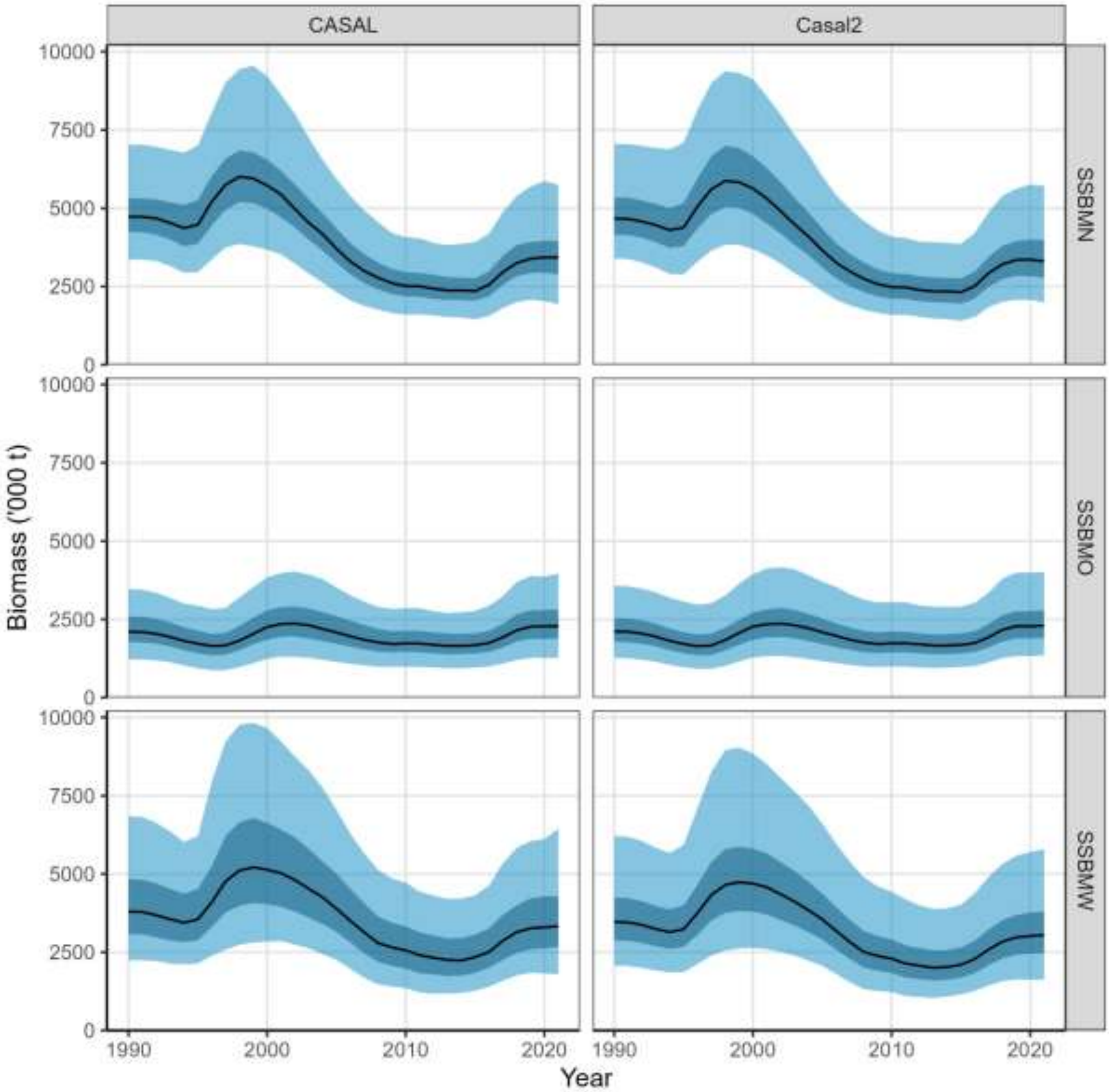

Figure 32: 2020 MCMC base case CASAL (left) and the equivalent Casal2 (right) model for SSB by year for 1990–2021.

3.2 Base case integrated model MPD results

MPD diagnostics for the SCI 3 base case integrated length-based model (model 02d) for areas MN, MO and MW are presented below, including the estimated spawning-stock biomass (SSB) trajectories and stock status, model fits to the relative abundance indices and length-composition data, one-step-ahead (OSA) residual diagnostics, estimated selectivity ogives, year class strength (YCS) estimates, and the stock-recruitment relationship.

The MN and MW stocks showed a similar overall pattern, with SSB increasing from the start of the model period to a peak in the late 1990s (around 140% B_0 for MN and 155% B_0 for MW), followed by a sustained decline to a minimum at around 2008–2010 (close to or below the 20% B_0 soft limit), and a partial recovery since around 2015 to current levels of approximately 58% B_0 (MN) and 58% B_0 (MW). The MO stock followed a less pronounced cycle, declining to around 50% B_0 by the early-to-mid 1990s before increasing to a peak of around 105–120% B_0 in the early 2000s, dipping to around 65% B_0 through the 2010s, and increasing again to its current level of around 118% B_0, above the 40% B_0 target throughout the time series (Figure 33).

The model fitted the relative abundance indices reasonably well for all three stocks, with predicted values tracking the main decline-and-recovery pattern evident in the commercial CPUE series (time steps 1 and 2) and broadly matching the photographic- and trawl-survey point estimates, allowing for their wider observation uncertainty and more limited temporal coverage. There was no strong evidence of systematic lack of fit (i.e., consistent over- or under-prediction) for any of the four index types within any stock (Figure 34).

Fitted length compositions from the trawl survey for area MO, MN and MW (Figure 35–Figure 37) and from the commercial fishery in time steps 1 and 2 for MO, MN, and MW (Figure 38–Figure 42) captured the general modal length and the consistent offset between sexes (with males typically attaining a larger modal length than females, consistent with the estimated growth and length-weight relationships), although the model fits, as expected, smoothed over some of the finer-scale, year-to-year variability evident in the raw observed length frequencies.

One-step-ahead (OSA) residual diagnostics for the fishery and survey length-composition data indicated an adequate overall fit, with the QQ-plots for all three stocks lying close to the 1:1 line across most of the distribution, with some divergence only in the extreme tails (Figure 43). The corresponding bubble plots of OSA residuals did not show strong, persistent patterns by year or length class within any data set, although there was some clustering of larger residuals (both positive and negative) at the smallest and largest length classes, where sample sizes are typically lower (Figure 44).

Estimated fishery selectivity ogives were similar in shape across the MN, MO and MW stocks within each time step, with full selection reached by around 50–60 mm and little difference between males and females. The trawl-survey selectivity ogive showed an earlier-rising, slightly dome-shaped pattern for males relative to females, consistent with the fully-selected female ogive approaching an asymptote of 1 at a greater length than males. The photographic-survey selectivity, with its alpha parameter fixed at 1, was estimated as a single logistic curve common to both sexes (Figure 45).

Estimated year class strengths (YCS) were variable about the assumed long-term average of 1 for all three stocks, with occasional very strong cohorts evident in the early 1990s (notably for MW, where the 1992/93 cohort was estimated at almost ten times the average, and for MN, where a comparable though smaller peak of around seven times the average occurred in the same period). More recent year classes were generally estimated closer to the long-term average, with YCS assumed equal to 1 from 2023 onwards, reflecting the limited information available to estimate the strength of the most recent cohorts (Figure 46). Data from the surveys and CPUE indices were consistent with the estimated year classes, and there was some agreement in the change in mean length observed from the length compositions. However, the length compositions were generally not informative for year classes entering the fishery.

Recruitment estimates were scattered widely about the deterministic Beverton–Holt stock-recruitment curve (steepness h=0.75) for all three stocks, reflecting the high estimated recruitment variability (year class strength) relative to any detectable stock-recruitment signal. Historical SSB has remained above roughly 30–50% B_0 for most of the time series in each stock, so the data provide little contrast at low stock size with which to estimate the shape of the stock-recruitment relationship independently of the assumed steepness (Figure 47).

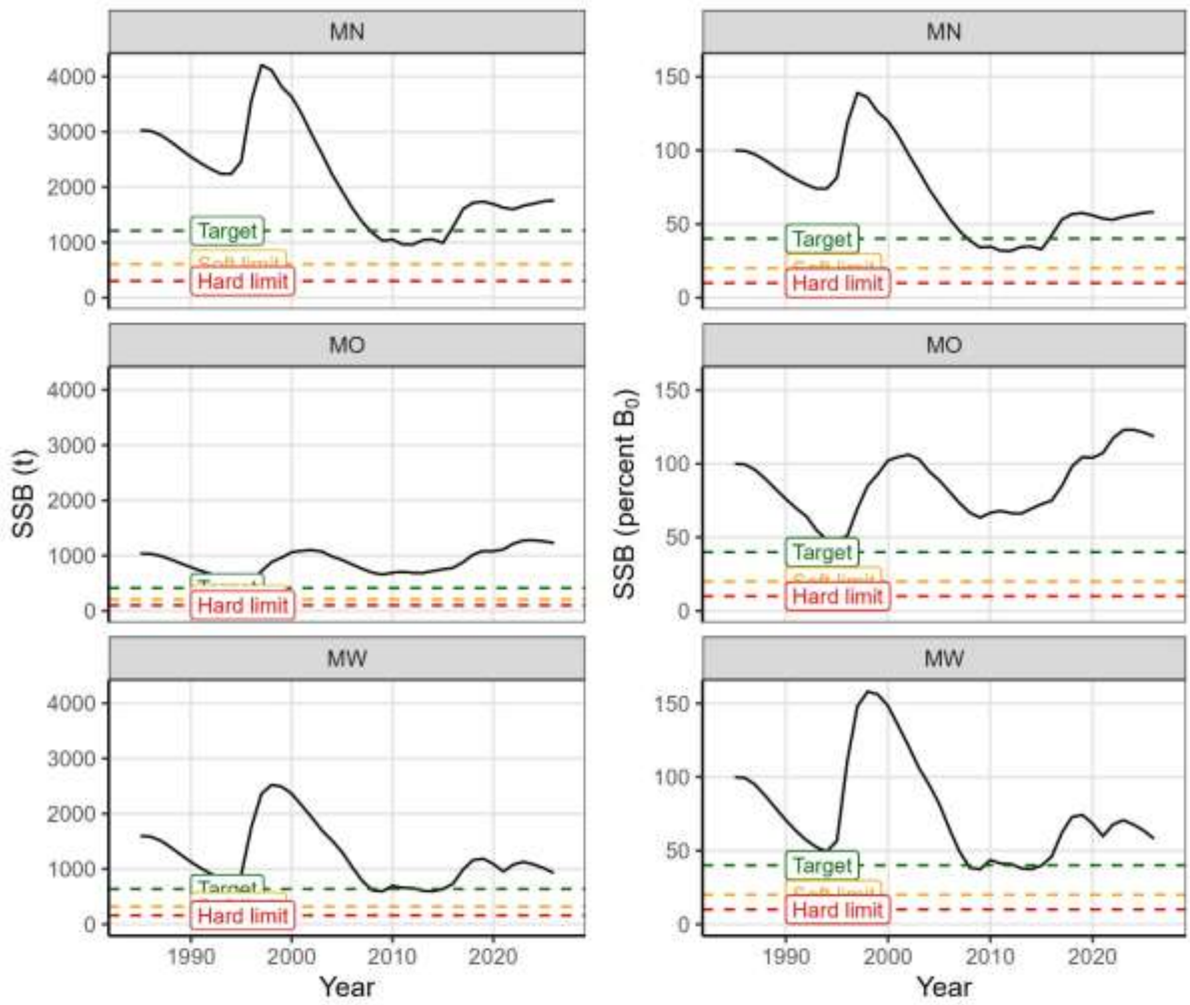

Figure 33: Base case model (02d) MPD trajectories for (left) *SSB* biomass and (right) stock status (*SSB*) as a percent of B_0 for MO, MN, and MW.

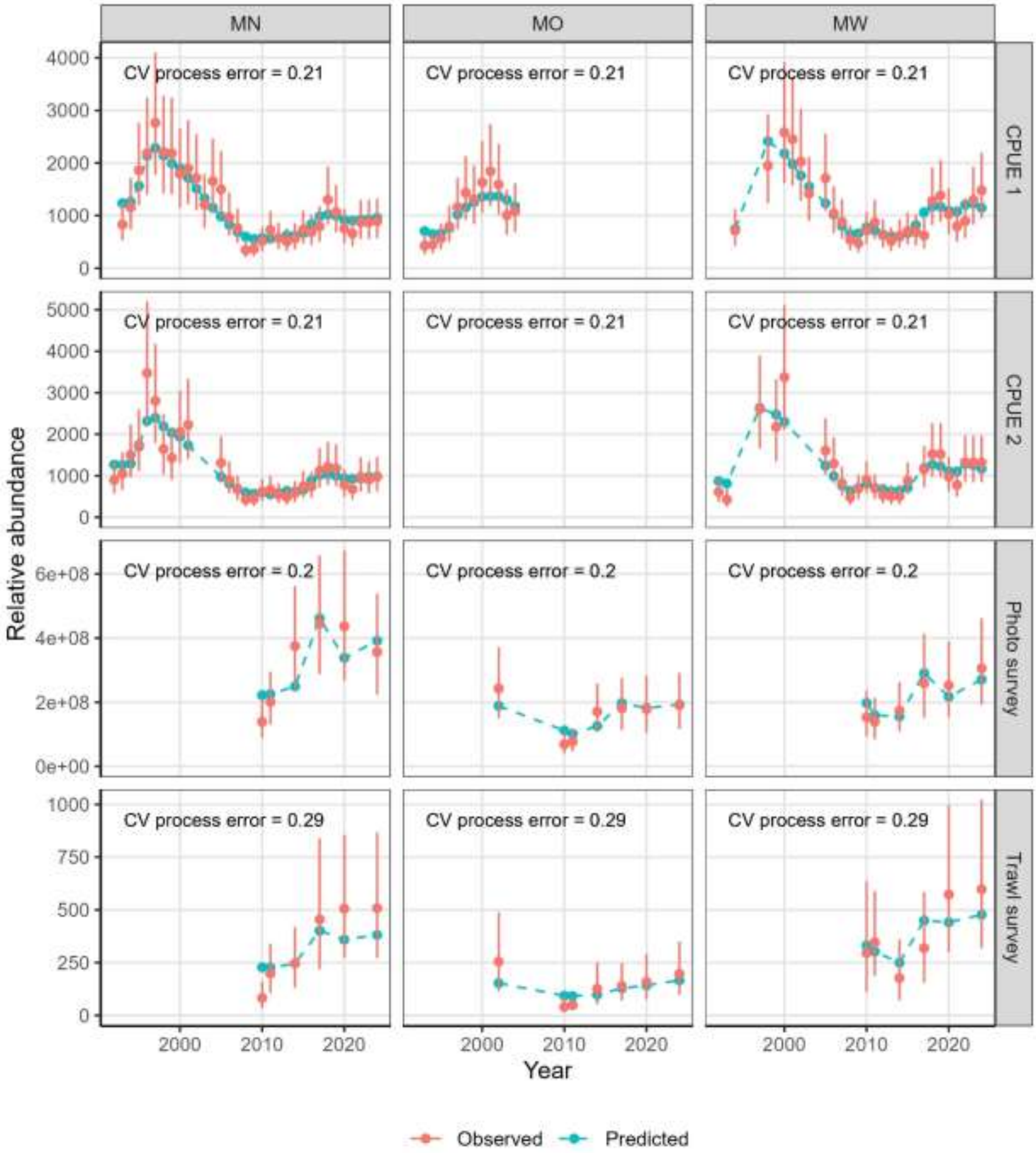

Figure 34: Base case model (02d) MPD model fits to the biomass and abundance time series (red circles and 95% confidence intervals indicated by the red lines) and expected values by blue points, for MO, MN, and MW.

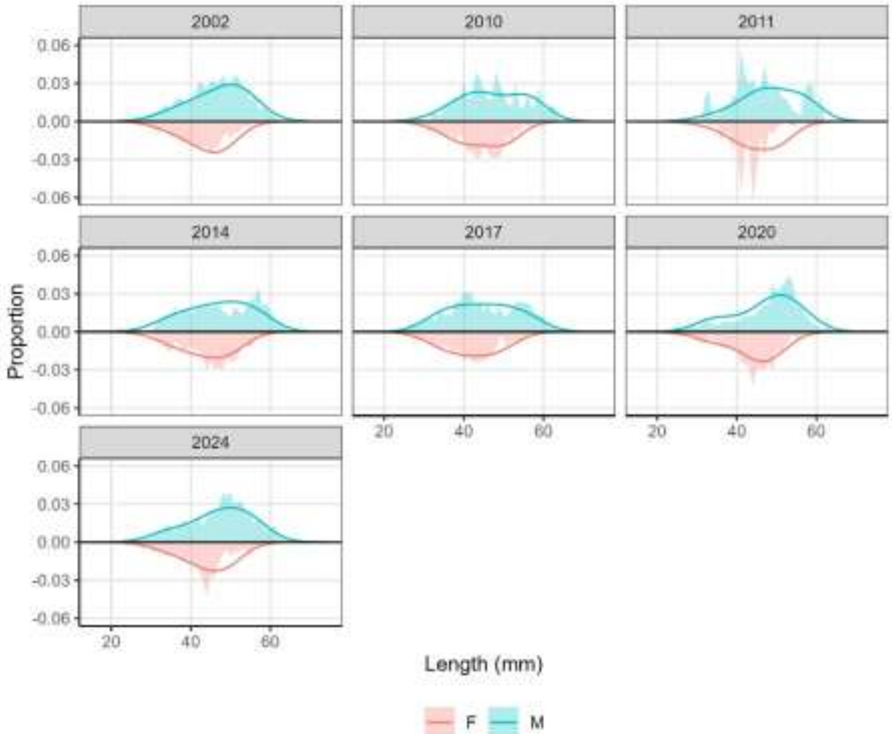

Figure 35: Base case model (02d) observed (solid lines) and expected (shaded polygons) length compositions for the trawl survey in MO for the base case model (02d), 2002–2024 (red=female and blue=male).

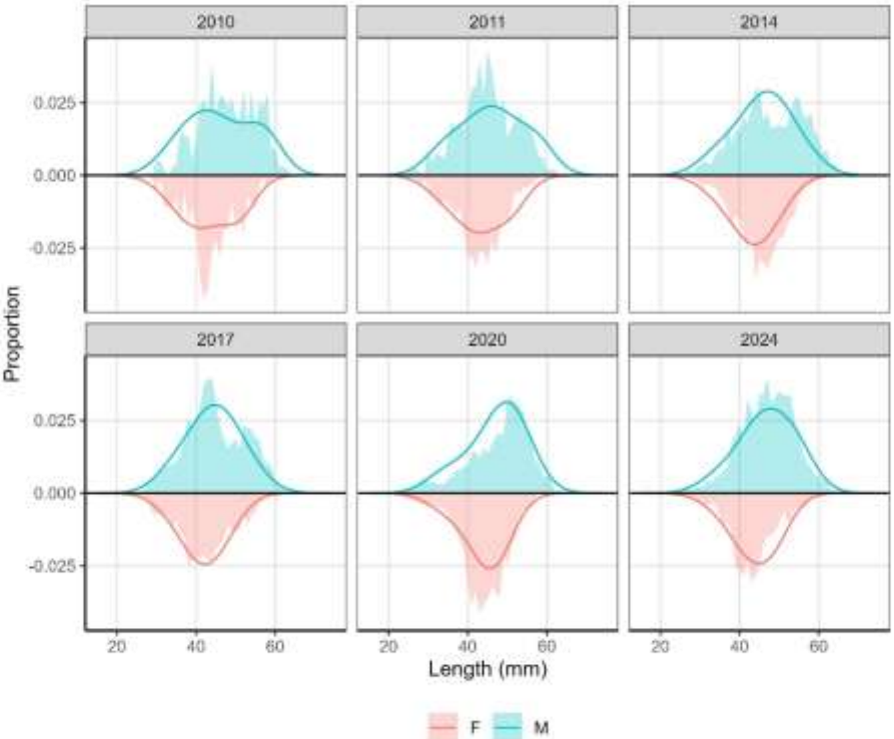

Figure 36: Base case model (02d) observed (solid lines) and expected (shaded polygons) length compositions for the trawl survey in MN for the base case model (02d), 2010–2024 (red=female and blue=male).

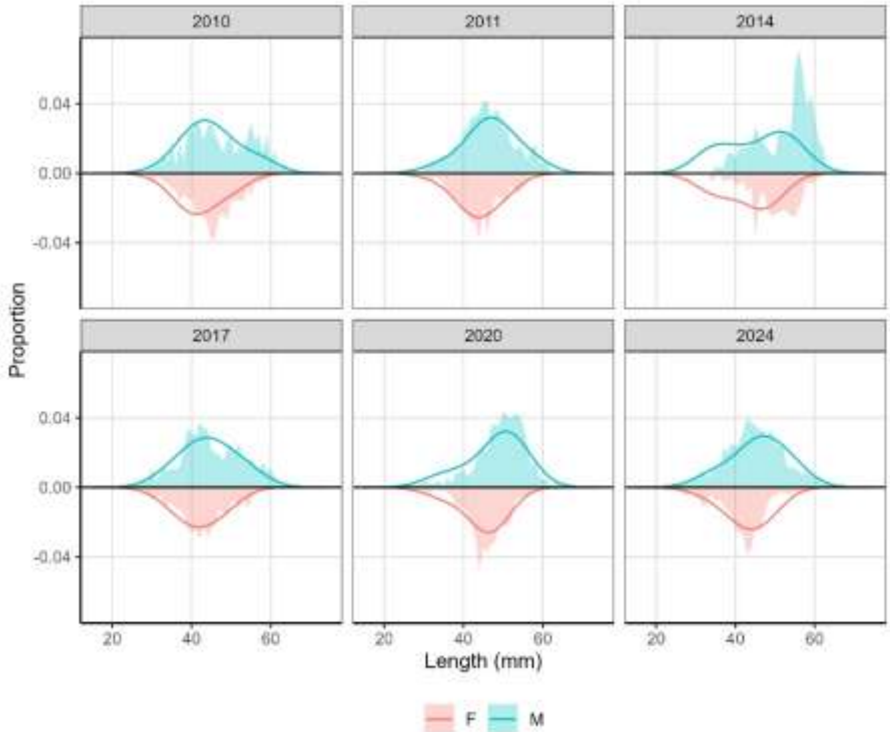

Figure 37: Base case model (02d) observed (solid lines) and expected (shaded polygons) length compositions for the trawl survey in MW for the base case model (02d), 2010–2024 (red=female and blue=male).

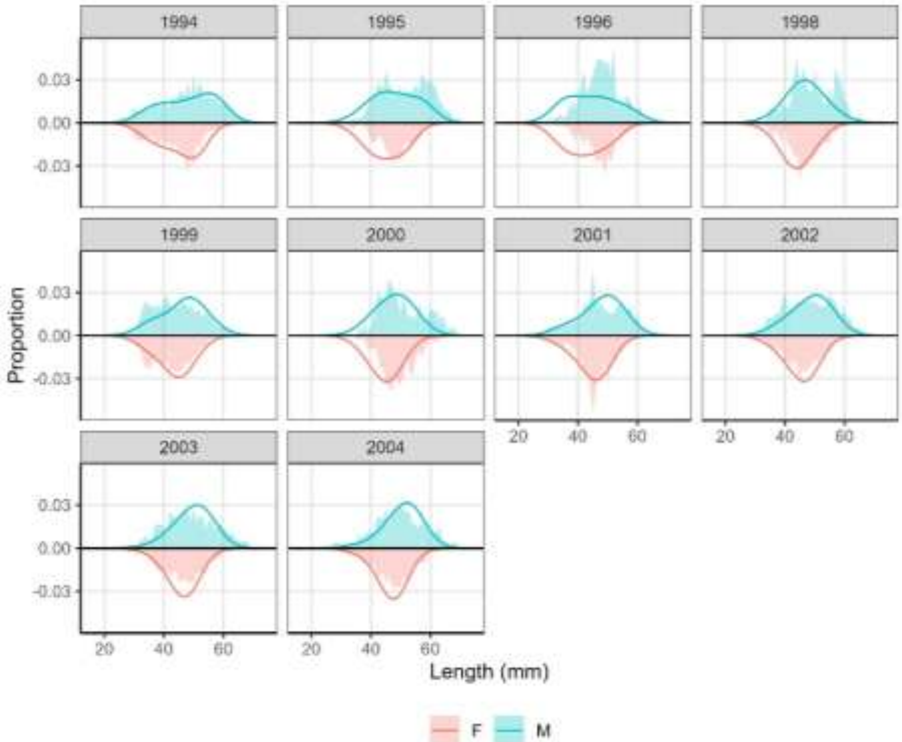

Figure 38: Base case model (02d) observed (solid lines) and expected (shaded polygons) length composition data from the commercial fishery in area MO in time-step 1 for the base case model (02d), 1994–2004 (red=female and blue=male).

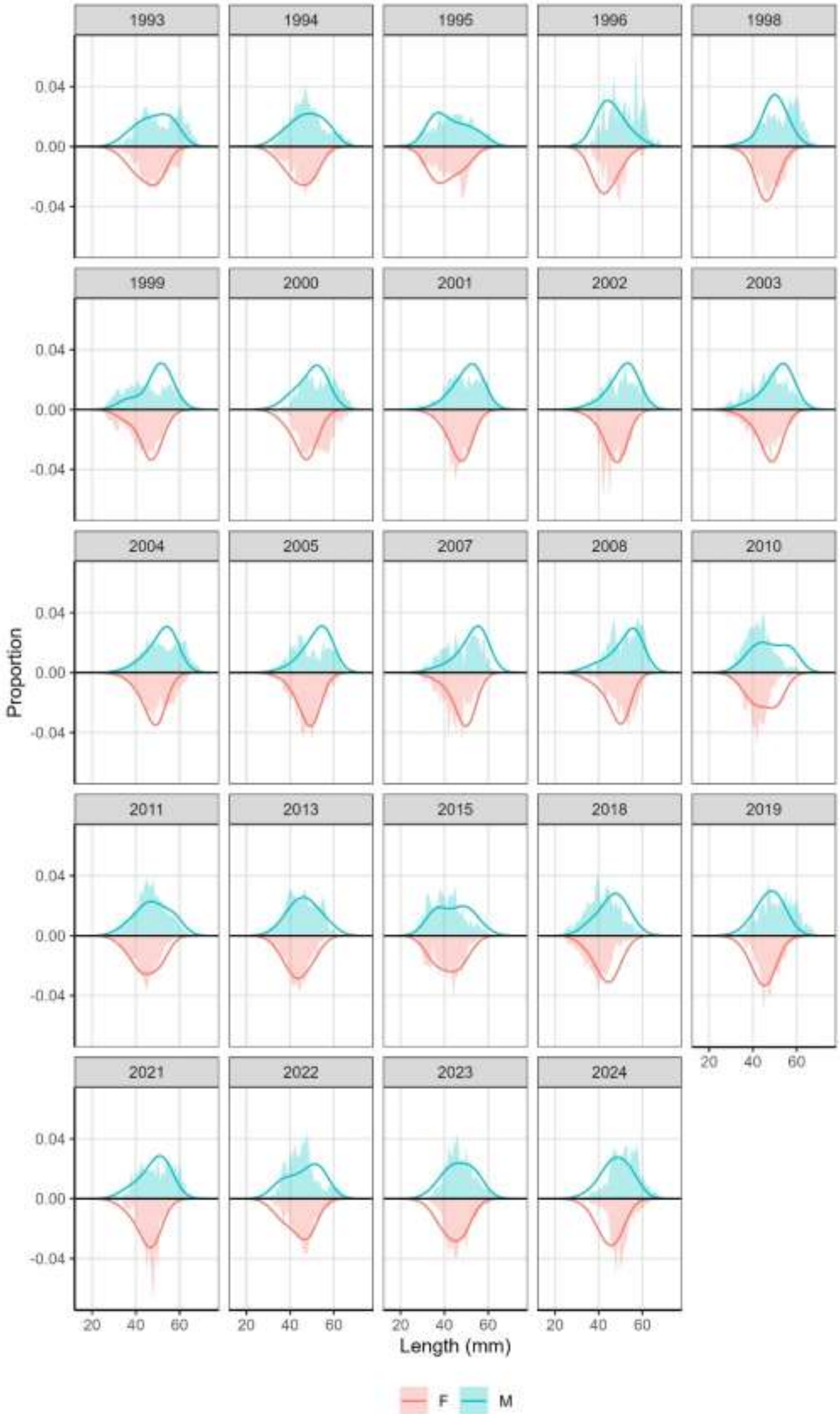

Figure 39: Base case model (02d) observed (solid lines) and expected (shaded polygons) length composition data from the commercial fishery in area MN in time-step 1 for the base case model (02d), 1993–2024 (red=female and blue=male).

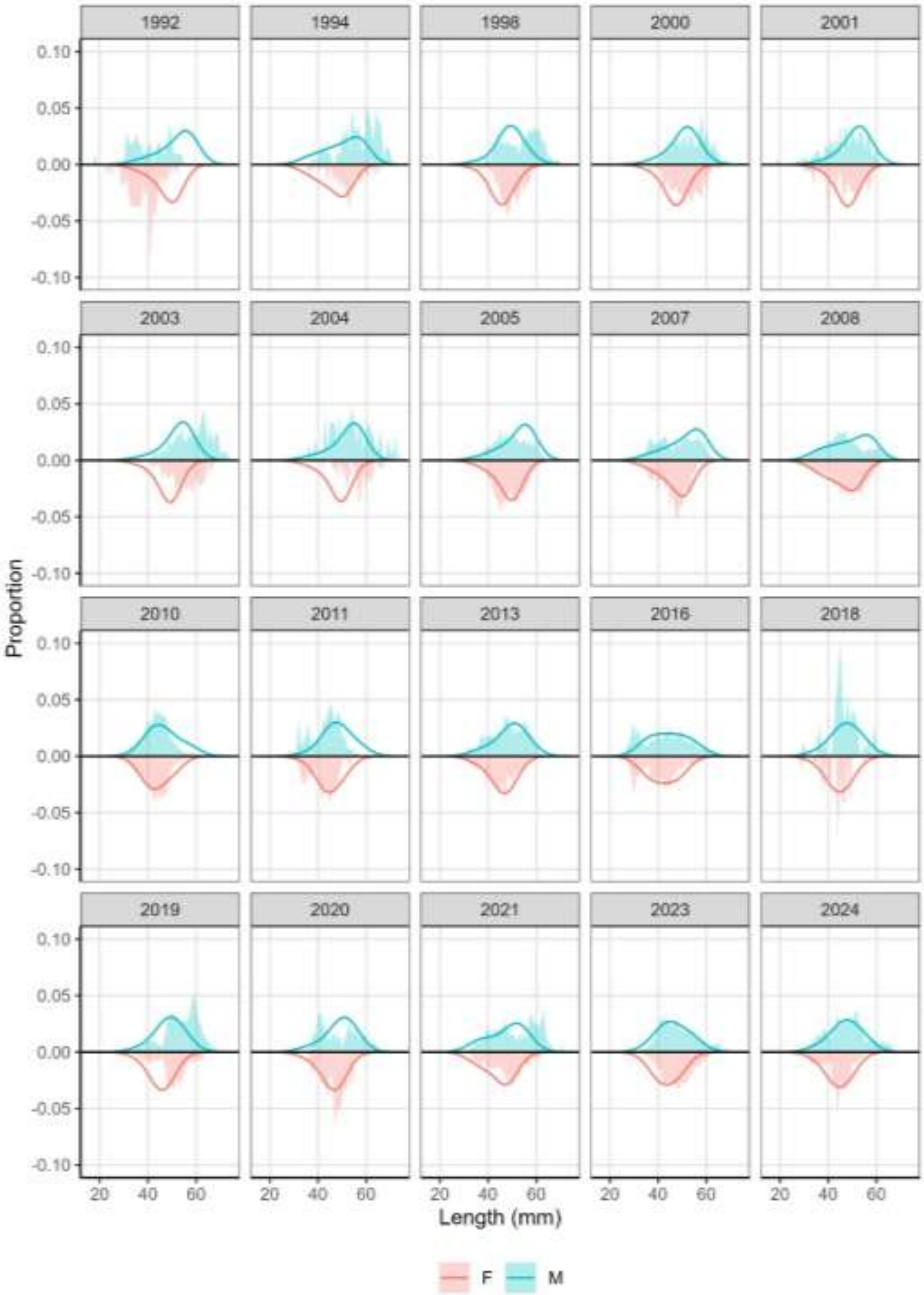

Figure 40: Base case model (02d) observed (solid lines) and expected (shaded polygons) length composition data from the commercial fishery in area MW in time-step 1 for the base case model (02d), 1992–2024 (red=female and blue=male).

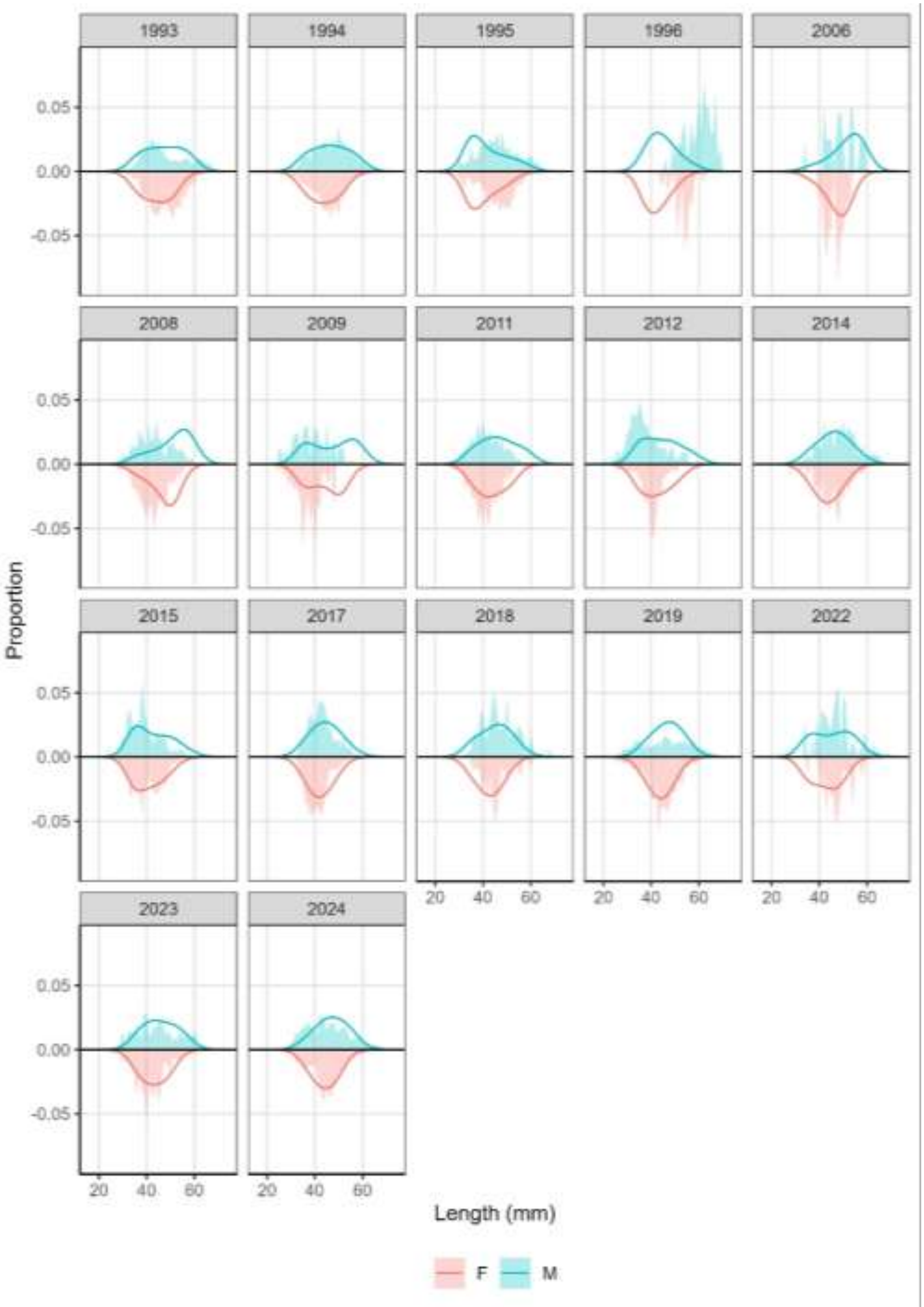

Figure 41: Base case model (02d) observed (solid lines) and expected (shaded polygons) length composition data from the commercial fishery in area MN in time-step 2 for the base case model (02d), 1993–2024 (red=female and blue=male).

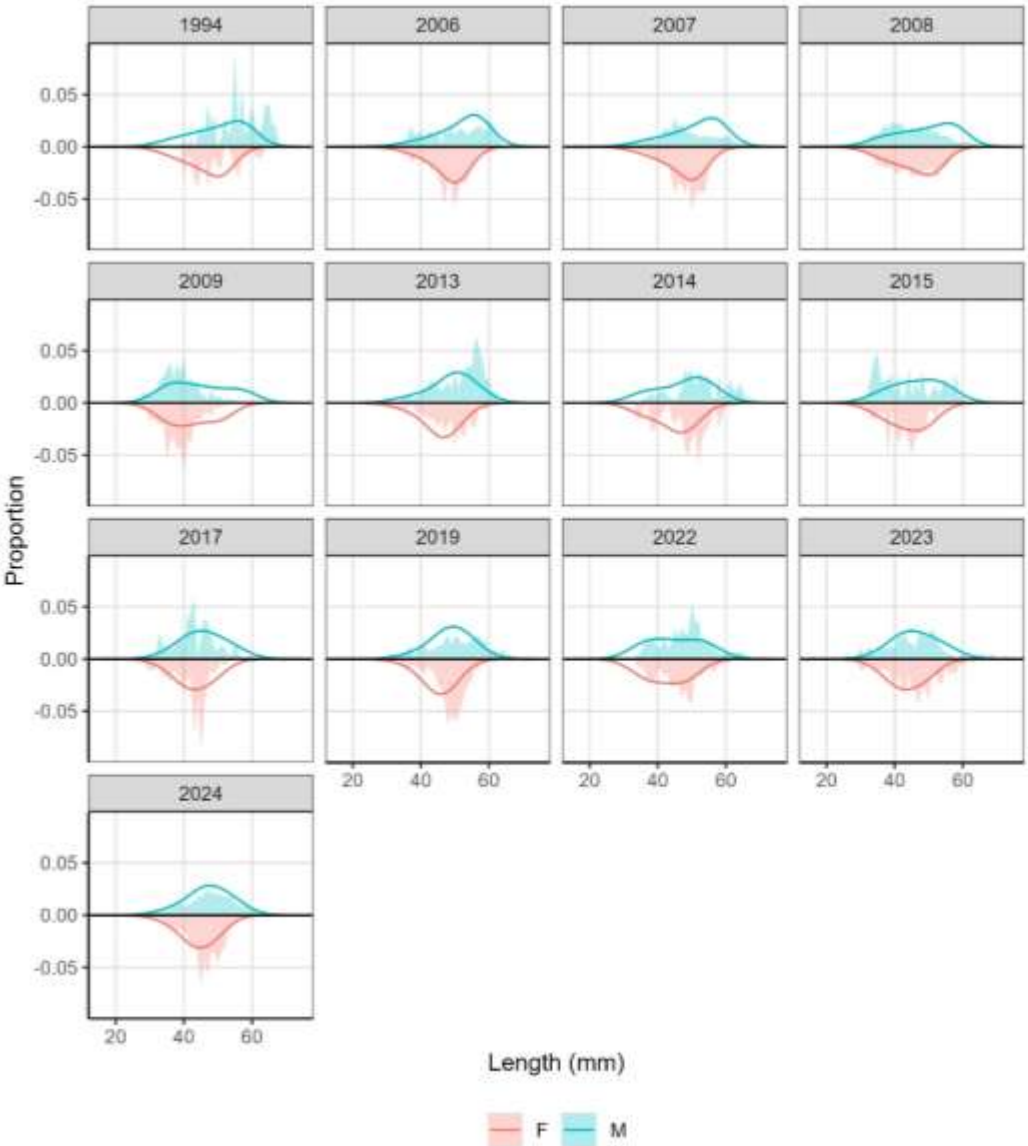

Figure 42: Base case model (02d) observed (solid lines) and expected (shaded polygons) length composition data from the commercial fishery in area MW in time-step 2 for the base case model (02d), 1994–2024 (red=female and blue=male).

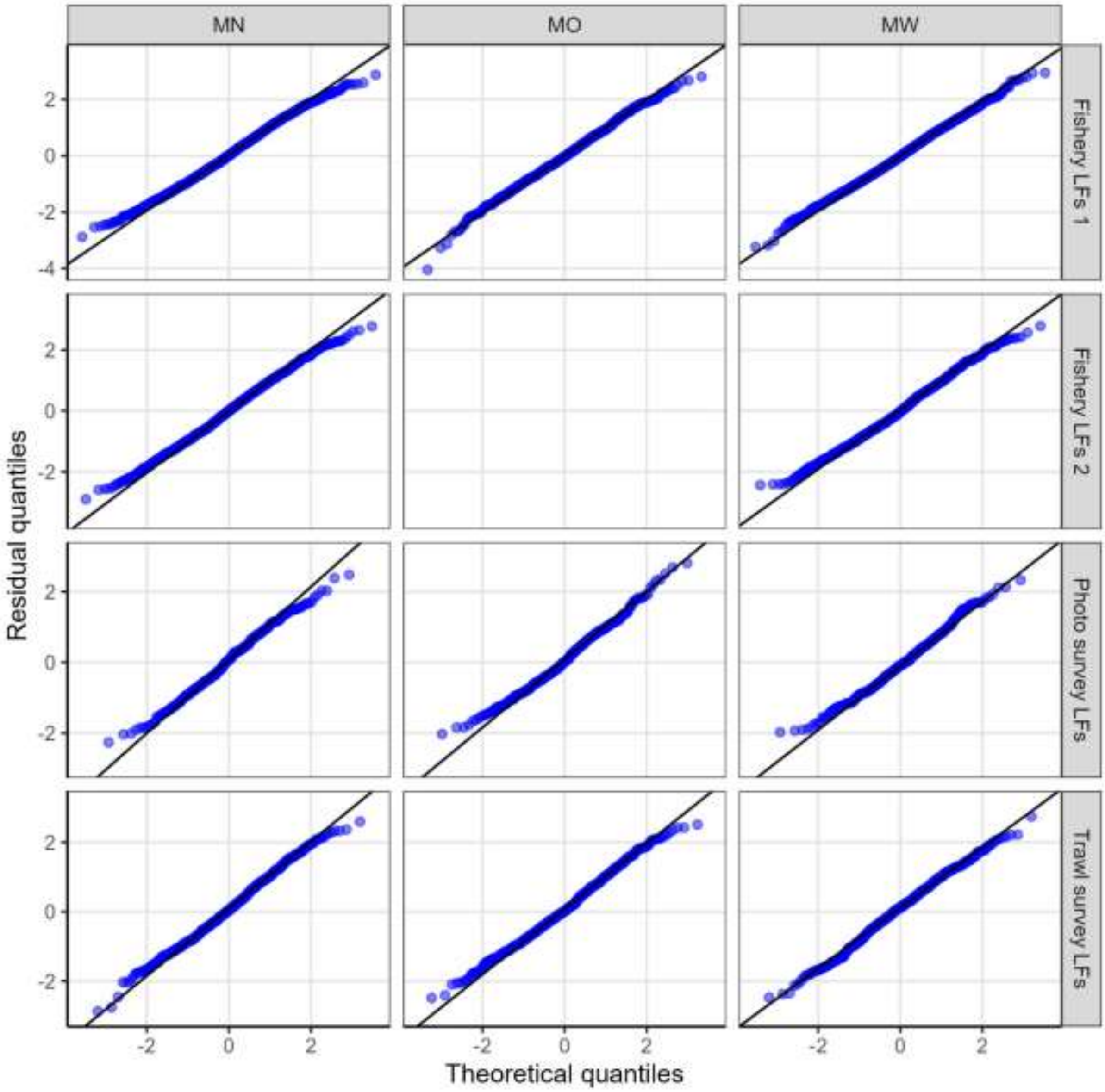

Figure 43: QQ-plots for the one-step-ahead (OSA) residuals for female and male length composition data from the commercial fisheries, trawl survey, and photo survey for areas MO, MN, and MW for the base case model (02d).

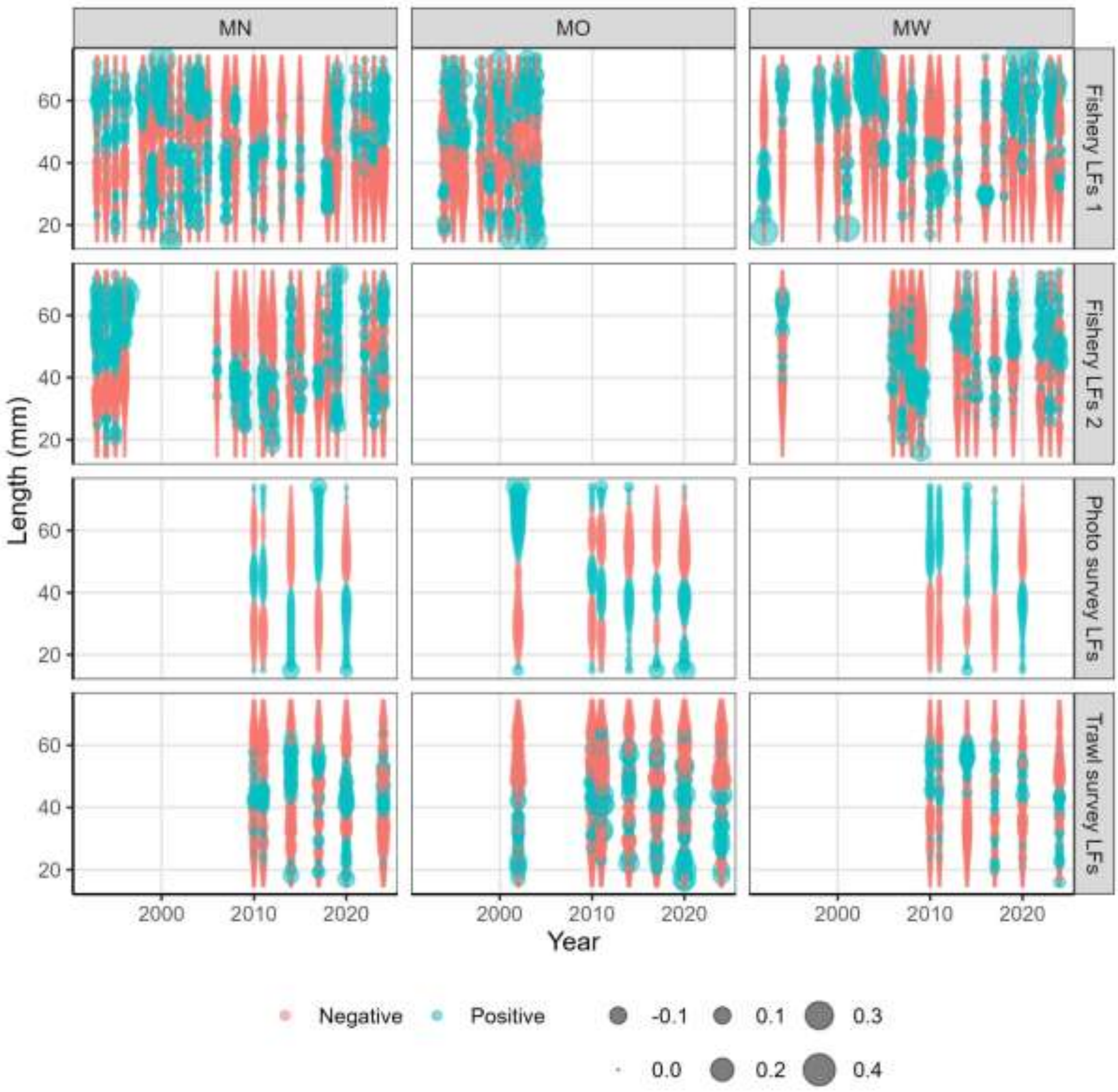

Figure 44: One-step-ahead (OSA) residuals for the base case model (02d) length composition data from the commercial fisheries, trawl survey, and photo survey for areas MO, MN, and MW, with red=positive and blue=negative residuals, and circle size proportional to the size of the residual.

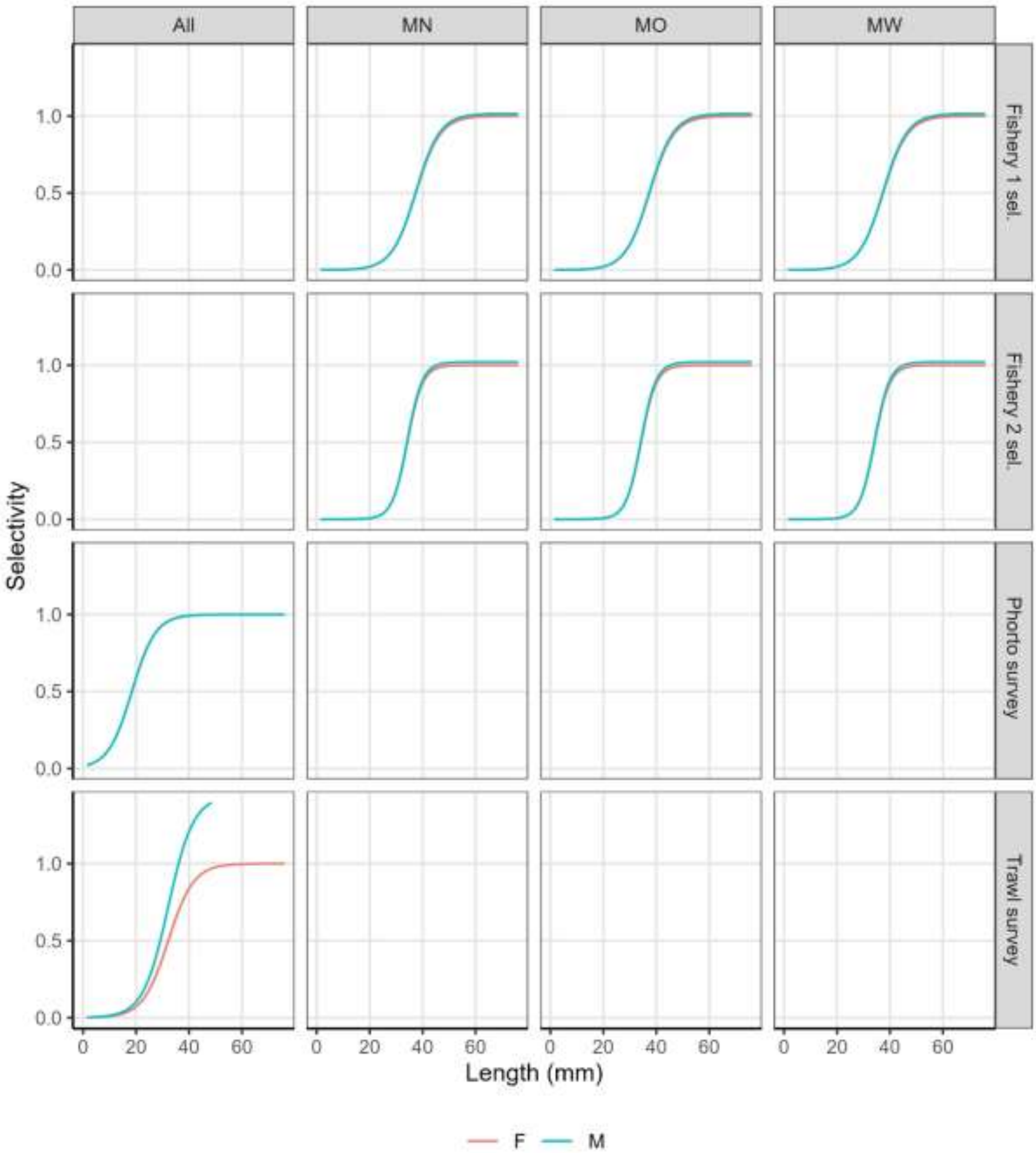

Figure 45: Base case model (02d) estimates of the selectivity parameters for the commercial catch, trawl survey, and photo survey selectivities for male (blue) and female (red) for areas MO, MN, and MW, and all areas combined.

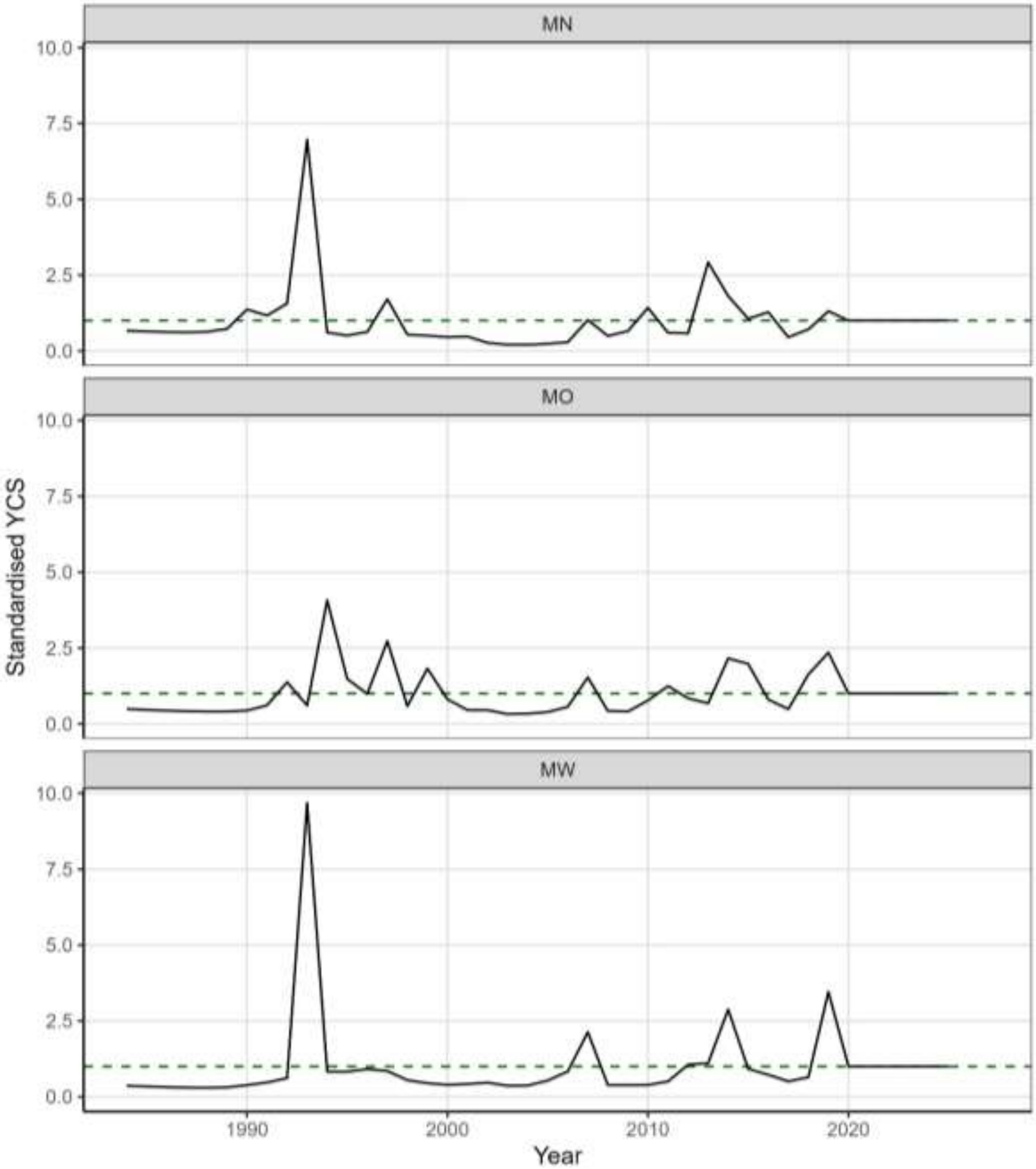

Figure 46: Base case model (02d) estimates of the relative year class strength parameters for areas MO, MN, and MW; estimated for 1984–2022 and assumed equal to 1 for 2023–2025.

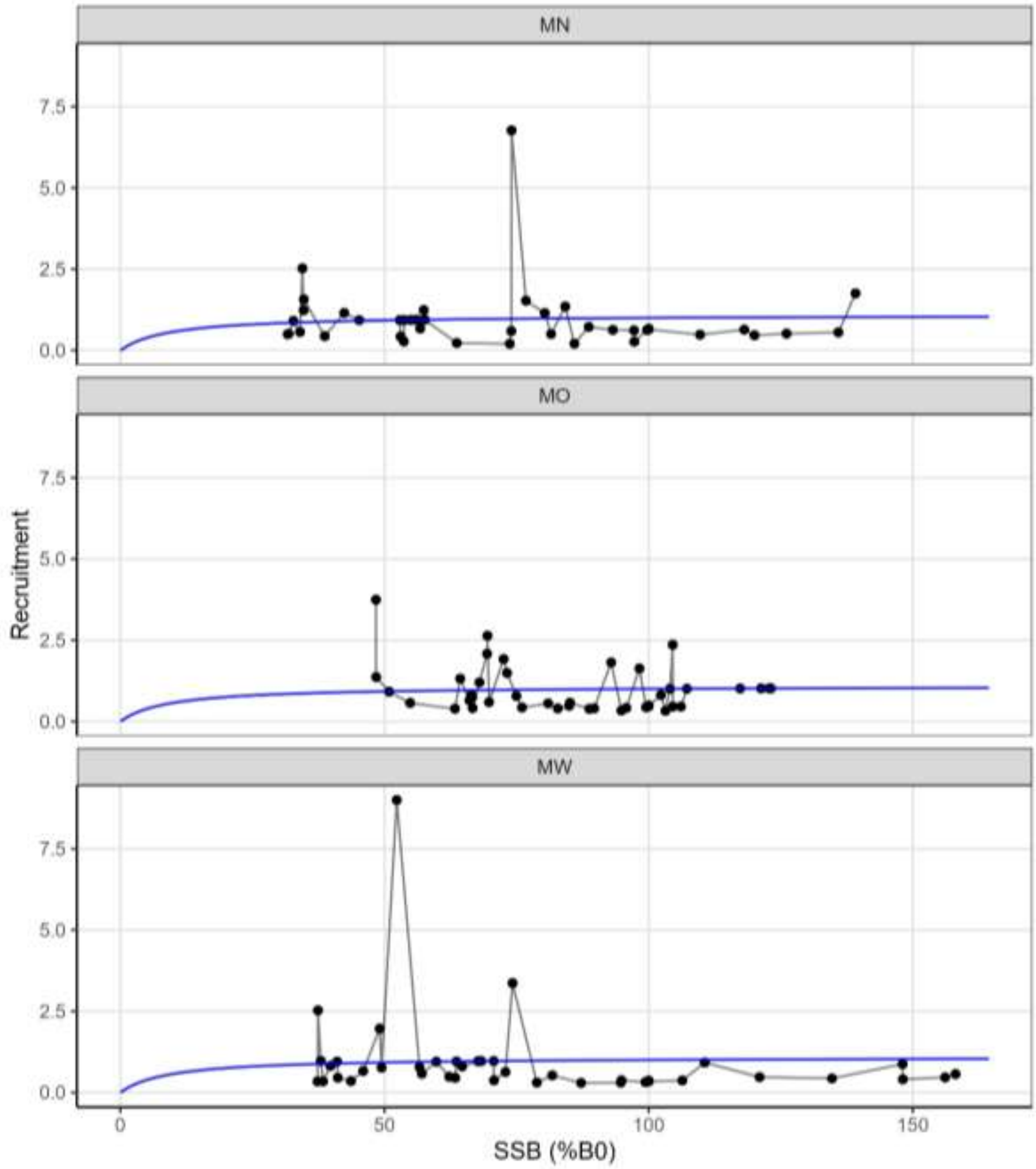

Figure 47: The stock recruitment relationship (Beverton-Holt with steepness *h*=0.75), and the relative recruitment values (y-axis) plotted against SSB (x-axis) for the base case model (02d).

3.3 MPD model retrospectives

Retrospective analyses of the base case model (02d) were carried out for each of the three stocks (MN, MO and MW). These sequentially removed each year's catch and observations and reduced the year class strengths estimated to exclude the most recent year(s) of data. This was done for 13 iterations, i.e., a retrospective peel was run for each of the 2013–2025 model years and compared with the full model fitted through to 2026. Models were refitted at the MPD, and the resulting spawning-stock biomass (SSB, as a percentage of B_0) trajectories are given in Figure 48, with the corresponding year class strength (YCS) estimates in Figure 49.

In general, the retrospective peels were consistent with one another for all three stocks over most of the time series, diverging mainly in the final two to three years before each peel's terminal year. For

MN and MW in particular, several of the more recent peels (e.g., the 2022 and 2023 model runs) estimated a higher terminal-year SSB than was subsequently supported once additional data were included; the pattern for MO was more mixed, with both upward and downward revisions evident among individual peels. These terminal-year divergences corresponded to the most recent year class strength initially being estimated above the long-term average in several peels (Figure 49), before being revised back towards the average as additional length-composition and survey information were incorporated in later model runs. This is a typical retrospective pattern for stocks with limited information on the most recent year classes and indicates a degree of uncertainty in the SSB and YCS estimates for the final two to three years of the assessment that should be considered when interpreting current stock status.

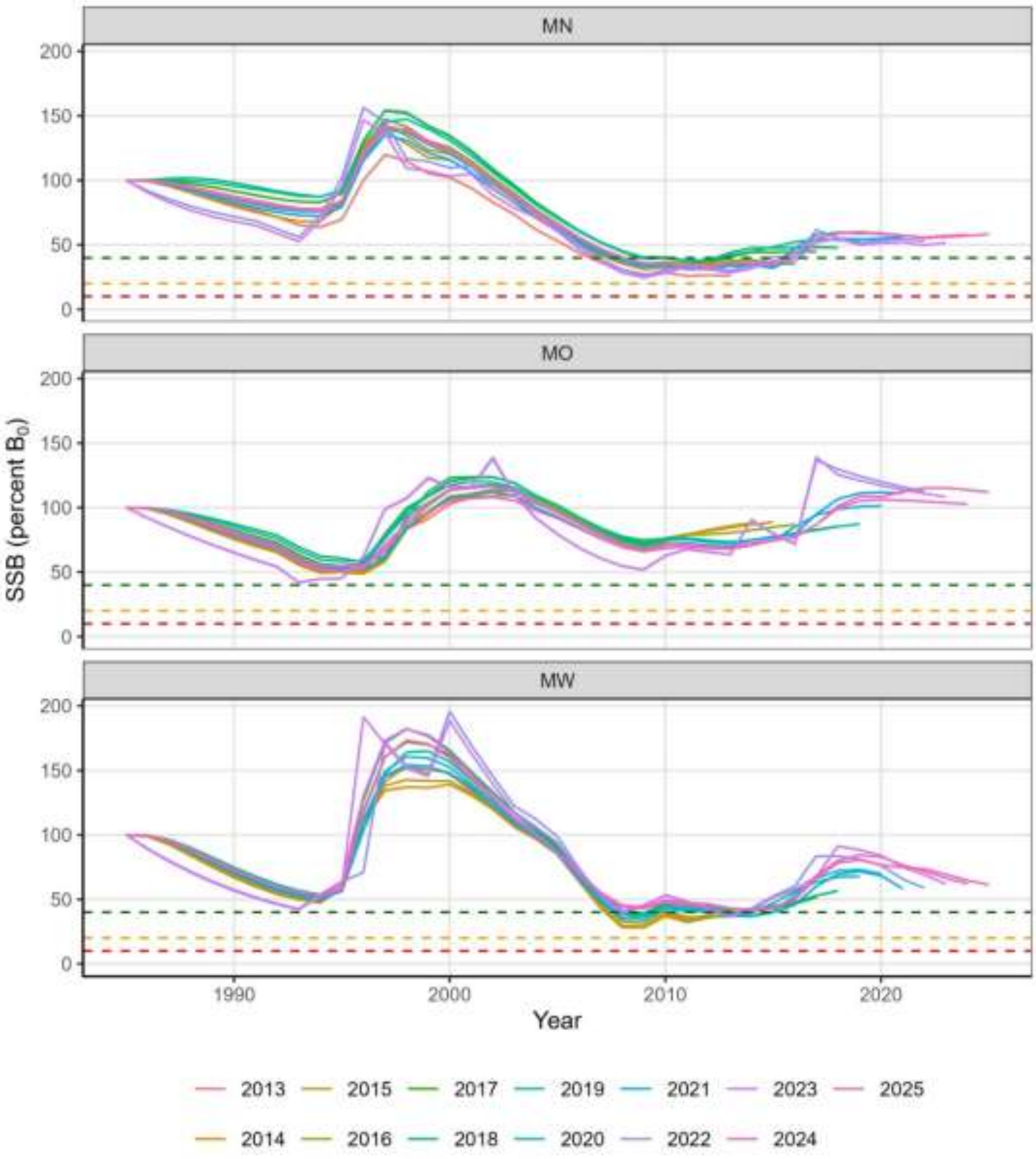

Figure 48: MPD retrospective estimates of spawning-stock biomass (SSB, as a percentage of B_0) for the base case model, by stock (MN, MO, MW), 2013–2025. Each line shows an MPD fit to the model with successive additional years of the most recent data excluded, compared with the full model fitted through to 2026. Dashed horizontal lines show the default hard (10% B_0, red), soft (20% B_0, orange) and target (40% B_0, green) reference points.

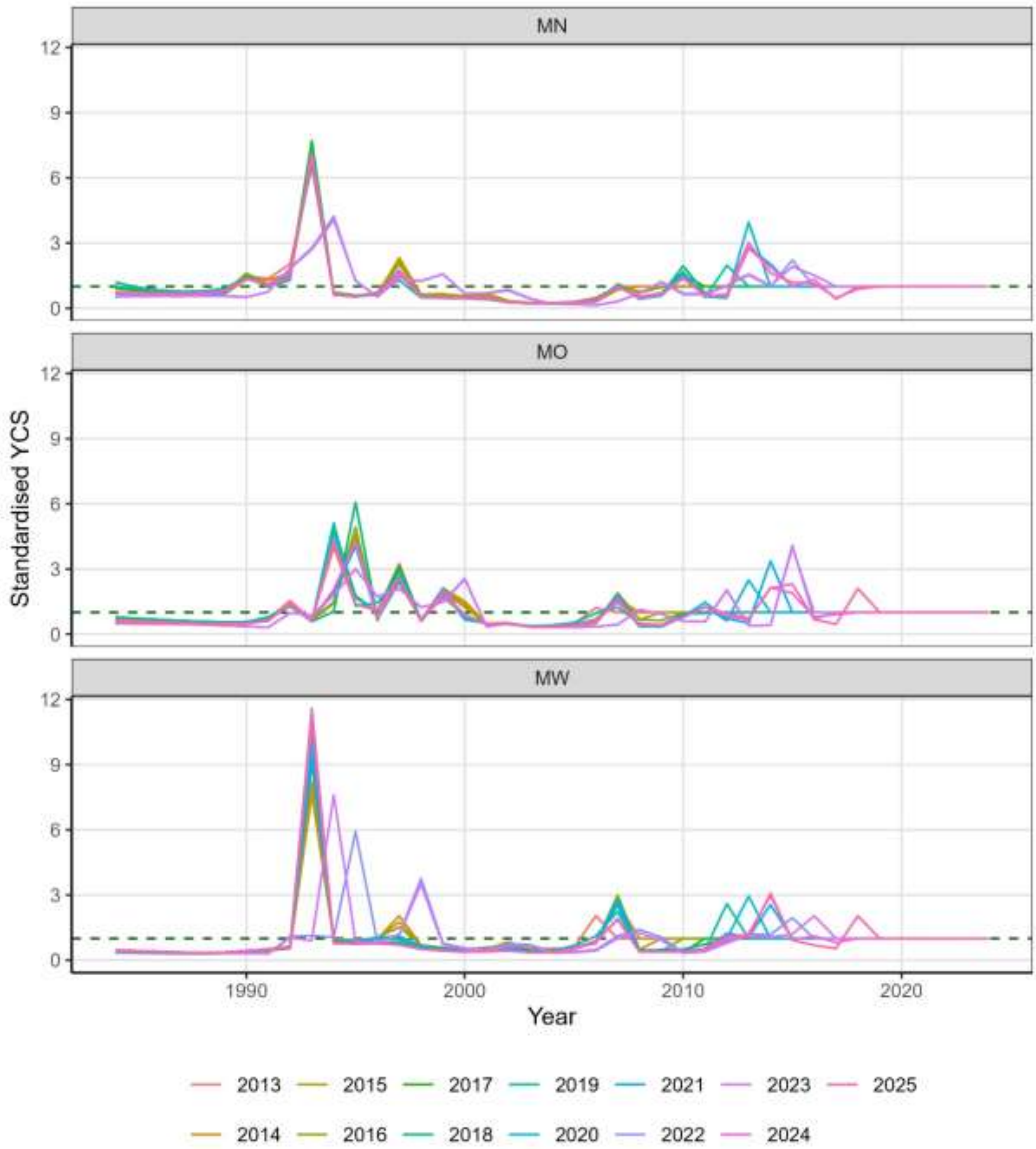

Figure 49: MPD retrospective estimates of standardised year class strength (YCS) for the base case model, by stock (MN, MO, MW), 2013–2025. Each line shows an MPD fit to the model with successive additional years of the most recent data excluded, compared with the full model fitted through to 2026. The dashed horizontal line indicates the long-term mean YCS of 1.

3.4 MCMC results

Plots of the posteriors from the MCMC chains for all estimated parameters (excluding YCS) for the SCI 3 (MN, MO and MW) base case model (02d) are given in Figure 50. Full diagnostic statistics ($\hat{r}$ and effective sample sizes) for all parameters are given in Appendix B.

Overall, most parameters showed acceptable convergence, with $\hat{r} \leq 1.01$ and effective sample sizes above 400. However, a number of parameters – mostly associated with the MO stock and the photographic- and trawl-survey selectivities and catchabilities, and the growth-increment parameters – showed weaker mixing, with $\hat{r}$ up to 1.72 and effective sample sizes as low as about 5 (bulk) and 32 (tail) for the male photographic-survey selectivity a_{50} parameter. The male growth-increment parameters (g_alpha, g_beta for both sexes) and the MO catchability and B_0 parameters also showed $\hat{r}$ in the range 1.02–1.06 and with effective sample sizes lower than 400. This indicates that, while the overall posterior distributions and reported medians and credible intervals are likely to be reasonably reliable, some individual parameters (specifically the photographic-survey male selectivity a_{50}) may benefit from a longer chain length or re-parameterisation. Sensitivity runs that excluded the photo survey, however, gave very similar results to the base case model, and it is unlikely that the poor mixing for these specific parameters impacted the outcomes from the model.

MCMC estimates of year class strengths (YCS) for the MN, MO and MW stocks are summarised in Figure 51. Posterior YCS estimates were uncertain in the earliest years of each stock's time series, with the strongest and most consistently estimated cohorts occurring in the early 1990s for MN and MW, and more moderate above-average cohorts spread across the 1990s and 2000s for MO; recent year classes (post-2023) were assumed equal to the long-term average (YCS=1), as there was little information available to estimate the strength of the most recent cohorts independently.

MCMC estimates of the relative abundance indices (commercial CPUE, photographic survey, and trawl survey) are shown in Figure 52 and indicated a reasonable fit of the MCMC posterior to the observed data across all three stocks, with predicted trajectories tracking the main features of the observed series within the reported confidence intervals. Model estimates of the selectivity parameters (Figure 53) indicated that the relative selectivity of males and females differed for the commercial fishery in both time steps, and that the trawl-survey selectivity ogive also differed between sexes; the photographic-survey selectivity ogive was estimated with considerably more uncertainty than the other selectivities, consistent with the weaker convergence noted above for this parameter.

Estimates of survey catchability (q) were generally within the specified priors. Catchability for the MO stock's CPUE, photographic-survey and trawl-survey indices was less precisely estimated and showed greater sensitivity to the choice of starting value than the corresponding MN and MW estimates, consistent with the smaller number of observations available for MO (Figure 50).

Vulnerable biomass exploitation rates by stock and time step are given in Figure 54. Exploitation rates increased markedly in the MN and MW stocks from around 2010–2011 as catches increased, declined through the mid-2010s, and increased again in recent years; exploitation of MO has been negligible since around 2005 in both time steps.

The base case model estimated the total SCI 3 initial spawning-stock biomass (B_0) as 5687 (95% CIs 4713–7209 t) and the 2025 biomass as 3874 (95% CIs 2868–5355 t), giving a current (2025) stock status of 68% B_0 (95% CIs 46–100% B_0) (Figure 55; Table 11). MN and MW were estimated at 58% B_0 , while MO remained well above the target at 112% B_0.

Table 11: MCMC estimates (t) of B_0 and current (2025) biomass (B_{2025} in t and as a percentage of B_0) for the SCI 3 base case model, by stock (MN, MO, MW) and for the total SCI 3. Values in parentheses are the lower and upper bound of the 95% credible interval.

Stock	B_0 (t)	B_{2025} (t)	B_{2025} (% B_0)
MN	3 110 (2 493–4 314)	1 815 (1 210–2 934)	58.3 (47.9–69.8)
MO	957 (639–1 510)	1 083 (666–1 809)	112.4 (96.8–133.4)
MW	1 553 (1 207–2 195)	899 (520–1 561)	58.0 (42.1–74.2)
SCI 3 (Total)	5 687 (4 713–7 209)	3 874 (2 868–5 355)	67.8 (46.4–99.6)

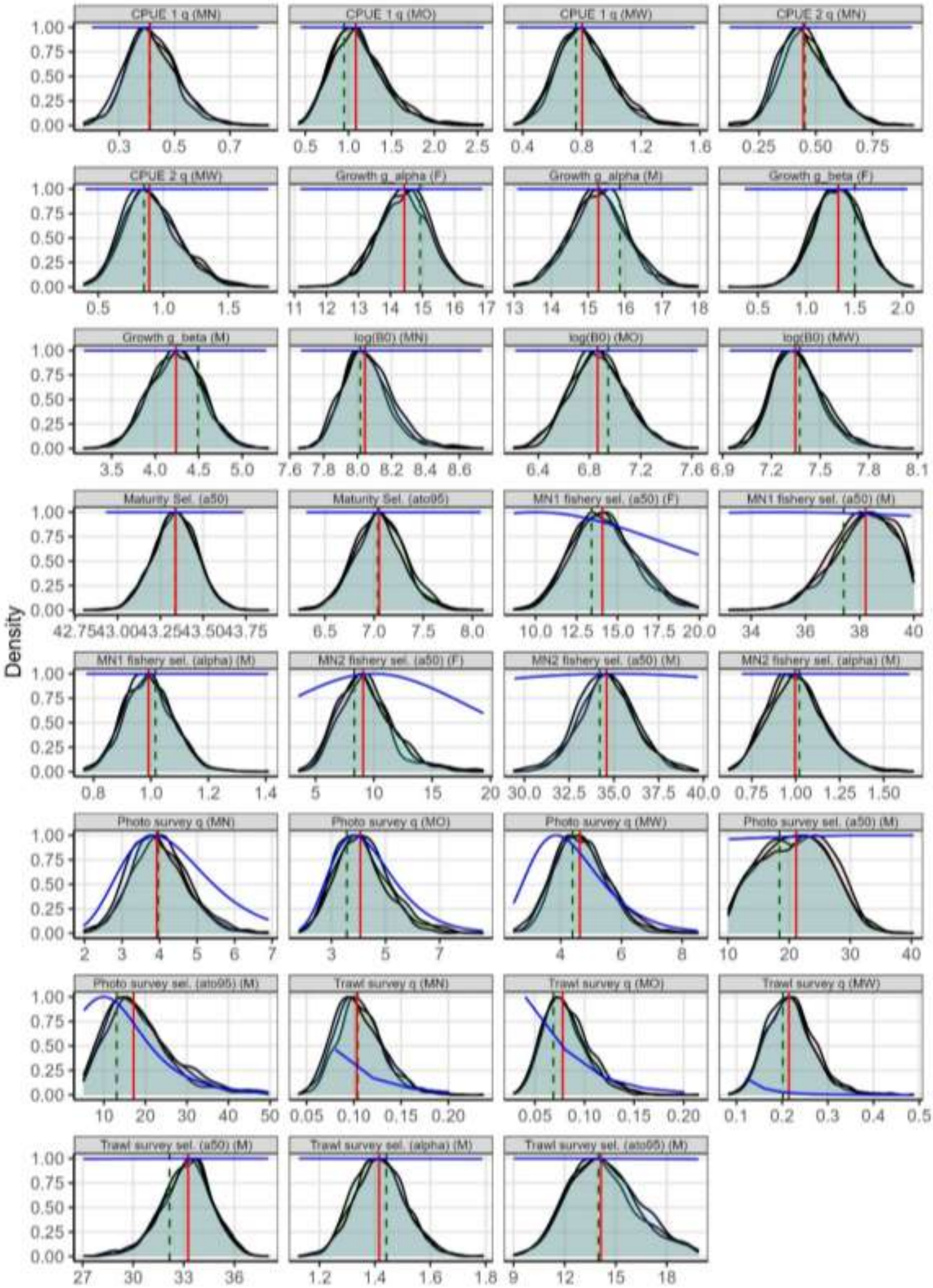

Figure 50: Base case model posterior distributions of estimated parameters (excluding YCS) for the SCI 3 areas (MN, MO, MW) model, pooled across MCMC chains. Priors over the range of estimated posterior values are shown as the blue lines, the median MCMC estimate as the vertical red line, and the MPD (the starting point for the MCMC) as the dashed green line.

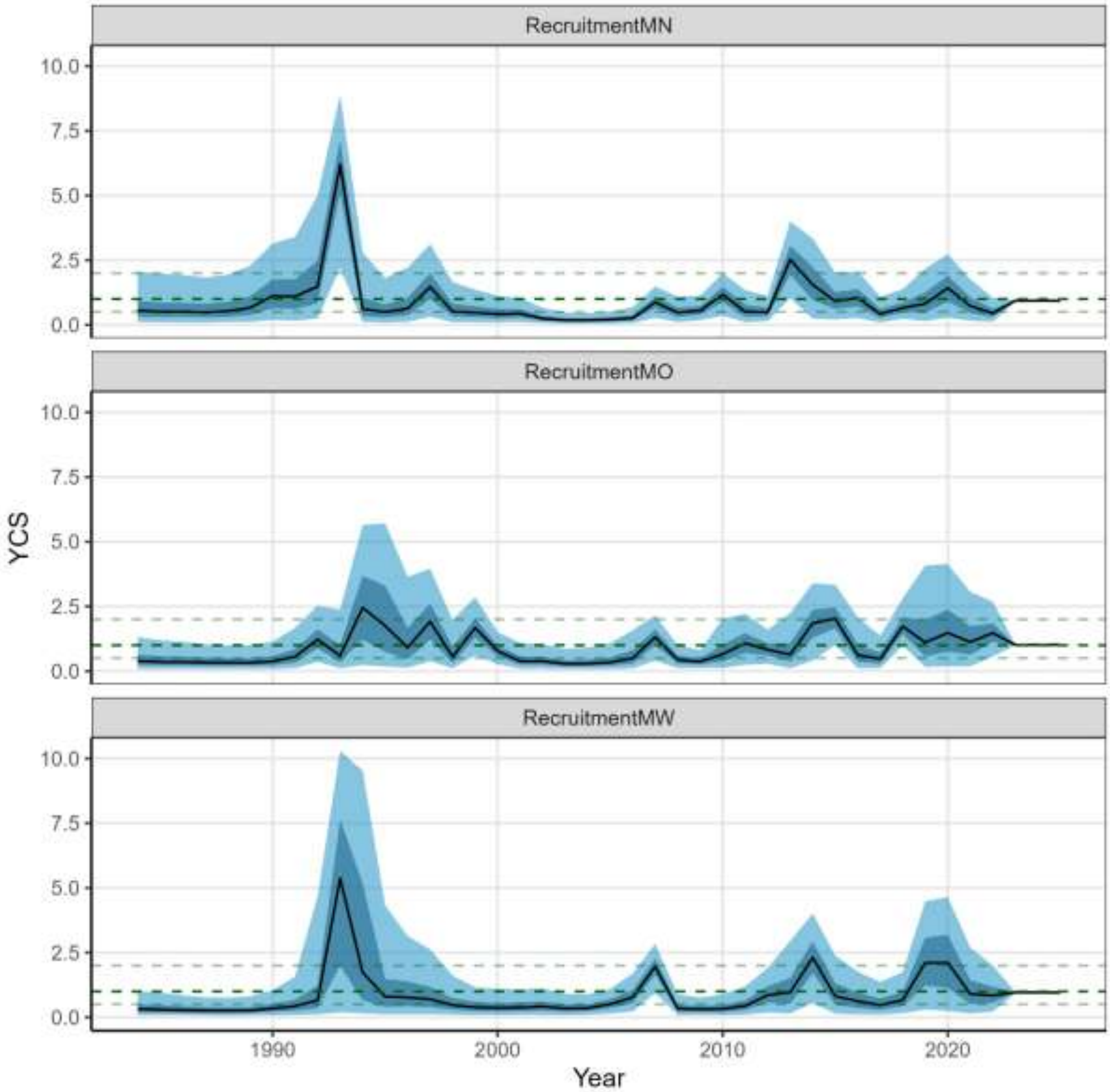

Figure 51: Base case model posterior distribution of year class strength (YCS) for the SCI 3 MN, MO and MW stocks, 1984–2026 (estimated 1984–2022). The solid line indicates the median, the dark shaded area the interquartile range, and the light shaded area the 95% CIs, for each stock. The horizontal dashed green line indicates the long-term average YCS of 1.

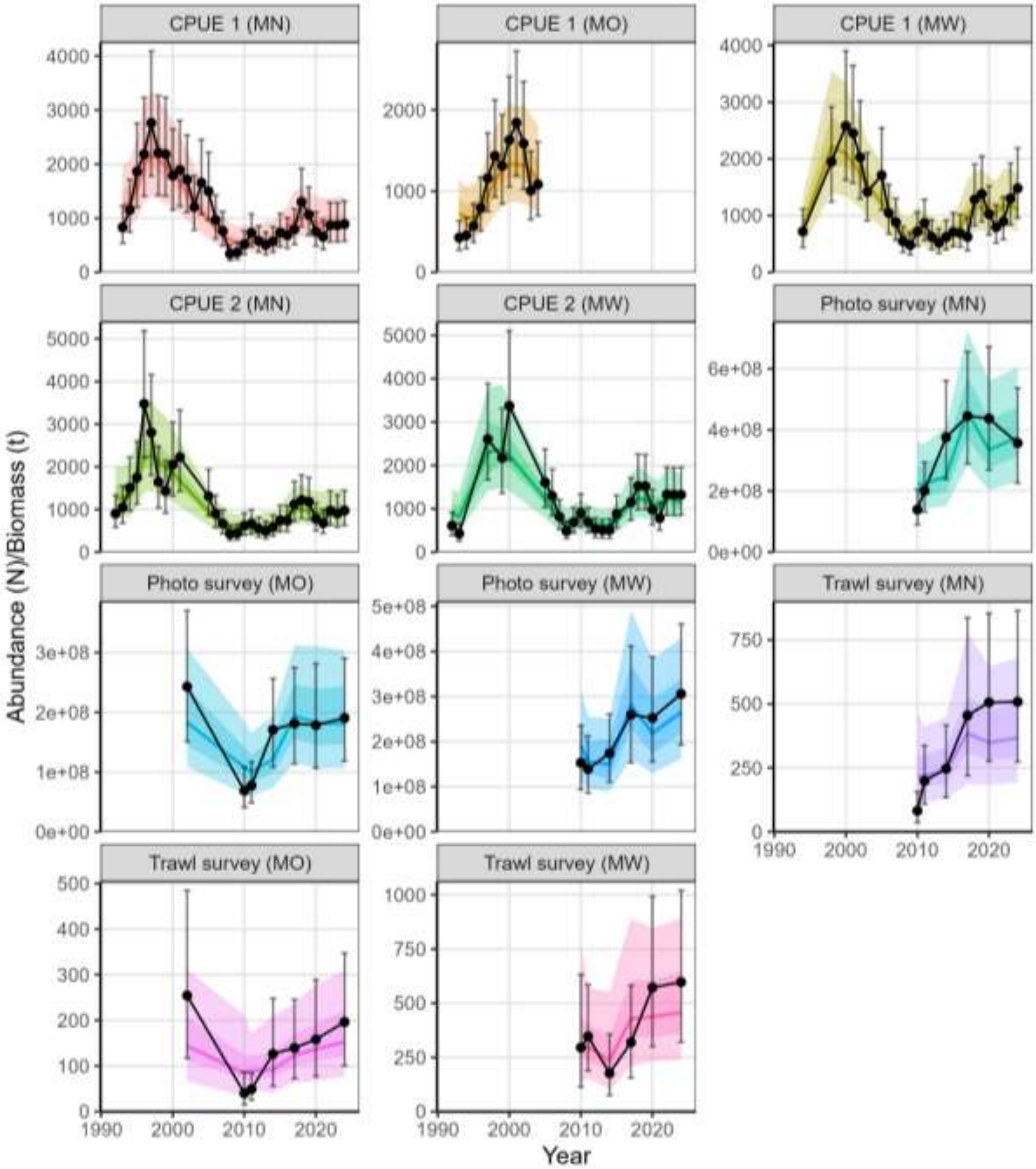

Figure 52: Base case model posterior distribution of the expected values for the commercial CPUE (time steps 1 and 2), photographic survey, and trawl survey relative abundance/biomass indices, by stock (MN, MO, MW). Observed values and 95% confidence intervals are shown as black points with vertical error bars. The coloured line indicates the median MCMC estimate, with the interquartile range (dark shading) and 95% CIs (light shading).

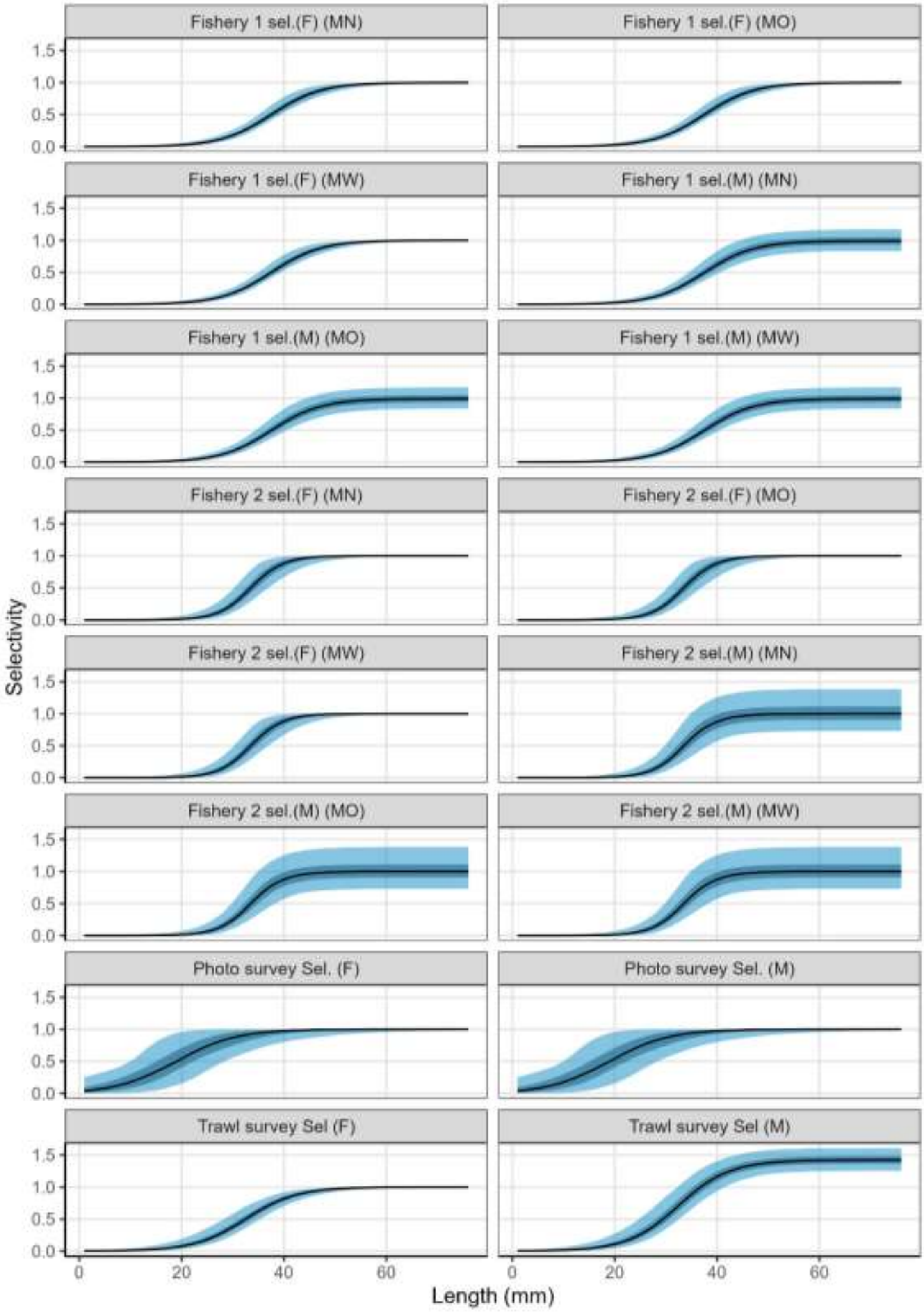

Figure 53: Base case model posterior distribution of the estimated selectivity ogives (by length, mm) for the commercial fishery (time steps 1 and 2, by stock and sex), the photographic survey (bottom, common across stocks), and the trawl survey (bottom, common across stocks). The solid line indicates the median, with the interquartile range (dark shading) and 95% CIs (light shading).

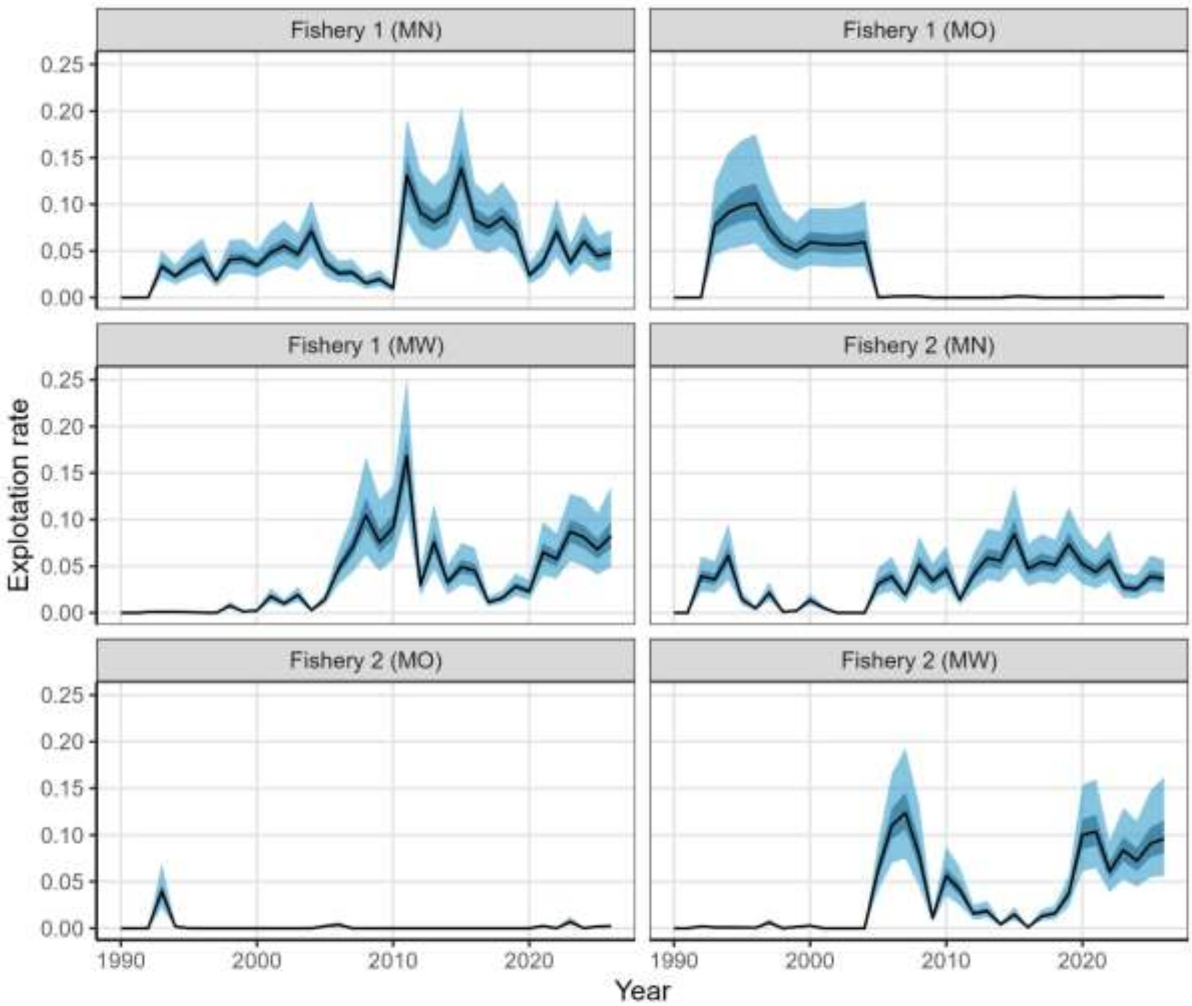

Figure 54: Posterior distribution of the historical (1990–2026) exploitation rates for the commercial fishery (time steps 1 and 2), by stock (MN, MO, MW), for the SCI 3 base case model. The solid line indicates the median trajectory, with the interquartile range (dark shading) and 95% CIs (light shading).

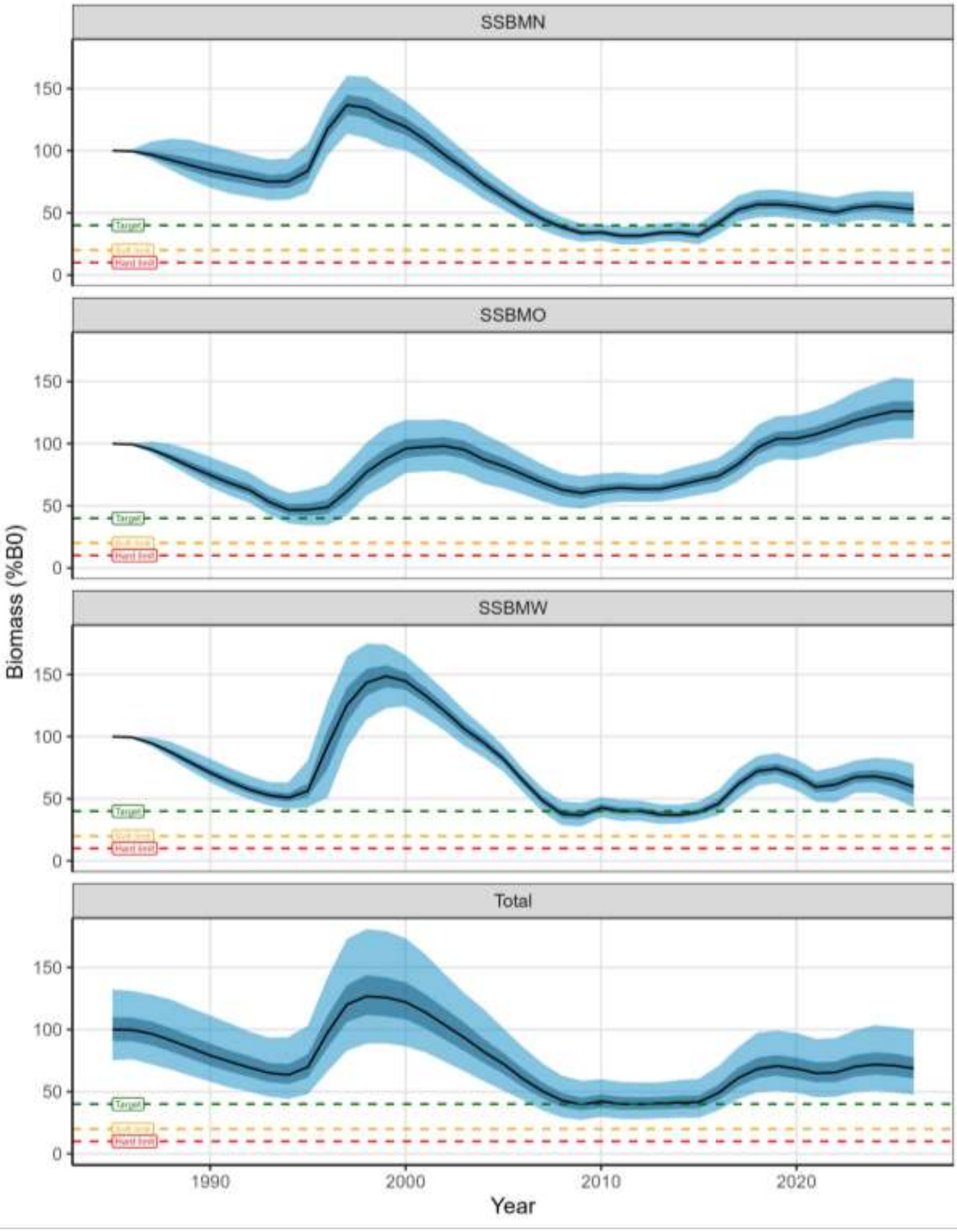

Figure 55: Posterior distribution of the historical (1985–2026) spawning-stock biomass (SSB, as a percentage of B_0) for the SCI 3 MN, MO, MW stocks and the SCI 3 total. The solid line indicates the median, with the interquartile range (dark shading) and 95% CIs (light shading). Target (green, 40% B_0), soft limit (orange, 20% B_0) and hard limit (red, 10% B_0) reference points are shown as horizontal dashed lines.

3.5 Model sensitivity runs

A series of MCMC model sensitivity runs was carried out for the SCI 3 (MN, MO and MW) integrated length-based base case model, using the base case as the starting point for each run. In general, the sensitivity runs considered gave a broadly similar picture of stock status to the base case, with total SCI 3 estimates of current stock status (B_{2026}/B_0) ranging from about 54% to 95% B_0 across all runs, and B_0 ranging from 4108 t to 6397 t (Table 12).

Varying natural mortality (*M*) had a modest effect on estimated stock status: the low-M sensitivity run (M=0.2 y^{-1}) gave a slightly lower total SCI 3 stock status (64.9% B_0) and the high-M (M=0.3 y^{-1}) sensitivity run gave a slightly higher status (70.7% B_0), bracketing the base case estimate of 67.8% B_0. Assuming a common photographic-survey catchability across the MN, MO and MW stocks (rather than estimating it separately for each) made very little difference to the overall result (67.0% B_0).

Sensitivity runs varying the choice of abundance indices had a larger effect on the estimated scale of the stock. Excluding the trawl- and burrow-count-survey calibration (uncalibrated burrow index) gave a total SCI 3 stock status (70.7% B_0) which is similar to the high-M sensitivity run.

Fitting to the trawl survey index alone (trawl index only) resulted in the highest estimates of both initial biomass (6397 t) and current stock status (95.1% B_0) among the sensitivity runs considered, particularly for the MN stock (95.8% B_0), reflecting the more limited information on recent trend available from this index alone relative to the CPUE and burrow-count indices used in the base case. Conversely, replacing the burrow-count index with the visible-scampi index (visible index replacing burrows) gave the lowest estimate of current stock status of any sensitivity run considered (54.1% B_0), and was the only sensitivity run with an appreciable probability of B_{2026} being below the 40% B_0 target for the total SCI 3 stock (Pr=0.97, compared with Pr=1.00 for the base case).

At the stock level, MO consistently showed the highest relative stock status of the three stocks across all sensitivity runs (ranging from 96.8% to 145.3% B_0), remaining well above the default target in every case. MN and MW were more variable between sensitivity runs, ranging from about 43.5% to 95.8% B_0 (MN) and 28.9% to 75.9% B_0 (MW), with the lowest status in both stocks occurring in the sensitivity run where the visible index replaced the burrow index, and the probability of B_{2026} exceeding 40% B_0 falling to 0.85 (MN) and 0.67 (MW) in that case.

None of the sensitivity runs considered changed the overall conclusion that the total SCI 3 stock was at or above the target of 40% B_0 in 2026, although the magnitude of the estimated initial and current biomass, and the degree of confidence in this conclusion, varied with the choice of abundance indices used, and to a lesser extent with the assumed value of natural mortality (Table 12).

A wider set of 16 MPD-level sensitivity runs was also carried out for SCI 3, extending the core MCMC sensitivity runs above to also examine the effect of fitting to individual abundance indices in isolation (CPUE only, CPUE time step 1 only, the burrow-count survey only, the trawl survey only, and the visible-scampi index only), removing informative catchability priors individually or jointly for the photographic and trawl surveys, up- and down-weighting the length-frequency data, and testing two alternative parameterisations of catchability (*q*) around the calibrated base case (Table 13 and Table 14).

The base case run (02d) gave a total SCI 3 B_0 of 5661 t and a current (2026) stock status of 69.2% B_0, consistent with the MCMC base case in Table 11. Most of the 18 MPD sensitivity runs fell within a broadly similar range, with total SCI 3 stock status from about 59% to 81% B_0 for runs that altered prior weighting, mortality, or catchability parameterisation alone (runs 08a/08b, 09a/09b/09c, 10a/11a, 42d/42e, and 50a/50d). Removing both the photographic- and trawl-survey catchability priors together (09c) gave the lowest B_0 (4286 t) and stock status (59.1% B_0) among this group, while down-weighting the length-frequency data (11a) gave one of the higher B_0 estimates (6614 t).

Fitting to individual abundance indices in isolation gave more divergent results. Fitting to the trawl survey alone (07a) gave the highest stock status of any sensitivity run considered (103.4% B_0). Fitting to the visible-scampi index alone (06a) gave a much larger B_0 (8151 t) than the base case, with a current status of 72.3% B_0. Fitting to CPUE time step 1 alone (04a) gave B_0 of 6105 t and a status of 81.4% B_0. Overall, the full set of MPD sensitivity runs spanned a total SCI 3 stock-status range of about 59% to 103% B_0, consistent with the range seen in the core MCMC sensitivity runs (Table 11) and reinforcing the conclusion that the SCI 3 stock is above the default 40% B_0 target under all credible alternative model configurations considered.

Table 12: Results from the integrated length-based model MCMC runs showing B_0, B_{2026} (t), and B_{2026}/B_0 estimates and 95% credible intervals for the base case (shaded) and sensitivity runs for SCI 3 (MN, MO, MW and the SCI 3 total).

Model	MN	MO	MW	SCI 3
Base – 2026 base case				
B_0 (t)	3 110 (2 493–4 314)	957 (639–1 510)	1 553 (1 207–2 195)	5 687 (4 713–7 209)
B_{2026} (t)	1 815 (1 210–2 934)	1 083 (666–1 809)	899 (520–1 561)	3 874 (2 868–5 355)
B_{2026} / B_0 (%)	58.3 (47.9–69.8)	112.4 (96.8–133.4)	58.0 (42.1–74.2)	67.8 (46.4–99.6)
P(B_{2026} > 40% B_0)	1.00	1.00	0.99	1.00
P(B_{2026} < 20% B_0)	0.00	0.00	0.00	0.00
Low *M* – Base with low *M*				
B_0 (t)	3 312 (2 766–4 228)	1 015 (655–1 621)	1 701 (1 365–2 311)	6 078 (5 182–7 380)
B_{2026} (t)	1 788 (1 198–2 767)	1 159 (689–1 969)	940 (552–1 631)	3 957 (2 929–5 439)
B_{2026} / B_0 (%)	53.8 (42.8–66.5)	113.9 (98.5–132.8)	55.2 (39.6–72.4)	64.9 (45.5–93.5)
P(B_{2026} > 40% B_0)	1.00	1.00	0.97	1.00
P(B_{2026} < 20% B_0)	0.00	0.00	0.00	0.00
High *M* – Base with high *M*				
B_0 (t)	2 995 (2 289–4 280)	919 (619–1 436)	1 447 (1 091–2 016)	5 413 (4 373–6 967)
B_{2026} (t)	1 873 (1 201–3 026)	1 029 (636–1 692)	873 (491–1 470)	3 826 (2 783–5 397)
B_{2026} / B_0 (%)	62.3 (51.6–72.9)	111.1 (95.7–132.7)	60.1 (43.8–75.0)	70.7 (47.9–103.7)
P(B_{2026} > 40% B_0)	1.00	1.00	0.99	1.00
P(B_{2026} < 20% B_0)	0.00	0.00	0.00	0.00
Same photo *q* – Base with same photo-survey *q* (MN, MO, MW)				
B_0 (t)	2 962 (2 419–3 878)	909 (685–1 262)	1 636 (1 286–2 233)	5 503 (4 514–7 223)
B_{2026} (t)	1 671 (1 152–2 539)	1 029 (723–1 500)	986 (605–1 611)	3 700 (2 644–5 435)
B_{2026} / B_0 (%)	56.4 (46.4–67.3)	112.6 (97.2–133.6)	60.2 (45.7–75.0)	67.0 (43.9–101.9)
P(B_{2026} > 40% B_0)	1.00	1.00	1.00	0.99
P(B_{2026} < 20% B_0)	0.00	0.00	0.00	0.00

Table 12 (continued): Results from the integrated length-based model MCMC runs showing B_0, B_{2026} (t), and B_{2026}/B_0 estimates and 95% credible intervals for the base case (shaded) and sensitivity runs for SCI 3 (MN, MO, MW and the SCI 3 total).

Uncalibrated burrow index – Base with uncalibrated burrow-count index				
B_0 (t)	3 189 (2 514–4 286)	910 (583–1 483)	1 544 (1 223–2 141)	5 715 (4 736–7 091)
B_{2026} (t)	1 931 (1 270–3 023)	1 103 (637–1 973)	926 (558–1 579)	4 056 (2 933–5 602)
B_{2026} / B_0 (%)	60.6 (49.7–72.2)	120.8 (101.5–145.3)	59.8 (43.9–76.3)	70.7 (48.6–102.7)
P(B_{2026} > 40% B_0)	1.00	1.00	0.99	1.00
P(B_{2026} < 20% B_0)	0.00	0.00	0.00	0.00
Trawl index only – Base fitted to the trawl survey index only				
B_0 (t)	3 414 (2 613–4 847)	908 (589–1 568)	1 968 (1 397–3 052)	6 397 (5 155–8 321)
B_{2026} (t)	3 280 (1 842–5 919)	1 134 (646–2 223)	1 500 (680–3 018)	6 090 (4 130–9 186)
B_{2026} / B_0 (%)	95.8 (68.0–128.8)	124.5 (100.3–155.5)	75.9 (45.8–114.2)	95.1 (58.9–152.0)
P(B_{2026} > 40% B_0)	1.00	1.00	0.99	1.00
P(B_{2026} < 20% B_0)	0.00	0.00	0.00	0.00
Visible index replacing burrow – Base with visible-scampi index replacing the burrow-count index				
B_0 (t)	2 335 (2 035–2 859)	482 (409–668)	1 254 (1 039–1 578)	4 108 (3 643–4 779)
B_{2026} (t)	1 068 (735–1 605)	569 (409–919)	545 (307–899)	2 222 (1 660–2 983)
B_{2026} / B_0 (%)	45.6 (35.7–56.8)	118.1 (96.9–145.4)	43.5 (28.9–58.7)	54.1 (39.2–74.2)
P(B_{2026} > 40% B_0)	0.85	1.00	0.67	0.97
P(B_{2026} < 20% B_0)	0.00	0.00	0.00	0.00

Table 13: MPD estimates of B_0 (t) for 16 MPD-level sensitivity runs for SCI 3, by stock (MN, MO, MW) and the SCI 3 total. The base case run (02d) is shaded.

Model	B_0 MN	B_0 MO	B_0 MW	B_0 SCI 3
(02a) 2025 initial (catch LFs)-PE	3 087	1 036	1 540	5 664
(02d) 2025 base case	3 027	1 039	1 595	5 660
(04a) 2025 CPUE (timestep 1)	3 206	1 123	1 777	6 105
(06a) 2025 Visible	6 374	468	1 309	8 151
(07a) 2025 Trawl	3 176	912	1 805	5 893
(08a) 2025 LowM	3 251	1 200	1 765	6 216
(08b) 2025 HighM	3 041	1 123	1 463	5 626
(09a) 2025 No photo prior	3 015	1 184	1 500	5 699
(09b) 2025 No trawl prior	2 884	830	1 381	5 095
(09c) 2025 No photo trawl prior	2 543	475	1 267	4 286
(10a) 2025 upweight LFs	2 211	1 027	1 151	4 389
(11a) 2025 downweight LFs	3 657	1 115	1 843	6 614
(42d) 2025 calibrated low M	3 191	1 111	1 756	6 058
(42e) 2025 calibrated high M	2 945	1 009	1 444	5 398
(50a) 2025 initial (catch LFs)-PE_q	2 860	792	1 549	5 201
(50d) 2025 calibrated_q	2 944	914	1 660	5 519

Table 14: MPD estimates of current (2026) stock status (as a percentage of B_0) for 16 MPD-level sensitivity runs for SCI 3, by stock (MN, MO, MW) and at the total SCI 3. The base case run (02d) is shaded.

Model	% B_0 MN	% B_0 MO	% B_0 MW	% B_0 SCI3
(02a) 2025 initial (catch LFs)-PE	60.1	129.6	60.1	72.8
(02d) 2025 base case	58.2	118.5	58.1	69.2
(04a) 2025 CPUE (timestep 1)	69.5	137.2	67.6	81.4
(06a) 2025 Visible	75.4	112.7	42.8	72.3
(07a) 2025 Trawl	102.1	137.4	88.7	103.4
(08a) 2025 LowM	55.8	130.3	59.9	71.4
(08b) 2025 HighM	64.5	128.3	60.3	76.1
(09a) 2025 No photo prior	59.2	131.3	58.7	74.1
(09b) 2025 No trawl prior	59.8	132.1	55.2	70.3
(09c) 2025 No photo trawl prior	53.8	116.7	48.0	59.1
(10a) 2025 upweight LFs	47.9	140.3	40.2	67.5
(11a) 2025 downweight LFs	64.5	123.7	65.2	74.7
(42d) 2025 calibrated low M	53.1	120.3	56.4	66.4
(42e) 2025 calibrated high M	62.7	116.5	59.9	72.0
(50a) 2025 initial (catch LFs)-PE_q	57.5	122.6	53.2	66.1
(50d) 2025 calibrated_q	57.1	117.0	59.9	67.9

4. SURPLUS PRODUCTION MODELS

MCMC mixing was good for all of the surplus production model parameters (Figure 56), and the posteriors updated the priors for the shared parameters (r, z, σ_p, τ) and for K in four of the five stocks (Figure 57). The exception was SCI 4AW (K[5]), for which the posterior closely tracked the prior, indicating that the available abundance and catch series for this stock were relatively uninformative about carrying capacity. The surplus production model fits to all abundance indices (commercial CPUE, trawl survey, and photo survey) were good across stocks and series (Figure 58).

Estimates of the parameters assumed common across stocks (intrinsic growth rate r, shape parameter z, process error σ_p, and additional observation error τ) are given in Table 15, together with the implied exploitation rate at 40% K (U_{40}). The posterior median of z (0.913, 95% CIs 0.605–1.370) was close to one, indicating production dynamics intermediate between, but closer to the symmetric

Schaefer form than the Fox form. The posterior median intrinsic growth rate was 0.287 (95% CIs 0.198–0.398).

Surplus production model stock-specific estimates of carrying capacity (K) ranged from a posterior median of 475 t for SCI 4AW to 3694 t for SCI 3MN (Table 16), and were broadly comparable in order of magnitude to independent estimates of virgin biomass (B_0) from the corresponding integrated length based stock assessments for SCI 3 in MN, MO, and MW (3100 t, 960 t, and 1550 t respectively), consistent with the shared-parameter surplus production approach providing similar productivity signals to the length-structured assessment where comparable estimates exist.

Surplus production model posterior estimates of annual process error indicated a substantial positive deviation in biomass during the 1990s across all stocks, consistent with a large recruitment event during this period (Figure 58).

The estimated surplus production model current biomass (B_{2025}) relative to carrying capacity (Table 16) indicated that all five stocks were above the 40% K target in the 2025 fishing year, with posterior median B_{2025}/K ranging from 0.492 (SCI 4AE) to 1.213 (SCI 4AW).

Overall, the shared-parameter Bayesian surplus production model provided a consistent and well-converged characterisation of stock productivity across the five scampi stocks, with all abundance series well fitted and all stocks estimated to be above the 40% K target reference point in the most recent assessment year.

Table 15: Surplus production model posterior median and 95% credible interval for model parameters assumed common across all five scampi stocks.

Parameter	Median	2.5%	97.5%
r (intrinsic growth rate)	0.287	0.198	0.398
z (shape parameter)	0.913	0.605	1.370
σ_p (process error)	0.319	0.271	0.382
τ (additional observation error)	0.169	0.124	0.223
U40 (exploitation rate at 40% K)	0.178	0.122	0.250

Table 16: Surplus production model stock-specific posterior median (95% credible interval) for carrying capacity (K), estimated 2025 biomass (B_{2025}), relative biomass status (B_{2025}/K), and projected 2031 biomass (B_{2031}), all in tonnes except B_{2025}/K.

Stock	K	B_{2025}	B_{2025} / K	B_{2031}
SCI 3MN	3 693.6 (2 188.5–6 998.7)	2 646.0 (1 256.2–5 347.6)	0.678 (0.337–1.459)	3 000.9 (609.5–6 403.7)
SCI 3MO	788.1 (460.3–1 500.0)	907.3 (360.3–1 935.7)	1.106 (0.508–2.184)	886.6 (141.6–1 907.6)
SCI 3MW	2 659.4 (1 457.5–5 213.9)	2 638.8 (1 195.8–5 594.2)	0.934 (0.479–1.864)	2 262.7 (175.0–5 399.8)
SCI 4AE	1 248.4 (664.2–2 600.9)	826.0 (201.0–2 218.9)	0.492 (0.303–0.781)	1006.3 (1.0–2 824.1)
SCI 4AW	475.0 (201.9–1221.0)	543.6 (161.4–1402.2)	1.213 (0.595–2.306)	497.9 (1.0–1 496.6)

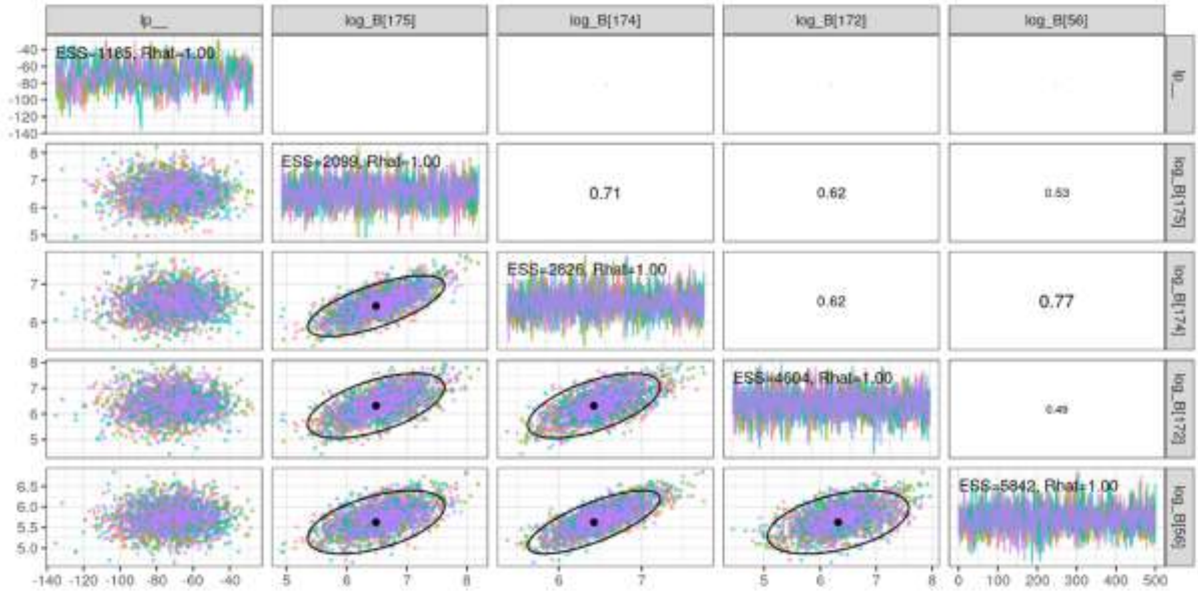

Figure 56: Surplus production model MCMC trace plots with effective sample size (ESS) and Rhat statistic for each parameter (diagonal), pair plots (lower triangle), and correlation coefficients (upper triangle) for the five slowest mixing model parameters.

Figure 57: Surplus production model prior versus posterior for all parameters.

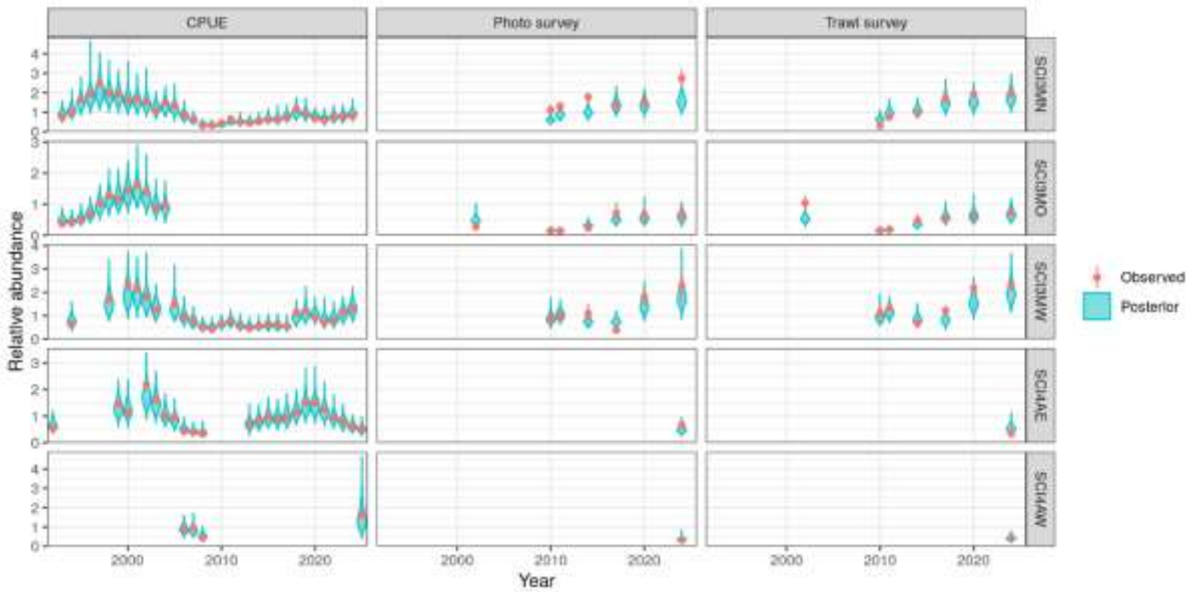

Figure 58: Surplus production model fit to abundance indices by year

5. PROJECTIONS AND YIELDS

5.1 Integrated assessment projections

Two sets of projection runs were carried out for the SCI 3 (MN, MO and MW) integrated length-based base case model, whereby the future annual catch for 2027–2031 was set at the level of the current TACC, with the catch split between stocks and time steps held at the values used for the final model year. Two alternative assumptions about future recruitment were considered: future year class strengths (YCS) resampled from the full set of estimated YCS (1984–2022, 'all YCS'), and future YCS resampled from the more recent estimated YCS only (2013–2022, 'recent YCS'), the latter reflecting the generally higher recruitment estimated over the most recent decade.

Results are shown in Table 17 for the estimated stock status (B_{2026} and B_{2031}, in tonnes and as a percentage of B_0) and in Table 18 for the projected probability of being above the target (40% B_0) or below the soft or hard limits (20% or 10% B_0 respectively), for each stock and for total SCI 3, under both recruitment assumptions. Figure 59 shows the SSB trajectories (as a percentage of B_0) under the assumption of TACC catch and recent (2013–2022) YCS, and Figure 60 shows the equivalent projection assuming TACC catch and the full (1985–2020) set of estimated YCS.

For the total SCI 3, stock status was projected to decline slightly over the five-year projection period under the all-YCS assumption, from a median of about 64% B_0 in 2026 to about 55% B_0 in 2031, as future recruitment set to the long-term average was insufficient to fully offset removals at the TACC; the probability of B_{2031} remaining above the 40% B_0 target fell from 1.00 in 2026 to 0.87 in 2031 under this assumption, although the probability of being below either the soft or hard limit remained low throughout (≤0.001). Under the recent-YCS assumption, stock status was instead projected to increase over the same period, from about 67% B_0 in 2026 to about 75% B_0 in 2031, with the probability of B_{2031} remaining above the target staying high at 0.99 (Table 17 and Table 18).

The projected pattern differed between stocks. MN and MW were projected to remain close to, or decline only slightly below, their 2026 levels under the all-YCS assumption (MN: 51.6% to 49.3% B_0; MW: 57.9% to 47.1% B_0), with the probability of remaining above the target falling to 0.67 (MN) and 0.61 (MW) by 2031, and a small but non-negligible probability of B_{2031} being below the soft limit (0.035 for MN, 0.077 for MW) or, for MW, the hard limit (0.015). Under the recent-YCS assumption, both stocks instead increased materially (MN: 54.2% to 66.6% B_0; MW: 61.9% to 75.6% B_0), with the probability of remaining above the target staying high at 0.90 (MN) and 0.93 (MW), and the probability of falling below either limit close to zero. MO, which started the projection period well above the target under both scenarios, was projected to decline somewhat under both recruitment assumptions, from about 125.8% to 89.3% B_0 (all YCS) and from about 129.1% to 114.9% B_0 (recent YCS), but remained virtually certain ($P \geq 0.996$) to stay above the target, and had essentially no probability of falling below either limit, in every case considered.

Overall, the projections indicate that the total SCI 3 stock is very likely to remain above the 40% B_0 target under TACC catches over the next five years regardless of the recruitment assumption used, although the probability of MN and, in particular, MW falling below the target is appreciably higher if future recruitment reverts to the long-term average rather than continuing at the levels estimated over the most recent decade (Table 18).

Table 17: Estimates of B_{2026} and B_{2031} (t and as a percentage of B_0) and 95% credible intervals for the SCI 3 base case model (MN, MO, MW and the SCI 3 total), assuming future catch equal to the TACC and future recruitment resampled from either the full (1984–2022) or recent (2013–2022) set of estimated year class strengths (YCS). 95% credible intervals are not shown for the SCI 3 total as they are not directly additive across stocks.

Stock	Future YCS	B_{2026} (t)	B_{2026} (% B_0)	B_{2031} (t)	B_{2031} (% B_0)
MN	All (1984–2022)	1 520 (930–2 750)	51.6 (37.4–81.1)	1 482 (492–4 083)	49.3 (18.1–129.4)
MN	Recent (2013–2022)	1 604 (965–2 631)	54.2 (38.9–75.4)	1 976 (772–3 785)	66.6 (28.9–119.3)
MO	All (1984–2022)	1 251 (766–2 192)	125.8 (102.5–156.6)	888 (384–1 866)	89.3 (50.0–147.5)
MO	Recent (2013–2022)	1 280 (776–2 295)	129.1 (103.9–160.6)	1 142 (524–2 326)	114.9 (68.2–175.3)
MW	All (1984–2022)	883 (485–1 655)	57.9 (38.9–91.5)	732 (177–2 347)	47.1 (13.0–140.8)
MW	Recent (2013–2022)	946 (540–1 664)	61.9 (42.1–89.8)	1 153 (424–2 342)	75.6 (31.3–137.6)
SCI 3	All (1984–2022)	3 655	64.3	3 102	54.5
SCI 3	Recent (2013–2022)	3 830	67.3	4 271	75.1

Table 18: The estimated projected probability of B_{2026} and B_{2031} being above the target (40% B_0), and of B2031 being below the soft (20% B_0) or hard (10% B_0) limits, for the SCI 3 base case model (MN, MO, MW and the SCI 3 total), assuming future catch equal to the TACC and future recruitment resampled from either the full (1984–2022) or recent (2013–2022) set of estimated year class strengths (YCS).

Stock	Future YCS	P(B_{2026} >40% B_0)	P(B_{2031}>40% B_0)	P(B_{2031}<20% B_0)	P(B_{2031}<10% B_0)
MN	All (1984–2022)	0.94	0.67	0.035	0.004
MN	Recent (2013–2022)	0.96	0.90	0.006	0.000
MO	All (1984–2022)	1.00	1.00	0.000	0.000
MO	Recent (2013–2022)	1.00	1.00	0.000	0.000
MW	All (1984–2022)	0.97	0.61	0.077	0.015
MW	Recent (2013–2022)	0.99	0.93	0.005	0.001
SCI 3	All (1984–2022)	1.00	0.87	0.001	0.000
SCI 3	Recent (2013–2022)	1.00	0.99	0.000	0.000

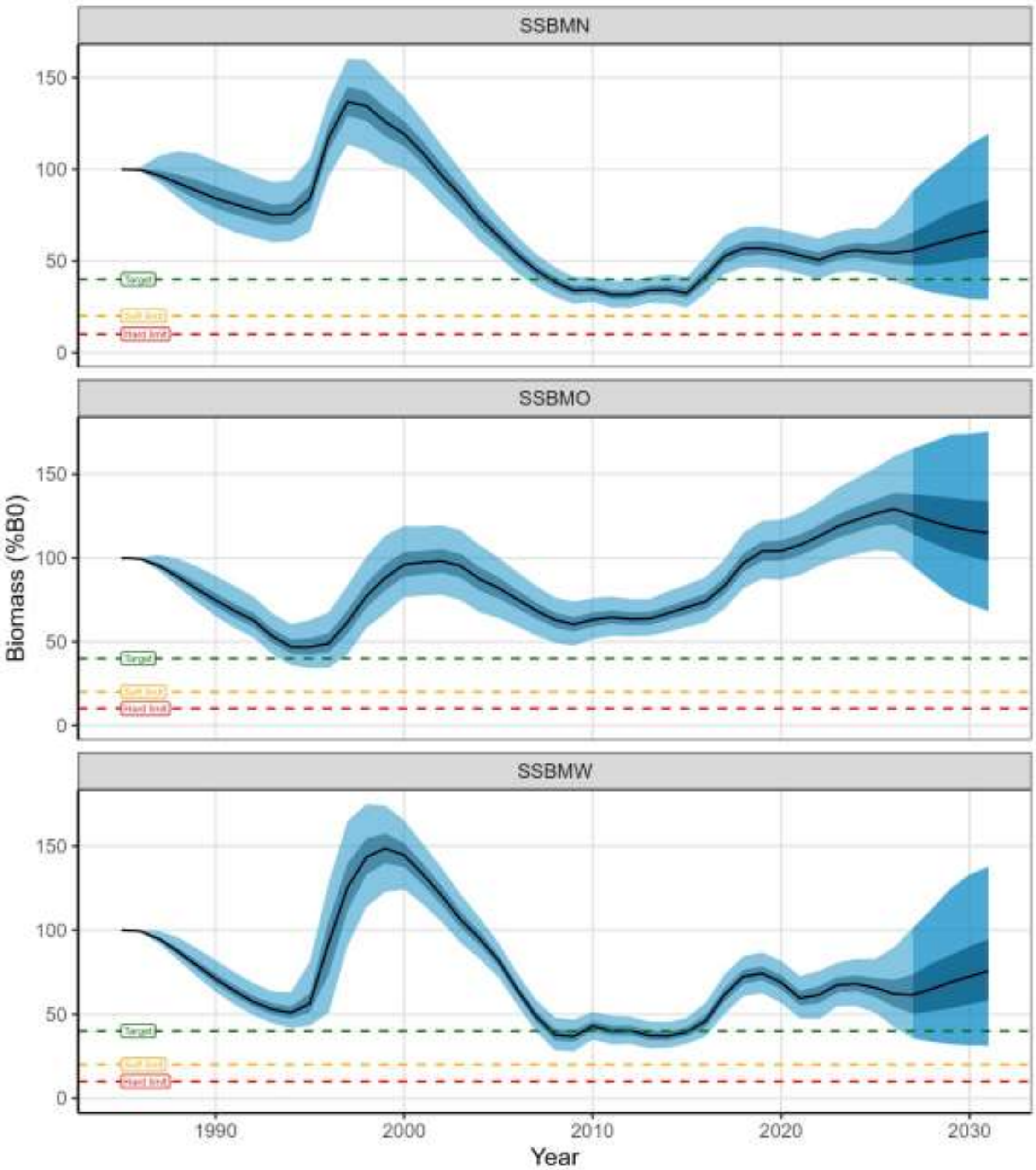

Figure 59: Posterior distribution of the historical (1985–2025) and projected (2026–2031, dark shaded region) spawning-stock biomass (SSB) as a percentage of B_0 for the SCI 3 MN, MO and MW stocks, assuming future catch equal to the TACC and recruitment resampled from the recent (2013–2022) estimated year class strengths. The solid line indicates the median trajectory, the dark shaded area indicates the interquartile range, and the light shaded area indicates the 95% credible interval. Horizontal dashed lines indicate the target (green, 40% B_0), soft limit (orange, 20% B_0), and hard limit (red, 10% B_0).

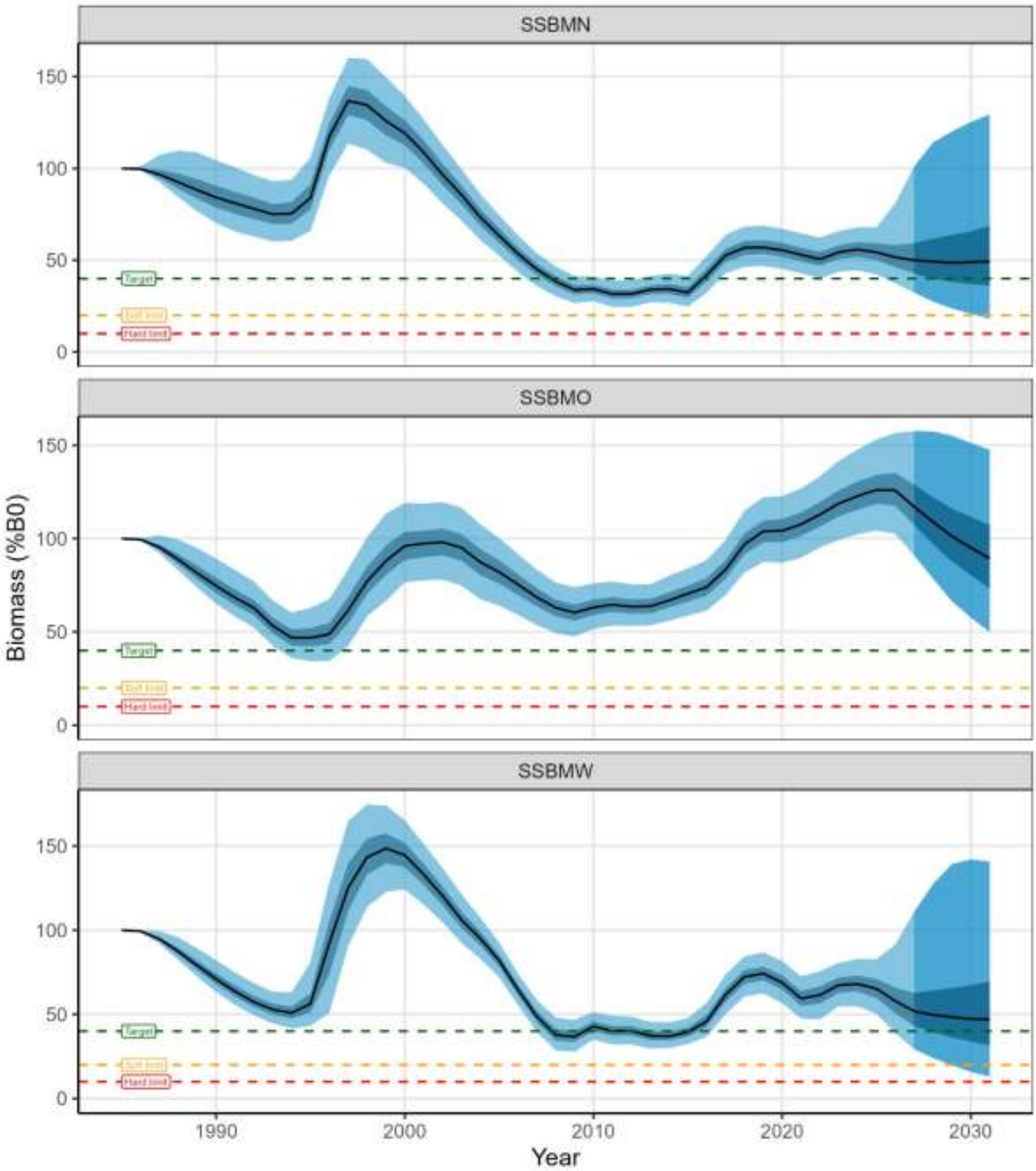

Figure 60: Posterior distribution of the historical (1985–2025) and projected (2026–2031, dark shaded region) spawning-stock biomass (SSB) as a percentage of B_0 for the SCI 3 MN, MO and MW stocks, assuming future catch equal to the TACC and recruitment resampled from the full (1984–2022) set of estimated year class strengths. The solid line indicates the median trajectory, the dark shaded area indicates the interquartile range, and the light shaded area indicates the 95% credible interval. Horizontal dashed lines indicate the target (green, 40% B_0), soft limit (orange, 20% B_0), and hard limit (red, 10% B_0).

5.2 Surplus production model projections

Projected biomass to 2031, based on catch continuing at recent levels and process error drawn from the mean and standard deviation of the 2015–2024 period, indicated that all stocks were expected to remain above 40% *K* over the projection period, although uncertainty intervals were wide, particularly for SCI 4AE and SCI 4AW where the lower bound of the projection approached zero (see Table 16 above).

6. DISCUSSION

This report provides the first integrated length-based stock assessment of scampi in SCI 3 (areas MN, MO, and MW) implemented in Casal2, updating the earlier CASAL assessment of McGregor et al. (2022), together with the first assessment for SCI 4A. As part of this work the catch-effort indices were re-estimated using GAMs, a Chatham Rise-specific length-weight relationship was derived for the first time, and the resource survey series were updated to include the 2024 trawl and photographic surveys, which extended the photographic survey to SCI 4A (areas 4AE and 4AW) for the first time (Wieczorek et al. 2024). In addition to the integrated assessment, a shared-parameter Bayesian state-space surplus production model was fitted jointly to all five scampi stocks (SCI 3 MN, MO, and MW, and SCI 4A east and west), providing a consistent basis for assessing the data-limited SCI 4A stocks alongside the more data-rich SCI 3 stocks.

The conversion of the length-based assessment from CASAL to Casal2 was validated by reproducing the McGregor et al. (2022) base case using the same model structure, parameters, and observations. The CASAL and Casal2 implementations gave very similar estimates of initial and current biomass, SSB trajectories, objective-function components, and year class strengths at both the MPD and MCMC levels. This provides confidence that the updated length-based implementation in Casal2 did not introduce material differences in model behaviour or stock-status estimates, and that differences between this assessment and the previous one reflect the additional data and revised model assumptions rather than the change of software platform.

For the SCI 3 stock as a whole, the base case model estimated initial spawning-stock biomass (B_0) at 5687 t (95% CI 4713–7209 t) and current biomass at 3874 t (95% CI 2868–5355 t), corresponding to a current stock status of about 68% B_0 (95% CI 46–100%). The stock is therefore assessed as Very Likely (> 90%) to be at or above the 40% B_0 management target and Exceptionally Unlikely (< 1%) to be below the soft (20% B_0) or hard (10% B_0) limits. This overall picture was robust across the range of MCMC and MPD sensitivity runs considered, which spanned a total SCI 3 stock status of roughly 54% to 103% B_0: none of the sensitivity runs changed the conclusion that the total SCI 3 stock was at or above the target. The status of the stock was, however, somewhat sensitive to the choice of abundance index, with the trawl-survey-only run giving the highest status (95% B_0) and the run replacing the burrow-count index with the visible-scampi index giving the lowest (54% B_0). This sensitivity analysis reflects the limited contrast among, and differing recent trends in, the available indices, and reinforces the value of maintaining the full suite of CPUE, trawl-survey, and photographic-survey series.

At the area level the three SCI 3 stocks showed contrasting dynamics. MN and MW followed a similar trajectory, rising to a peak in the late 1990s, declining to a minimum close to or below the soft limit around 2008–2010, and recovering to about 58% B_0 at present. MO declined early in the time series but has since increased and remained well above the target throughout, at about 112% B_0 currently, reflecting the substantial reduction in catch from this area following the introduction of scampi to the QMS in 2004. Although the total SCI 3 stock is above the target, exploitation rates in MN and MW increased again in recent years as catch increased, and overfishing ($U > U_{40\%B0}$) was estimated to be Likely (> 60%) to be occurring in MW. This stock structure is an important consideration for management, because catch is not evenly distributed among the areas and the aggregate status masks the more heavily exploited MN and MW stocks.

The surplus production model was applied alongside the integrated length-based assessment for three connected reasons; the main differences between the two approaches are summarised in Table 19. First, the surplus production model is structurally much simpler than the integrated model: it requires fewer assumptions and parameters, depends only on catch and relative abundance indices rather than on the biological and length-composition data needed by the integrated model, and is faster to fit and easier to interpret. Second, where the two approaches could be compared directly — for the three SCI 3 stocks — they gave very similar answers. The stock-specific carrying capacity (*K*) estimates from the surplus production model (3694 t for MN, 788 t for MO, and 2659 t for MW) were of the same order of magnitude as the corresponding B_0 estimates from the integrated assessment (about 3100 t, 960 t, and 1550 t), and both approaches estimated all three SCI 3 stocks to be above their respective target reference points. This agreement between two structurally different models, fitted to the same abundance information, increases confidence in the SCI 3 assessment and demonstrates that the simpler surplus production model is able to reproduce the stock dynamics and status estimated by the more complex integrated model for these stocks. Third, and most importantly, because the surplus production model performed well for SCI 3 and does not require the biological and length-composition data that are unavailable for SCI 4A, it could be extended to provide the only quantitative assessment of the data-limited SCI 4A east (4AE) and SCI 4A west (4AW) stocks, fitted jointly with the SCI 3 stocks in a single shared-parameter model. The surplus production model estimated a shape parameter (z=0.913) close to the symmetric Schaefer form and an intrinsic growth rate (r=0.287), and estimated all five stocks, including both SCI 4A stocks, to be above the 40% *K* target in the most recent year.

A recurring feature of both modelling approaches was a marked, broadly synchronous increase in productivity across the stocks during the 1990s. In the integrated assessment this appeared as very strong estimated year classes in the early 1990s (most pronounced for MW and MN), and in the surplus production model as a large positive process-error deviation over the same period. Recruitment was estimated to be highly variable, and preliminary model fits indicated that the recruitment variability assumed in previous assessments (σ_R=0.4) was too low to be consistent with the changes in abundance observed over the history of the fishery, with values closer to σ_R=1.1 being more plausible. The cause of this variability, and whether it reflects environmental or climate-driven changes in productivity, is not known. This recruitment variability has direct consequences for the projections: under TACC catches the total SCI 3 stock was projected to remain above the target over the next five years under both recruitment assumptions, but stock status increased when future recruitment was resampled from the recent (higher) period and declined when resampled from the full time series. The probability of remaining above the target in 2031 fell appreciably for MN and, in particular, MW under the long-term-average recruitment assumption, indicating that the favourable projected outlook depends on recent recruitment levels being maintained.

A number of uncertainties should be borne in mind when interpreting these results. First, retrospective analysis showed a consistent pattern in which the most recent year classes, and hence terminal-year SSB, were initially estimated above the long-term average in several peels before being revised back towards the average as additional data were incorporated. This is a typical pattern for stocks with limited information on the most recent cohorts and indicates that the SSB and YCS estimates for the final two to three years of the assessment are more uncertain than the credible intervals alone suggest. Second, several biological parameters — natural mortality, growth, stock-recruitment steepness, and maturity — are poorly known for New Zealand scampi and were either fixed or estimated from sparse or borrowed information; the assessment was, however, relatively insensitive to the assumed value of natural mortality. The newly estimated Chatham Rise length-weight relationship is an improvement over the previously assumed SCI 1 & 2 relationship and indicated longer, thinner scampi than in those northern stocks. Third, the interpretation of the photographic survey may change over time due to reader experience and viewing conditions and this may affect the indices used in the assessment. Although the reader calibration of McGregor et al. (2024) reduces this effect, some of the MCMC chains for the photographic-survey selectivity and catchability parameters (and for the data-poor MO stock generally) mixed poorly; sensitivity runs excluding the photographic survey nonetheless gave very similar results, so this is unlikely to have affected the overall conclusions.

The SCI 4A assessment remains substantially more uncertain than that for SCI 3. SCI 4A supports a more recently developed fishery, has only a single year of resource-survey information (2024), and could only be assessed using the surplus production model. The posterior for the carrying capacity of the western stock (4AW) closely tracked its prior, indicating that the available catch and abundance data for this stock are largely uninformative about its absolute scale. The conclusion that both SCI 4A stocks are above 40% K should therefore be treated with caution, and the projections for these stocks had wide uncertainty intervals with lower bounds approaching zero. Continued collection of survey and catch-effort information will be required before the status of the SCI 4A stocks can be estimated with any confidence.

Overall, the assessment indicates that the SCI 3 scampi stock is in a healthy state, very likely to be above the management target and unlikely to be approaching the limit reference points, and that under current catch levels it is likely to remain so over the medium term provided recent recruitment is maintained. The data-limited SCI 4A stocks appear to be above the target but are assessed with considerably lower confidence. Areas for future work include continuation of the trawl and photographic survey time series (including for SCI 4A), further development and validation of the photographic survey reader calibration, improved information on scampi growth, natural mortality, and stock structure, and continued monitoring of recruitment variability and its possible links to environmental and climate-driven change.

Table 19: Summary of the differences in assumptions and aspects of surplus production models versus integrated length-based models.

Aspect	Surplus production models	Integrated length-based models
Simplicity vs. Complexity	Simpler, requiring fewer assumptions and parameters.	More complex, incorporating detailed biological and fishery data.
Data Requirements	Relies on abundance indices (e.g., CPUE, photo surveys, trawl surveys) and catch data.	Requires additional data, such as length frequencies, growth rates, and recruitment patterns.
Handling Recruitment	Captures recruitment variability through process error, reflecting fluctuations in productivity.	Explicitly estimates recruitment deviations, often informed by length frequency data.
Flexibility and Speed	Faster to run and easier to interpret; suitable for management procedures (MPs).	More computationally intensive and effort-intensive to update.
Performance and Outputs	Produces biomass estimates and dynamics similar to integrated models for Scampi stocks.	Provides detailed outputs, such as sex-specific selectivity and growth patterns.
Applicability to Data-Limited Stocks	Ideal for data-limited stocks, such as SCI 4A, where biological data are sparse.	Better suited for data-rich stocks with detailed biological and fishery data.
Use in Management	Useful for annual updates and MPs due to simplicity and speed.	Provides richer insights for certain management decisions and validation purposes.

Reference points for scampi in SCI 3 (MN, MO and MW) are the default management target of 40% B_0, a soft limit of 20% B_0, and a hard limit of 10% B_0. The overfishing threshold was assumed to be $F40\%B_0$, calculated as the catch over spawning-stock biomass exploitation rate $U40\%B_0$ at the target biomass for the base case model, giving $U40\%B_0$=0.178 for MN, $U40\%B_0$=0.201 for MO, $U40\%B_0$=0.153 for MW, and $U40\%B_0$=0.194 for the total SCI 3 stock (Figure 61). B_{2026} was estimated to be 68% B_0 for the total SCI 3 stock, Very Likely (> 90%) to be at or above the target, and Exceptionally Unlikely (< 1%) to be below the soft or hard limit, for the base case and most of the sensitivity runs considered. Overfishing is Exceptionally Unlikely (< 1%) to be occurring in MO and Very Unlikely (< 10%) to be occurring in MN but is Likely (> 60%) to be occurring in MW; at the SCI 3 stock scale, overfishing is Very Unlikely (< 10%) to be occurring (Figure 61).

Based on the projections carried out, the stock is predicted to remain above 40% B_0 for the total SCI 3 stock for the next five years under current catches (TACC), provided year class strengths remain at recent levels; if year class strengths return to the long-term average, the stock is predicted to decline more quickly. The probability of the current catch or TACC causing biomass to remain below or decline below the soft limit is Very Unlikely (< 10%), and below the hard limit is Exceptionally Unlikely (< 1%). The probability of the current catch or TACC causing overfishing to continue or commence at the SCI 3 stock scale is Very Unlikely (< 10%), although overfishing is more likely to continue in the MW stock specifically at these catch levels.

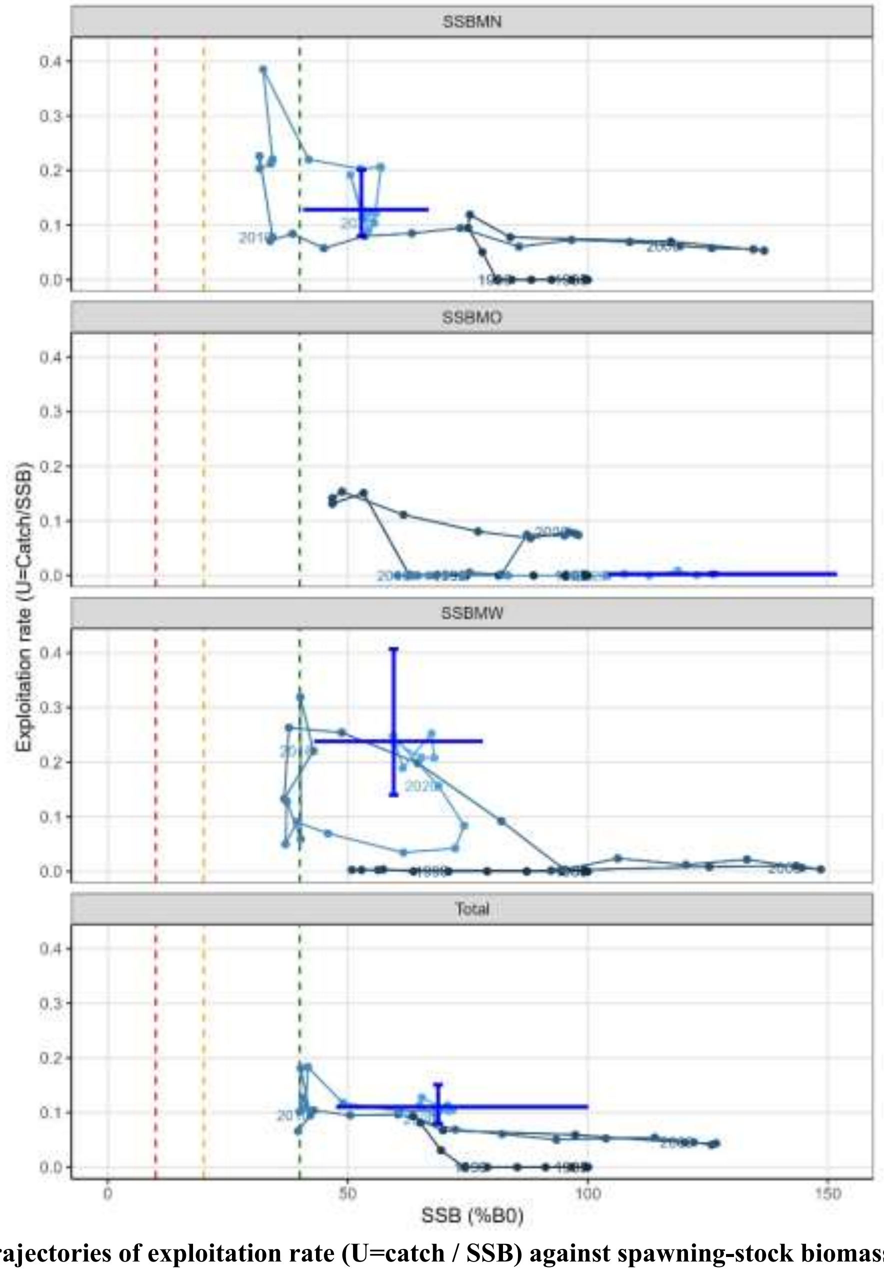

Figure 61: Trajectories of exploitation rate (U=catch / SSB) against spawning-stock biomass (SSB, as a percentage of B_0) for the SCI 3 MN, MO and MW stocks and the SCI 3 total, from the start of the assessment period to 2026. Points are labelled by year and connected in temporal sequence. Vertical dashed lines show the default hard limit (10% B_0, red), soft limit (20% B_0, orange) and target (40% B_0, green) reference points; the horizontal dashed line shows the exploitation rate at the target biomass (*$U40\%B_0$*) for each stock and the SCI 3 total. The dark blue cross shows the median (and 95% credible interval) of SSB (%B_0) and exploitation rate for the final model year.

6.1 Monitoring of changes that may be due to climate change and environmental variability

Pinkerton et al. (2018, 2023) proposed methods for a qualitative evaluation of potential effects of environmental or climate change on the stock assessment. This approach evaluates where productivity may have changed due to environmental fluctuations or climate change and hence may be important to consider in the scientific or management advice for the stock. A summary of the qualitative evaluation determined by the Deepwater Working Group is given in Table 20.

Table 20: Summary of the changes that may be due to climate change and environmental variability for SCI 3 and SCI 4A scampi.

Parameter	Summary
Recruitment	Large changes in productivity over time, but unknown if these relate to climate change. Strong evidence of a recruitment/productivity pulse in mid-1990s, weak recruitment up to 2008 and an increase in mean recruitment since about 2010
Age-at-maturity	Not enough information from which to evaluate effects
Stock recruitment steepness and variability	It is not known if there have been changes in the stock-recruit steepness parameter (h). Stock size has remained high and changes in steepness may not be apparent. Variability in recruitment is high and has potentially changed over the history of the fishery.
Natural mortality	Not enough information from which to evaluate effects
Growth	Not enough information from which to evaluate effects
Length-weight	Not enough information from which to evaluate effects
Spatial distribution	Based on the fishery distributions, there was no evidence of spatial distribution changes in the distribution of the population over time. However, scampi are constrained to areas where the substrate is predominantly mud or fine sediments, and may not have the opportunity to move in response to climate related environmental changes
Stock structure	Not enough information from which to evaluate effects

7. ACKNOWLEDGEMENTS

We thank the Fisheries New Zealand Data Management Team for the data extracts used in these analyses and the additional assistance and information on interpretation. We also thank Geoff Tingley, Vidette McGregor, Ian Tuck, and Gretchen Skea for their comments and advice, as well as the members of the Deepwater Fisheries Assessment Working Group for their input and discussions that improved the work presented in this report. This report was funded by Fisheries New Zealand under Project Code SCI 2024-02.

8. REFERENCES

Bentley, N.; Kendrick, T.H.; Starr, P.J.; Breen, P.A. (2012). Influence plots and metrics: tools for better understanding fisheries catch-per-unit-effort standardizations. *ICES Journal of Marine Science 69*, 84–88.

Beverton, R.J.H.; Holt, S.J. (1957). *On the dynamics of exploited fish populations.* HMSO, London.

Bull, B.; Dunn, A.; McKenzie, A.; Gilbert, D.J.; Smith, M.H.; Bian, R.; Fu, D. (2012). CASAL (C++ algorithmic stock assessment laboratory) User Manual v2.30-2012/03/21. *NIWA Technical Report 135.* National Institute of Water and Atmospheric Research, Wellington, 280 p.

Casal2 Development Team (2024). Casal2 user manual for age-based models, v24.08. *NIWA Technical Report 139*. NIWA. (Using source code from https://github.com/alistairdunn1/CASAL2:Development), Wellington, New Zealand, 311 p.

Casal2 Steering Group (2026). Casal2 user manual for length-based models, v26.05. Technical Report. (Using source code from https://github.com/alistairdunn1/CASAL2.git:master), Wellington, New Zealand, 313 p.
Charnov, E.L. (1993). *Life history invariants: some explorations of symmetry in evolutionary ecology*. Oxford University Press, Oxford.
Cryer, M. (2000). A consideration of current management areas for scampi in QMAs 3, 4, 6A and 6B. Final Research Report for Ministry of Research Project MOF199904K Objective 1. 52 p. (Unpublished report held by Fisheries New Zealand.).
Cryer, M.; Stotter, D.R. (1997). Trawling and tagging of scampi off the Alderman Islands western Bay of Plenty, September 1995 (KAH9511). *New Zealand Fisheries Data Report No. 84*. 26 p.
Cryer, M.; Stotter, D.R. (1999). Movement and growth rates of scampi inferred from tagging, aldermen islands, western bay of plenty. *NIWA Technical Report 49.* 36 p.
Dunn, A. (2025). gamInflu: Influence Analysis for Generalized Additive Models. Wellington, New Zealand, https://github.com/alistairdunn1/gamInflu.
Fisheries New Zealand (2025). Report from the Fishery Assessment Plenary, May 2025: stock assessments and stock status. Compiled by the Fisheries Science Team, Fisheries New Zealand. Ministry for Primary Industries, Wellington, New Zealand, 1955 p.
Fox, W.W. (1970). An Exponential Surplus-Yield Model for Optimizing Exploited Fish Populations. *Transactions of the American Fisheries Society 99*, 80–88. https://academic.oup.com/tafs/article/99/1/80/7893616. https://doi.org/10.1577/1548-8659(1970)99%3C80:AESMFO%3E2.0.CO;2
Francis, R.I.C.C. (2011). Data weighting in statistical fisheries stock assessment models. *Canadian Journal of Fisheries and Aquatic Sciences 68*, 1124–1138.
Gelman, A.; Carlin, J.B.; Stern, H.S.; Dunson, D.B.; Vehtari, A.; Rubin, D.B. (2015). *Bayesian Data Analysis*, 3rd ed. Chapman and Hall/CRC, New York. https://doi.org/10.1201/b16018
Gelman, A.B.; Carlin, J.S.; Stern, H.S.; Rubin, D.B. (1995). *Bayesian data analysis*. Chapman and Hall, London.
Gilks, W.R.; Richardson, S.; Spiegelhalter, D.J. (1998). *Markov chain Monte Carlo in practice*, CRC Interdisciplinary Statistics. Chapman & Hall.
Harley, S.J.; Myers, R.A.; Dunn, A. (2001). Is catch-per-unit-effort proportional to abundance? *Canadian Journal of Fisheries and Aquatic Sciences 58*, 1760–1772. https://doi.org/10.1139/f01-112
Hilborn, R.; Walters, C.J. (1992). *Quantitative fisheries stock assessment. Choice, dynamics and uncertainty*. Chapman and Hall, New York.
Kristensen, K. (2026). RTMB: “R” Bindings for “TMB.”
Marra, G.; Wood, S.N. (2011). Practical variable selection for generalized additive models. *Computational Statistics & Data Analysis 55*, 2372–2387. https://www.sciencedirect.com/science/article/pii/S0167947311000491. https://doi.org/10.1016/j.csda.2011.02.004
Marsh, C.; Dunn, A. (2024). r4Casal2: R package for post processing Casal2 model output. https://github.com/alistairdunn1/r4Casal2:Development. Version 1.04. NIWA and Ocean Environmental, Wellington, New Zealand.
McGregor, V.L.; Hartill, B.W.; Tuck, I.D.; Bian, R. (2022). Characterisation, CPUE, and length-based assessment model for scampi on the Mernoo Bank (SCI 3) 1989–90 to 2019–20. *New Zealand Fisheries Assessment Report 2022/18*. New Zealand, 222 p.
McGregor, V.L.; Holmes, S.J.; Underwood, M.J. (2024). Review of photo calibration methods for scampi (*Metanephrops challengeri*) photo surveys. *New Zealand Fisheries Assessment Report 2024/05*. 34 p.
Monnahan, C.C. (2024). Toward good practices for Bayesian data-rich fisheries stock assessments using a modern statistical workflow. *Fisheries Research 275* https://linkinghub.elsevier.com/retrieve/pii/S0165783624000882. https://doi.org/10.1016/j.fishres.2024.107024
Morizur, Y. (1982). Estimation de la mortalité pour quelque stocks de langoustine, *Nephrops norvegicus*. report. *Annual Science Conference 1982 - K - Shellfish committee.* https://doi.org/10.17895/ices.pub.21378252.v2

Pauly, D. (1980). On the interrelationships between natural mortality, growth parameters, and mean environmental temperature in 175 fish stocks. *Journal du Conseil Permanent International pour l'Exploration de la Mer 39,* 175–192.

Pella, J.J.; Tomlinson, P.K. (1969). A generalized stock production model. *Inter-American Tropical Tuna Commission Bulletin 13*, 419–496.

Pinkerton, M.; Devine, J.; Dunn, A.; Mormede, S. (2023). Monitoring the effects of environmental variability and climate change on toothfish assessments. WS-CC-2023/20. CCAMLR, Hobart, Australia, 10 p.

Pinkerton, M.; Dunn, A.; Mormede, S.; Parker, S. (2018). Monitoring and managing the effects of environmental change on toothfish assessments. WG-SAM-18/22. CCAMLR, Hobart, Australia, 14 p.

Polacheck, T.; Hilborn, R.; Punt, A.E. (1993). Fitting Surplus Production Models: Comparing Methods and Measuring Uncertainty. *Canadian Journal of Fisheries and Aquatic Sciences 50*: 2597–2607. http://www.nrcresearchpress.com/doi/10.1139/f93-284. https://doi.org/10.1139/f93-284

Punt, A.E. (2003). Extending production models to include process error in the population dynamics. *Canadian Journal of Fisheries and Aquatic Sciences 60*: 1217–1228. https://cdnsciencepub.com/doi/10.1139/f03-105. https://doi.org/10.1139/f03-105

R Core Team (2022). R: A language and environment for statistical computing. R Foundation for Statistical Computing, Vienna, Austria.

Schaefer, M.B. (1954). Some aspects of the dynamics of populations, important for the management of the commercial marine fisheries. *Inter-American Tropical Tuna Commission Bulletin 1*, 27–56.

Simpson, G.L. (2024). gratia: Graceful ggplot-Based Graphics and Other Functions for GAMs Fitted using mgcv. https://gavinsimpson.github.io/gratia/.

Stan Development Team (2020). Stan Modelling Language: User's Guide and Reference Manual Version 2.24. Stan Governing Body.

Tuck, I.D. (2014). Length-based population model for scampi (*Metanephrops challengeri*) in the Bay of Plenty (SCI 1) and Wairarapa / Hawke Bay (SCI 2). *New Zealand Fisheries Assessment Report 2014/33.* 172 p.

Tuck, I.D. (2017). Characterisation and a length-based assessment model for scampi (*Metanephrops challengeri*) at the Auckland Islands (SCI 6A). *New Zealand Fisheries Assessment Report 2017/56*. 178 p.

Tuck, I.D. (2019). Characterisation and a length-based assessment model for scampi (*Metanephrops challengeri)* on the Mernoo Bank (SCI 3). *New Zealand Fisheries Assessment Report 2019/61*. 248 p.

Tuck, I.D. (2020). Characterisation and CPUE standardisation of scampi in SCI 4A. *New Zealand Fisheries Assessment Report 2020/04*. 48 p.

Tuck, I.D.; Dunn, A. (2012). Length-based population model for scampi (*Metanephrops challengeri*) in the Bay of Plenty (SCI 1), Wairarapa / Hawke Bay (SCI 2), and Auckland Islands (SCI 6A). *New Zealand Fisheries Assessment Report 2012/01*. 125 p.

Vehtari, A.; Gelman, A.; Gabry, J. (2017). Practical Bayesian model evaluation using leave-one-out cross-validation and WAIC. *Statistics and Computing 27*, 1413–1432. https://doi.org/10.1007/s11222-016-9696-4

Wieczorek, A.M.; Underwood, M.J.; Evans, O.; Hall, J.; Hamill, J.; Armiger, H.; Smith, M.; Spong, K.; Drury, J.; Barry, F.; Miller, A.; Stevens, D.W.; Wood, B.A.; Clinchard, S.; Stotter, D.R. (2024). Estimation of the abundance of scampi on the Chatham Rise in SCI 3 and SCI 4A using trawl and photographic surveys. *New Zealand Fisheries Assessment Report 2024/62.* 41 p.

Wood, S.N. (2003). Thin-plate regression splines. *Journal of the Royal Statistical Society (B) 65*, 95–114.

Wood, S.N. (2004). Stable and efficient multiple smoothing parameter estimation for generalized additive models. *Journal of the American Statistical Association 99*, 673–686.

Wood, S.N. (2011). Fast stable restricted maximum likelihood and marginal likelihood estimation of semiparametric generalized linear models. *Journal of the Royal Statistical Society (Series B) 73*, 3–36.

Wood, S.N. (2017). *Generalized Additive Models: An Introduction with R*, 2nd ed. Chapman and Hall/CRC.

Wood, S.N.; Pya, N.; Säfken, B. (2016). Smoothing parameter and model selection for general smooth models (with discussion). *Journal of the American Statistical Association 111*, 1548–1575.

APPENDIX A: MPD SUMMARY FIGURES

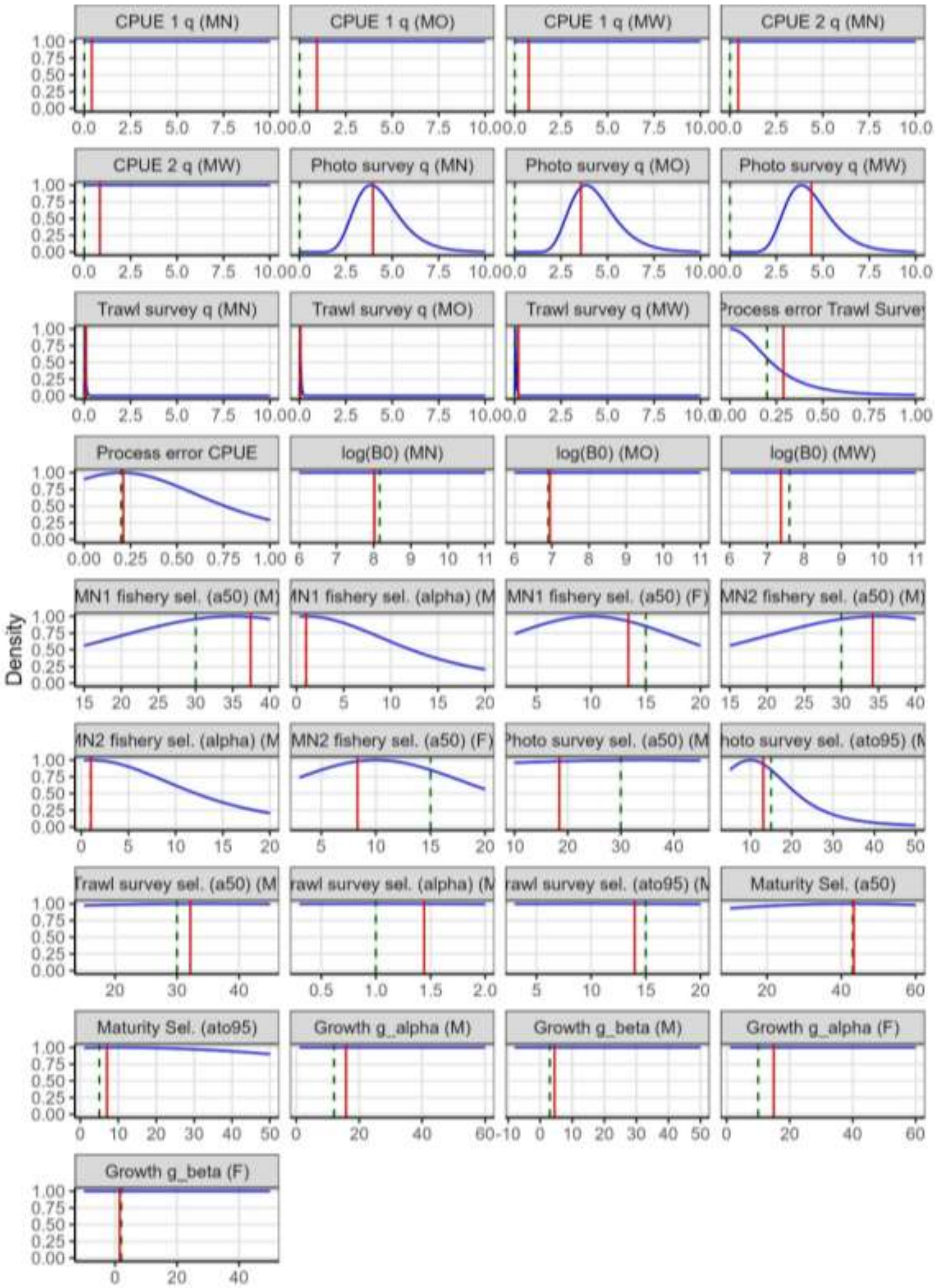

Figure 62: Base case model MPD estimates for all parameters excluding YCS. Priors are shown as the blue lines, the MPD estimates as the vertical red lines, and the starting points for estimation as the dashed green lines. The x-axis range indicates the bounding values for each parameter.

APPENDIX B: MCMC SUMMARY TABLES AND FIGURES

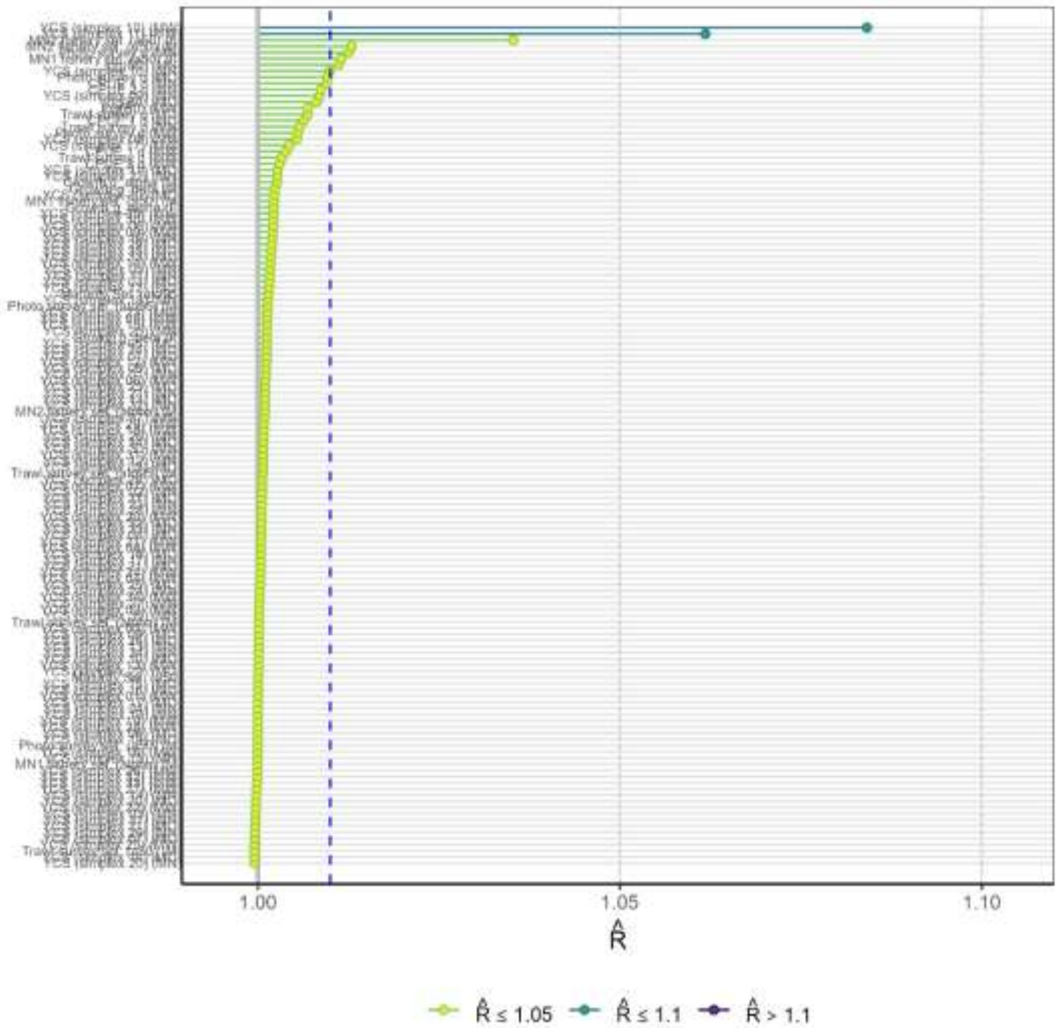

Figure 63: Base case model MCMC $\hat{r}$ statistics for all parameters from the three independent chains ($\hat{r}$ values less than 1.05 suggest no evidence of non-convergence).

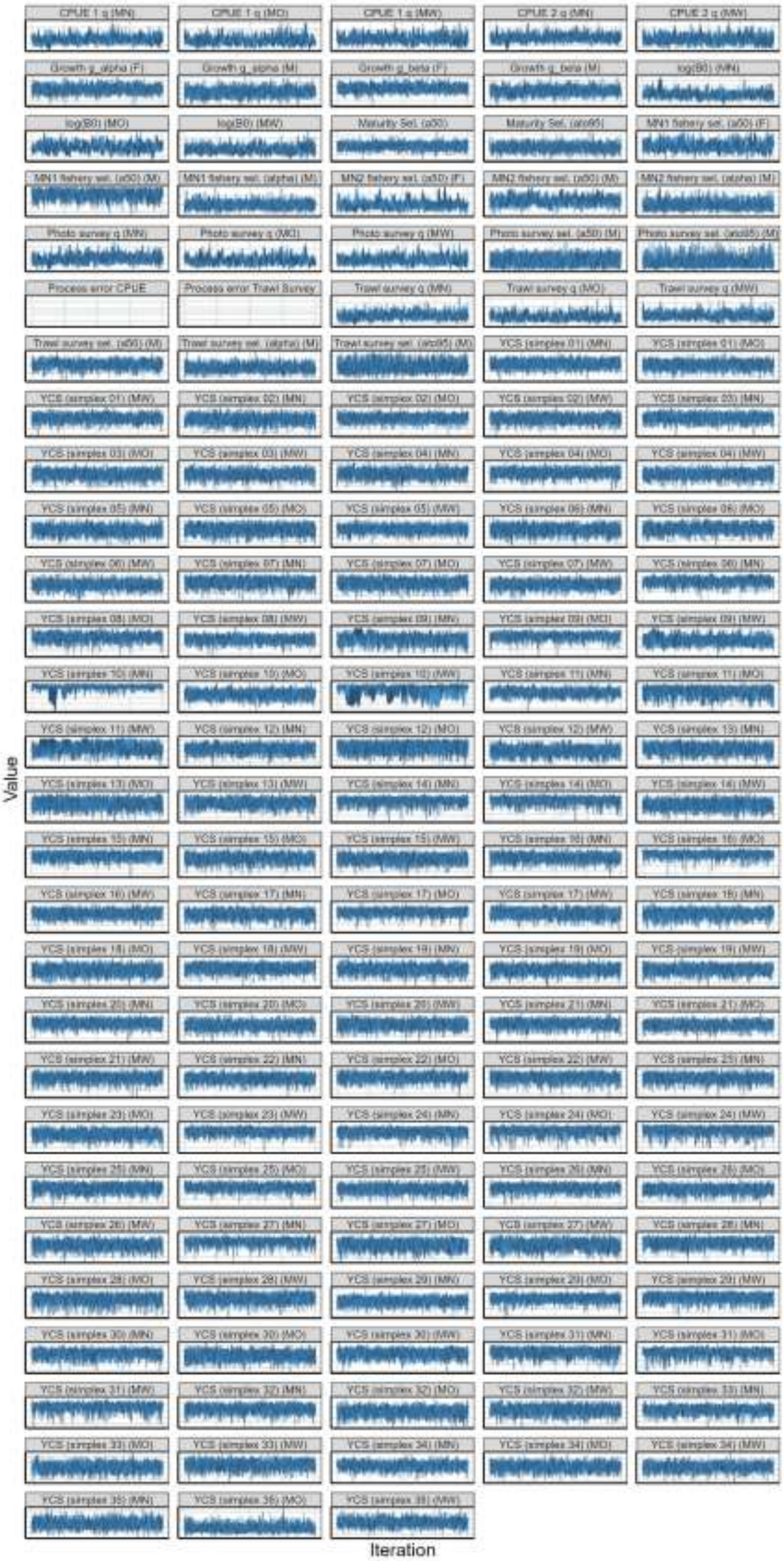

Figure 64: Base case model MCMC estimates for all parameters from the three independent chains (colour shades)